UNIVERSITY OF
LINCOLN

RECQL4: linking DNA replication to bone tumorigenesis

By Lisa Chacko

13383076

MSc by Research: Life Science

School of Life Sciences

Research supervisor: Csanad Bachrati

December 2017

This is to certify that I am responsible for the work submitted in this thesis, that the original work is my own, except as specified in the acknowledgements and in references, and that neither the thesis nor the original work contained therein has been previously submitted to any institution for a degree.

Signature:

Name: Lisa Anne Chacko

Date: 08/12/2017

Abstract

RECQL4 is a gene that encodes a 1208 amino acid protein. RECQL4 protein is required during DNA replication initiation and DNA end resection. A lack of RECQL4 is therefore associated with a decrease in DNA damage repair. There are three unrelated autosomal recessive diseases that are linked with mutations in *RECQL4.* Rothmund Thomson Syndrome is rare disorder which has documented mutations within *RECQL4* which has been linked to an increased tendency to develop osteosarcomas.

To study the effect of RECQL4 depletion, shRNA knockdowns, ASC52Telo cells, osteo-differentiated cells and osteo-differentiated cells in long term PHA-767491 treatment were subjected to a series of experiments. The trilineage differentiation capability, growth characteristics, expression of cell proliferation and bone formation markers, drug sensitivity and chromosomal instability was tested for each of the cell lines. These results could be used to identify any differences in expressions and behaviours between the RECQL4 depleted cells and the control cells.

All the cell lines were able to differentiate into adipocytes and osteoblasts, with p44 pLK0.1 and p44 shRQ-9 having a decreased adipocyte differentiation in comparison to the others. No significant difference was observed in the growth assay between the cells in which RECQL4 was depleted and their controls. The p44 shRQ-9 cells showed the lowest foci count when tested for 53BP expression but the highest Ki67 expression. There were no significant results between the RECQL4 depleted cells and their controls when looking at marker gene expressions. The drug sensitivity assays also show no significant differences however p14 shRQ-10 and P44 shRQ-10 appear less sensitive in the mid-range concentrations. The chromosomal analysis showed that OD+PHA, p44 shRQ-9 and p44 shRQ-10 have an increased degree of aneuploidy and tetraploid cells.

Acknowledgements

To my supervisors, Dr. Csanad Bachrati and Dr. Timea Palmai-Pallag, for all your help throughout the entire duration of my MSc by Research. Words cannot describe how grateful I am to the both of you for all the support and guidance you have provided me with. I can only hope this thesis does your guidance some justice.

To Anika and Frances for all your help and support whilst in the laboratory. Your help was invaluable on a daily basis.

To Alex Aithen for ensuring all equipment in the laboratory is working and providing guidance to the best of your ability.

To all the staff and students at the University of Lincoln whom I have had the pleasure to know over the last four years. Thank you for all your support and kind words over the years and I wish you all the very best in the future.

To all my work colleagues, past and present, for your continued support and encouragement each day.

Thank you to my best friend Dominque Sade for keeping a smile on my face even when I felt stressed. You were my rock during my masters and I cannot thank you enough for always being there for me.

To my sister for all of your guidance throughout my undergraduate degree and my masters. Without your knowledge I would not have been as successful.

To my boyfriend for being there when I needed support, no matter what time of day it is. You help remind me how far I have come and how far I have the potential to go.

To my parents for being by my side throughout all of my time at university. You support me in every possible way that you can and help me overcome any obstacles I may face during the process. I am sorry for any of the grey hairs you may have gained in the process.

Table of Contents

Table of Figures

List of Tables

Abbreviations

ASCs	Adipose-derived Stem Cells
BGS	Baller Gerold Syndrome
BM	Bone Marrow
CIN	Chromosomal Instability
DSB	Double Strand Break
HR	Homologous Recombination
HRDC	Helicase & RNAase D C-Terminal
HSCs	Hematopoietic Stem Cells
hTERT	Human Telomerase Reverse Transcriptase
hTR	Human Telomerase RNA
MSCs	Mesenchymal Stem Cells
NHEJ	Non-Homologous End Joining
RQC	RecQ C-Terminal
RTS	Rothmund-Thomson Syndrome
Runx2	Runt Related Transcription Factor 2
SNPs	Single-Nucleotide Polymorphisms
TGF-β	Transforming Growth Factor-β
UCB	Umbilical Cord Blood
UCM	Umbilical Cord Matrix

1. Introduction

1.1 Mesenchymal Stem cells

Evidence was first provided by Friedenstein *et al*. (1970) that a population of hematopoietic stem cells (HSCs) and a rare population of plastic-adherent cells was present in the bone marrow (BM). During the 1980's it was shown that mesenchymal stem cells (MSCs) had the capability of differentiating to osteoblasts, chondrocytes and adipocytes (Williams and Hare, 2011). Since then MSCs have been shown to be present in a variety of foetal and adult tissues including cord blood, amniotic fluid, foetal blood and, in some cases, adult peripheral blood. Many researchers have had a keen interest in MSCs due to their therapeutic potential in tissue repair and immune modulation (Roberts, 2004). Owing to their ease of isolation, expansion and their multi-lineage differentiation ability, MSCs are applied in a range of experimental and medical applications. Some examples include the enhancement of HSC engraftment, the amelioration of acute graft-versus-host disease and regenerative medicine approaches, in particular for bone and cartilage ((Xiao *et al*., 2013)

1.1.1 MSC defining Characteristics

A universal definition of an MSC is difficult to decide on since there are no unique unambiguous cell surface markers to distinguish MSCs from HSCs. When undifferentiated, the shape of MSCs resemble the spindle shape of fibroblasts making them hard to distinguish (Williams and Hare, 2011). Stem cells have traditionally been defined by their multipotency and self-renewal capability (Nombela-Arrieta *et al*., 2011). Some researchers are unsure whether MSCs are true stem cells or multipotent precursor cells. A standard criteria has been developed by the International Society of Cellular Therapy that defines MSCs by three characteristics: "1) adherence to plastic in standard culture conditions, 2) expression of CD105, CD73 and CD90 and no expression of CD45, CD34, CD14, CD11b, CD79b, CD19 and HLA-DR and 3) capacity to differentiate into osteoblasts, chondroblasts and adipocytes *in vitro,* termed trilineage differentiation potential" (Xiao *et al*., 2013).

Phenotypically, MSCs express many different markers, although none of these are specific to MSCs. However, cell surface CD markers can be used to distinguish between MSCs and HSCs. For example MSCs lack the haematopoietic markers CD34, CD45, CD14, CD11 and HLA-DR. MSCs can also express markers including myofibroblasts, neurons and transforming growth factor-β (TGF-beta) (Ding *et al*., 2011). As well as the adhesion molecules mentioned in the standard criteria, MSCs also express some cytokine receptors (e.g. IL-1R, TNF-αR) and some stromal cell markers (e.g. SH-2, SH-3 and SH-4) (Roberts, 2004, Chamberlain *et al*., 2007).

1.1.2 Sources of MSCs

MSCs can be obtained from various tissues including the umbilical cord, endometrial polyps, bone marrow, peripheral blood, skeletal muscle and adipose tissue (Ding *et al*., 2011, Wagner *et al*., 2005). These are ideal sources due to the quantity that can be obtained and ease of harvesting the cells (Ding *et al*., 2011). The most researched and most accessible source of MSCs is the BM, even though the number of cells present are low in frequency (0.01-0.0001% of nucleated cells in BM) (Roberts, 2004). Although BM represents the main source of MSCs, the number of BM MSCs available decreases with age and can be affected when there is a high degree of viral infection. Obtaining BM MSCs from a patient is also a highly invasive procedure, making it necessary to look for alternative sources of MSCs (Romanov *et al*., 2003, Kern *et al*., 2006).

Recently it has been shown that stem cells can be derived from the umbilical cord matrix and blood. Umbilical cord blood (UCB) is a much less invasive method that causes no harm to the mother of the infant (Kern *et al*., 2006). It is established that UCB is a rich source of HSCs, but the ability to establish MSC cultures from UCB is controversial. Some studies have proven to isolate MSCs from UCB at a sufficient yield to use in clinical application, but other studies have clearly failed (Zeddou *et al*., 2010). Researchers from Kansas State University concluded that cells from the matrix of the umbilical cord (UCM) had stem cell properties and thus could prove a rich source of primitive cells (Mitchell *et al*., 2003), with Zeddou *et al*. (2010) confirming it is possible to isolate MSCs from UCM in their experiment.

Most of the evidence obtained so far suggests the MSCs are not present in the peripheral blood of healthy adults, only in specific circumstances. These can include patients with malignant diseases and healthy women during and after pregnancy (Roberts, 2004). There is, however, evidence that MSCs can be collected from menstrual blood (Ding *et al*., 2011). Around 400 menstrual cycles occur in each women's reproductive years, with the average blood loss each menstruation around 35ml (Ding *et al*., 2011, Toyoda *et al*., 2007). Menstrual blood is usually discarded but could represent a new source of human MSCs to be used in regenerative medicine (Ding *et al*., 2011). Many of MSCs collected from this source have myogenic differentiation potential, especially towards forming cardiac muscle cells (Toyoda *et al*., 2007).

Another alternative source of stem cells, which is less invasive and available in larger quantities, is adipose tissue (Kern *et al*., 2006). With the current increase in obesity across the world, subcutaneous adipose tissue is easily accessible and in abundance. Thousands of

liposuction surgeries are carried out each year and the lipoaspirate tissue is discarded (Bunnell *et al*., 2008). In the past a variety of names have been used to try and describe that plastic adherent cell population that can be isolated from adipose tissue. To help avoid confusion, the International Fat Applied Technology Society adopted the term “adipose-derived stem cells” (ASCs) to describe this cell population (Bunnell *et al*., 2008). ASCs are pluripotent cells with characteristics similar to BM-derived MSCs. Studies have shown that ASCs contain similar surface markers and gene profiling to the MSCs found in BM (Kim *et al*., 2007).

1.1.3 Differentiation of MSCs

As mentioned before, MSCs have the ability to differentiate into a variety of lineages of mesodermal origin. Their tri-lineage potential to differentiate into bone, cartilage and fat *in vitro* can be used to further help identify MSC populations (Ding *et al*., 2011).

To promote adipogenesis differentiation, MSCs are induced through incubation with dexamethasone, insulin, isobutyl-methylxanthine and indomethacin for a period of 2-3 weeks. An accumulation of lipid-rich vacuoles within the cells can be seen which express peroxisome proliferation-activated receptor y2, lipoprotein lipase and aP2: a fatty acid-binding protein (Pittenger *et al*., 1999). These lipid vacuoles can be assayed histologically by staining lipid droplets in cells using Oil Red O solution (Figure 1A) (Ding *et al*., 2011). These adipocytes were shown to remain healthy for at least 3 months in culture (Pittenger *et al*., 1999).

Osteogenic differentiation has been widely induced *in vitro* by incubating a confluent monolayer of MSCs with a mixture of dexamethasone, β-glycerophosphate and ascorbic acid phosphate for a period of 2-3 weeks (Chamberlain *et al*., 2007). A study by Pittenger *et al*. (1999) showed the isolated MSCs formed aggregates which could be viewed by staining with Alizarin Red (Figure 1B). Any osteo-differentiation MSCs stain a bright orange-red colour. Their quantitative assays also showed that there was a 4-10 fold increase in alkaline phosphatase activity and that after 1 week of incubation there was evidence of calcium accumulation (Pittenger *et al*., 1999).

Chondrogenic differentiation is promoted through the culturing of MSCs in the presence of TGF-β. Histological analysis using toluidine blue indicated the presence of glycosaminoglycans within the extracellular matrix (Chamberlain *et al*., 2007). The presence of glycosaminoglycans can also be shown with Alcian Blue staining (Figure 1C).

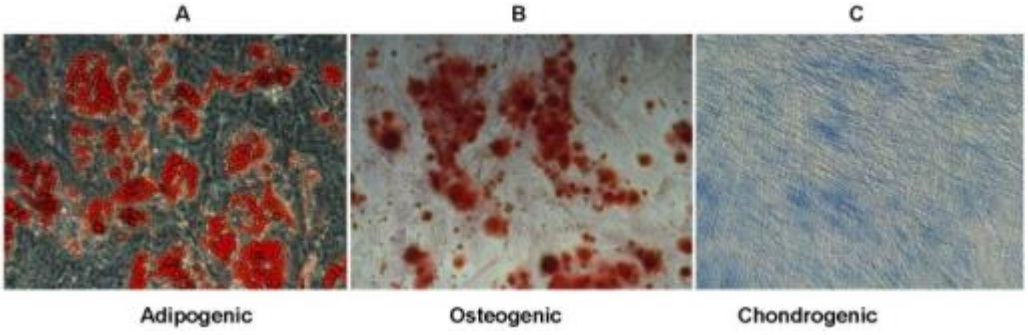

Figure 1. Trilineage potential of MSCs. Differentiation of MSCs into A) Adipocytes stained with Oil Red O, B) Osteoblasts stained with Alizarin Red and C) Chondrocytes stained with Alcian Blue (Dolley-Sonneville *et al*., 2013).

Previous studies have also demonstrated that BM-derived MSCs have the ability to differentiate into myoblasts that can fuse into rhythmically beating myotubes, after treatment with 5-azacytidine and amphotericin B (Wakitani *et al*., 1995).

All these differentiation events are accompanied by changes in gene expression and are tightly regulated by signalling events and transcription factors (Ding *et al*., 2011).

1.1.3.1 Regulation of differentiation

There are two main molecular pathways that describe the regulation of the differentiation of MSCs into cartilage and bone: the WNT canonical pathway and the TGF-β superfamily pathway (Augello and De Bari, 2010). It is likely that many different growth factors will interact with these pathways to help control MSC differentiation (Williams and Hare, 2011).

The TGF-β pathway is involved in skeletal growth and the regulation of the chondrogenic differentiation of MSCs. TGF-β3 promotes chondrogenic differentiation in MSCs via several intracellular cascades, including the SMAD proteins, mitogen-activated protein kinases and extracellular-signal regulated kinases (Williams and Hare, 2011).

WNT glycoproteins are soluble glycoproteins that activate receptor complexes composed of Lrp5 and Lrp6 proteins, which induces a series of intracellular events that monitor cell differentiation and proliferation (Westendorf *et al*., 2004). This WNT pathway has been shown to play an important role during skeletogenesis by promoting osteoblast proliferation and suppressing chondrocyte formation (Westendorf *et al*., 2004). WNT signalling leads to the stimulation of four different signalling pathways, the canonical pathway being the best characterised (Etheridge *et al*., 2004). This pathway regulates β-catenin stability, an integral part in transducing WNT signals to the nucleus (Westendorf *et al*., 2004). Disruptive mutations in the LRP5 receptor have been associated with a decreased bone mass and decreased osteoblast proliferation, whereas activating mutations in LRP5 can result in a high bone-mass

phenotype and increased osteoblast proliferation (Etheridge *et al*., 2004). There are a number of WNT ligands and receptors expressed on MSCs, each controlling MSC differentiation. For example WNT3A promotes undifferentiated MSC proliferation and suppresses osteogenic differentiation (Boland *et al*., 2004).

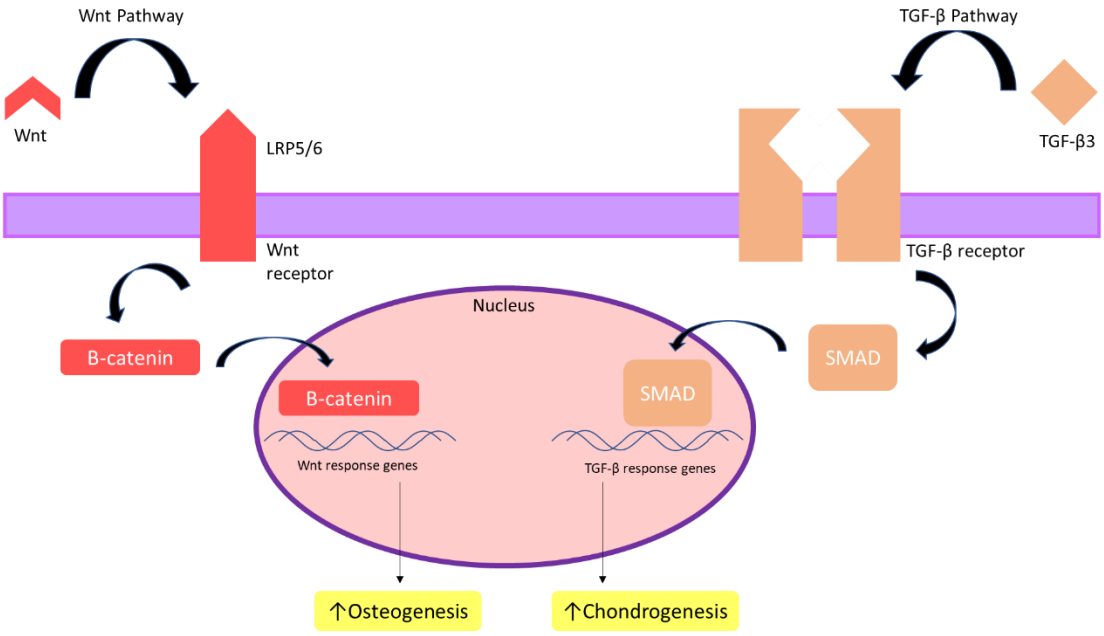

Figure 2. Molecular regulation of MSC differentiation. WNT and TGF-β signalling pathways that regulate differentiation of MSCs (Adapted from (Williams and Hare, 2011) using PowerPoint)**.**

One of the genes shown to be a target of β-catenin is runt-related transcription factor 2 (RUNX2), resulting in the stimulation of bone formation (Gaur *et al*., 2005). RUNX2 plays an essential role in osteoblast differentiation and during the later stages of chondrocyte differentiation. RUNX2 has been shown to upregulate osteoblast-related genes such as *ALP, BGLAP, OCN, BSP* and *COL1A1* (Florencio-Silva *et al*., 2015). Another transcription factor involved in the regulation of bone formation and osteoblast differentiation is zinc finger transcription factor Osterix , which has been shown to be regulated by RUNX2 (Nishio *et al*., 2006). RUNX2 is the first transcription factor required to determine the osteoblast lineage, with canonical WNT signalling and Osterix further directing the outcome by blocking their differentiation into chondrocytes (Komori, 2008).

1.1.4 Therapeutic uses of MSCs

Due to their tri-lineage potential, ease of expansion and isolation, MSCs have therapeutic potential in a variety of medical applications. The ability of MSCs to maintain pluripotency after prolonged culturing offers the use of cultured MSCs in autologous and allogeneic transplants. Other medical applications that have seen the use of MSCs are in cardiac repair,

reducing graft-versus-host disease, enhancing marrow engraftment and in generating connective tissue elements that may be abnormal (Ng *et al*., 2008). The immunological characteristics of MSCs further enhance their therapeutic appeal (Javazon *et al*., 2004).

1.1.5 Immunological characteristics of MSCs

The immunological phenotype of MSCs is widely described as MHC I^+, MHC II^-, $CD40^-$, $CD80^-$ and $CD86^-$. This phenotype is regarded as non-immunogenic and therefore when used in transplantations, the allogeneic host may not require the use of immunosuppression. It is possible that MHC class I may activate T cells, but due to the absence of any costimulatory modules there would be no secondary signal (Javazon *et al*., 2004). There have been multiple studies that suggest MSCs have immunosuppressive properties, in particular that MSCs have the ability to modulate many T-cell functions, including cell activation. However, this suppression is independent of any MHC matching between the T cells and MSCs (Chamberlain *et al*., 2007).

1.1.6 hTERT immortalisation of MSCs

Human cell lines that have been derived from non-cancerous tissues have a finite lifespan when cultured under laboratory conditions meaning senescence occurs after a limited number of divisions. This limitation to the cell lines has proved to be a major obstacle in previous experiments and it also limited their use as therapeutic agents. Multiple forms of senescence have been shown to exist with telomere-controlled senescence proving a common form (Lee *et al*., 2004). The onset of telomere senescence is shown through the shortening of the telomeres. Telomeres shorten each time cell division occurs, providing a “molecular clock” for cell lines (Bernadotte *et al*., 2016). This shortening ultimately leads to mortality stage 1 (M1) and stage 2 (M2). It has been shown that in cells of renewal tissues a DNA polymerase, named telomerase, is present and has the ability to synthesise telomeric repeats, which compensates for the end replication problem that is caused by the shortening of telomeres (Bernadotte *et al*., 2016). Telomerase is made up of two core components: human Telomerase Reverse Transcriptase (hTERT) and human Telomerase RNA (hTR). The first core component is involved in providing catalytic activity, and its expression is normally suppressed in human somatic cells. When expressed exogenously it can sufficiently reconstitute telomerase activity, preserving the length of the telomeres and ultimately preventing the onset of M1 and M2 (Lee *et al*., 2004).

1.1.7 Osteoblasts to Osteocytes

Osteoblasts are defined as bone forming cells that originated from MSCs. They are found along the bone surface and make up 4-6% of the composition of bone cells (Florencio-Silva *et al*., 2015). Osteoblast cells secrete osteoid, a non-mineralised bone matrix, and become incorporated in mineralised bone matrix as osteocytes (Franz-Odendaal *et al*., 2006). Osteocytes comprise 90-95% of all bone cells, making them undoubtedly the most abundant cellular component of mammalian bones (Feng *et al*., 2006, Franz-Odendaal *et al*., 2006). The morphology of osteocytes depends on the type of bone. For example, osteocytes found in the trabecular bone are more rounded in appearance in comparison to those found in cortical bone. It is suggested that osteocytes on average have a half -life of around 25 years, much greater than the average lifespan of an osteoblasts which is only three months. (Florencio-Silva *et al*., 2015). Osteocytes have the ability to communicate not only with one another, but with all cells present at the bone surface through a meshwork of cell processes in the bone matrix that run through canaliculi (Palumbo *et al*., 1990). This ensures that all cells involved in the formation of bone remain connected during all stages (Franz-Odendaal *et al*., 2006)

There are three different modes of ossification that transform osteoblasts into osteocytes; intramembranous, perichondral and endochondral. The mode used is dependent on what type of bone is being generated (woven or lamellar bone), the location of bone formation and the age/gender of the individual. Intramembranous bone formation forms membrane bones and occurs when bone is formed without the replacement of a cartilaginous model. In the presence of a cartilaginous precursor, perichondral ossification is the most common mode of bone formation. Endochondral ossification is normally seen in long bones and involves a cartilaginous template that is either remodelled or is replaced by bone through a series of co-ordinated steps (Franz-Odendaal *et al*., 2006).

There are four different fates for osteoblasts at the end of a bone-forming phase. They can become osteocytes embedded in the bone, become bone lining cells, undergo apoptosis or occasionally transdifferentiate into cells that deposit chondroid bone (Franz-Odendaal *et al*., 2006). Parfitt (1990) reported that 65% of osteoblasts in cancellous bone undergo apoptosis and around 30% undergo osteocyte transformation.

1.2 Osteosarcoma- Tumours of the bone

Osteosarcoma is the most prevalent malignant bone tumour which is presumed to derive from cells of an osteoblastic lineage. It is characterised by the production of immature osteoid by neoplastic cells (Poos *et al*., 2015). Osteosarcoma most often presents itself in the femur (42%

with 75% occurring in the distal femur), humerus (10% with 90% in the proximal humerus) or the tibia (19% with 80% occurring in the proximal tibia) of patients. The age distribution of osteosarcoma is defined as bimodal, the first peak being during adolescence and the second peak during late adulthood (Ottaviani and Jaffe, 2010). The first peak normally occurs in the pubertal growth spurt in 10-14 year olds. The deaths due to osteosarcoma represent 8.9% of childhood and adolescent cancer deaths. The average 10 year survival rate is currently just over 65.8%, but only 24% in patients with formed metastases at the time of presentation (Duchman *et al*., 2015). Elderly patients have the poorest survival chances (Ottaviani and Jaffe, 2010). There are many factors affecting the prognosis of osteosarcoma, a few of the factors being response to chemotherapy, presence of metastases, tumour site and tumour size (Clark *et al*., 2008). The current therapy to manage osteosarcoma consists of preoperative chemotherapy, complete surgical resection and postoperative chemotherapy. Owing to the advances in imaging techniques and the positive effect of the use of preoperative chemotherapy, amputation of the affected limb is rarely required as surgery can normally be limb-sparing (Luetke *et al*., 2014).

Molecular markers and pathways that help contribute to the development of osteosarcoma have been a recent area of research to determine their significance as clinically predictive tools. These markers can be useful in predicting a patient's response to chemotherapy, the overall prognosis and developing therapeutic agents to help with the treatment (Clark *et al*., 2008).

1.2.1 Molecular markers in osteosarcoma

The current standard prognostic markers carry a level of inaccuracy and bear a number of limitations. This has presented the need for quantitative measures to help improve treatment planning. The table below outlines some of the molecular factors that have been associated with the prognosis of osteosarcoma (Clark *et al*., 2008).

Table 1. Molecular factors shown to be associated with the prognosis of osteosarcoma. Modified from Clark *et al*. (2008).

Factor	Role in osteosarcoma	Level present in osteosarcoma	Any correlation with prognosis?	Potential for therapeutic use
VEGF	Angiogenesis	↑	Controversial	Yes

MMP2, MMP9	Extra-cellular matrix invasion	↑	Correlation	Yes, positive results from other cancers
PLAU/PLAUR	Increases plasmin. Pro invasion	↑	Correlation	Yes, reduced invasion when regulated
P-glycoprotein	Drug resistance	↑	Correlation	Undetermined
CXCR4	Chemotaxis, organ specific metastasis	↑	Correlation	Yes
TP53	Cell cycle control	↓/mutated	Correlation	Undetermined
ERBB2	Cell signalling, proliferation	Mixed results	Controversial	Undetermined
Survivin	Inhibits apoptosis	↑	Correlation	Undetermined
HLA class I	Absence allows immune system invasion	↓	Correlation	Undetermined
Ezrin	Cell signalling, metastasis	↑	Correlation	Yes
RB1	Tumour suppressor	↓/mutated	Correlation	Undetermined
FOS	Transcription	↑	Indirect correlation	Undetermined

1.2.2 Genomic instability in osteosarcoma

Genomic instability has been shown to play a critical role in the development and progression of cancer, and has also shown to have implications on the aging progress (Petkovic *et al.*, 2005). Osteosarcoma exhibits a complex karyotype due to the high levels of genomic instability, particularly chromosomal instabilities (Poos *et al*., 2015). Over the years, many cytogenetic studies and genomic analyses of osteosarcomas have been carried out using multiple techniques such as karyotyping, comparative genomic hybridisations, quantitative PCR and many others. More recently, studies utilising single-nucleotide polymorphisms (SNPs) have been carried out to understand more about osteosarcoma genomics. There is still a lot of uncertainty around the genetic etiology, but there are some consistent findings. Many studies have shown that there is a higher prevalence to develop osteosarcoma in individuals with familial Li-Fraumeni syndrome (*TP53* inactivation), Rothmund-Thomson syndrome (*RECQL4*

inactivation), Bloom syndrome (*BLM* inactivation) and Werner syndrome (*WRN* inactivation). The genes linked with these latter three syndromes encode DNA helicases of the RecQ family, involved in the maintenance of DNA (Martin *et al*., 2012).

Osteosarcoma is susceptible to aneuploidy with a large number of chromosomal alterations being present (Nishijo *et al*., 2004). Previous cytogenic analysis of the cancerous cells in osteosarcoma has shown a clear change in the number of chromosomes and a tendency to develop structural chromosomal aberrations. (Al-Romaih *et al*., 2003). There are two subtypes of chromosomal instability (CIN): numerical CIN and structural CIN. The processes resulting in numerical CIN are those that result in copy number alterations. It is evident in polyploidy which can be caused by errors in mitosis, deletions, amplifications, translocations and aneuploidy. Structural CIN normally results from ineffective DNA damage response mechanisms induced by genotoxic insults, replication errors that can lead to chromosomal breakages and genomic rearrangements.

1.2.3 Mutations linked with osteosarcoma

The pathogenesis of osteosarcoma has previously been linked to mutations in several genes including *RB1* and *TP53*, genes important for mitotic checkpoints (Cao *et al*., 2005, Maire *et al*., 2009). It has also been shown that there is a significant correlation between the mutation of *TP53* and increased levels of genomic instability in osteosarcoma, while studies involving *RB1* mutation show a contribution to the loss of heterozygosity in mice (Overholtzer *et al*., 2003, Coschi *et al*., 2010). A study by Maire *et al*. (2009) of 18 osteosarcoma cases showed a link between the overexpression of *RECQL4*, a gene that encodes a DNA helicase, and structural CIN. However, there are many studies suggesting other genes that may contribute to the development of osteosarcoma.

1.3 DNA damage and repair: the role of DNA helicases

During DNA replication, recombination and repair double stranded DNA must become partially unwound to form single stranded DNA intermediates (Lohman, 1993). DNA helicases are ubiquitous enzymes responsible for unwinding double stranded DNA and are involved in many of the cells basic cellular processes (Wang *et al*., 2003). DNA helicases utilise the energy produced from the hydrolysis of ATP to play an important role in DNA metabolism, participating in replication, transcription, repair and chromatin organisation (Croteau *et al*., 2012, Mohaghegh and Hickson, 2001). It is possible that any interruptions to the function of these helicases could reduce genomic stability resulting in an increased chance of tumorigenesis (Wang *et al*., 2003).

1.3.1 RecQ family helicases

Helicases of the RecQ family play a critical role in ensuring efficient repair of DNA damage. RecQ helicases are members the SF2 superfamily involved in the resolution of DNA structure and travel in a 3'-5' direction on single stranded DNA (Bernstein *et al*., 2010).

There are five known RecQ homologues in humans and germ-line mutations in three of these are linked with premature aging and/or cancer predisposition (Bachrati and Hickson, 2003).

RecQ proteins contain many different structural domains with all containing a core helicase domain. WRN, BLM and RECQ1 contain a helicase and RNAse D C-terminal (HRDC) and nuclear localisation sequences and all except RECQL4 contain a RecQ C-terminal (RQC) domain. It is thought that the HRDC and RQC domains are involved in the mediation of interactions with nucleic acids and other proteins. All the RecQ helicases except RECQL5 contain an acidic region, which enables protein-protein interactions. WRN is the only human RecQ protein that contains an exonuclease domain (Figure 3) (Bernstein *et al*., 2010).

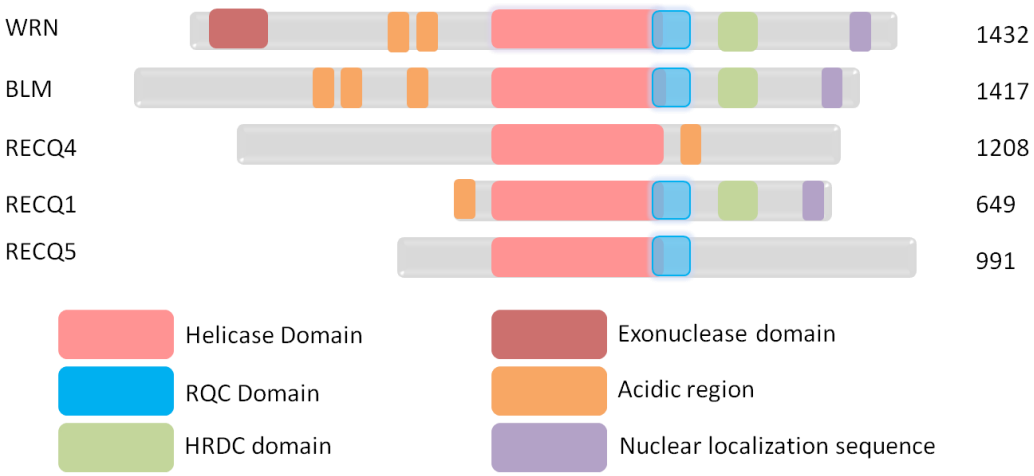

Figure 3. The structural domains of each member of the human RecQ helicases. Adapted from Bernstein *et al*. (2010).

RecQ helicases are also important at various steps during DNA replication. The absence of RecQ helicase activity can result in stalled or collapsed replication forks, which requires repairing in order to prevent double strand breaks (DSBs). RecQ helicases can help the association of polymerases with the replication fork and unwind any DNA structures that could ultimately lead to replication fork stalling.

1.3.2 RECQL4

The *RECQL4* gene encodes an 1208 amino acid protein and is located on human chromosome 8q24.3 (Kitao *et al*., 1999, Wang *et al*., 2003). Although *RECQL4* displays many domain

characteristics of the RecQ family, it lacks some features such as the domains that are used in DNA binding. Many previous experiments have shown that RECQL4 is required to assemble the machinery used in DNA replication initiation (Sangrithi *et al*., 2005). A study by Im *et al*. (2015) showed that RECQL4 is required during DNA replication initiation for Mcm10 and Ctf4 to associate with replication origins. Mcm10 and Ctf4 are crucial parts of the pre-replication complex and they are responsible in the recruitment of RECQL4 into the pre-replication complex to subsequently initiating replication. A lack of RECQL4 would prevent DNA replication initiation from occurring.

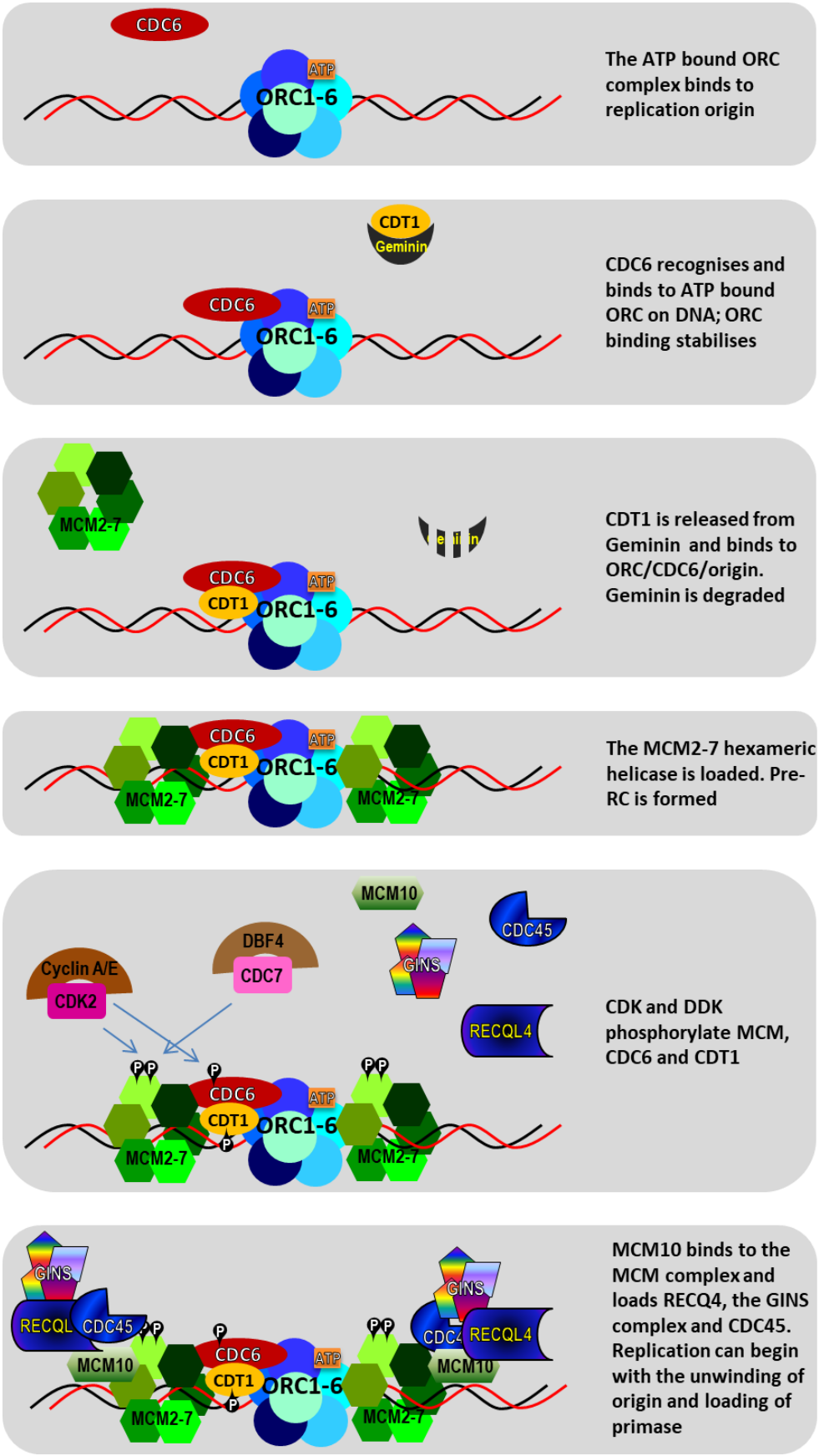

Figure 4. Schematic diagram showing the assembly of the pre-replication complex. (Adapted by Csanad Bachrati from (Diffley, 2004, Labib, 2010, Symeonidou *et al.*, 2012).

RECQL4 has been shown to have intrinsic ATPase activity and also single stranded DNA annealing activity (Singh *et al*., 2010). A study by (Lu *et al*., 2016)) identified a role for *RECQL4* in DNA end resection, an essential step of homologous recombination dependent DNA double strand break repair. When a depletion of *RECQL4* is seen, there is a subsequent reduction in homologous recombination mediated repair and end resection. An interaction is seen between *RECQL4* and MRE11-RAD50-NBS1 (MRN), which identifies DSBs and initiates DNA end resection with the recruitment of CtIP. *RECQL4* is also seen directly interacting with CtIP at DSBs via its N-terminal domain, recruiting CtIP to the MRN complex (Lu *et al*., 2016).

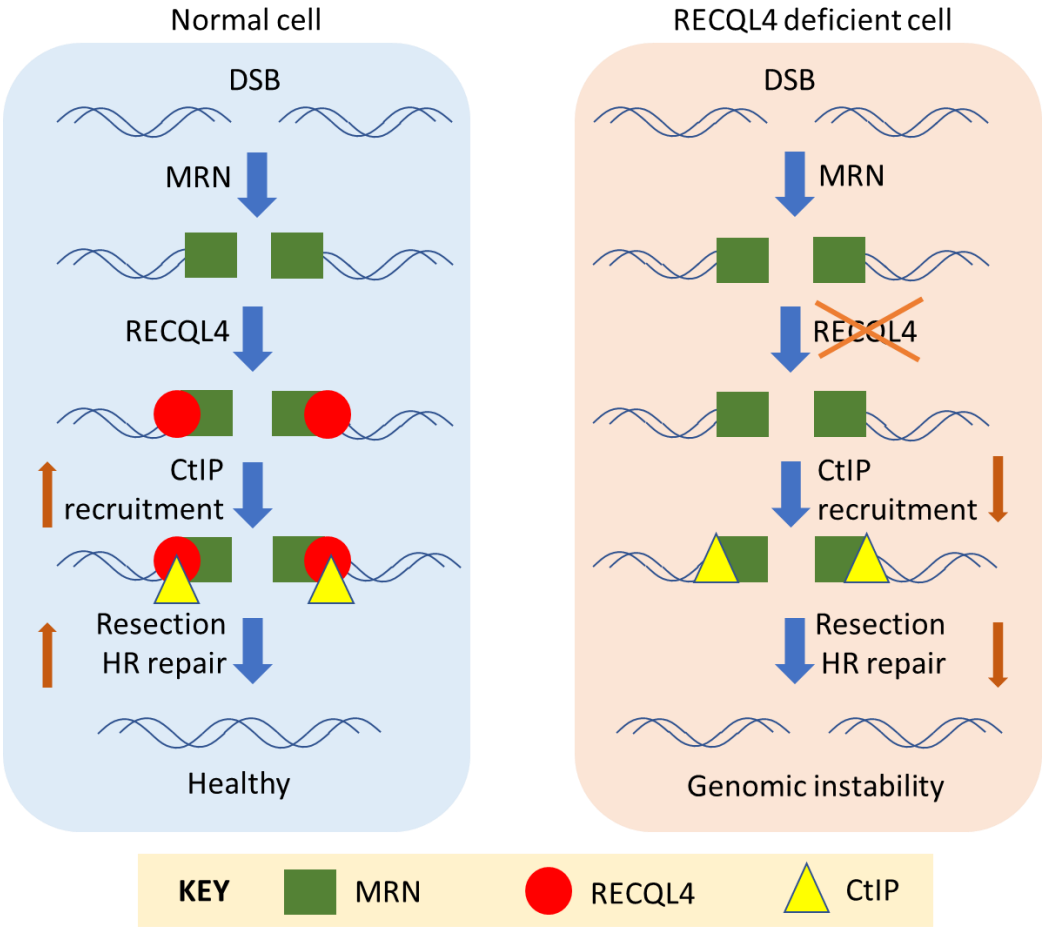

Figure 5. The role of *RECQL4* in DSB repair. Adapted from Lu *et al*. (2016).

1.3.3 DNA damage

DNA damage occurs in many different forms and can result from defects in any part of DNA metabolism. In response to DNA damage, cells have developed a range of pathways to arrest the cell cycle and induce DNA repair (Mohaghegh and Hickson, 2001). Mutations can frequently occur in DNA repair genes, which results in genome destabilisation, consequently causing an increase in mutations at other loci. The maintenance of genomic stability is

important in the prevention of cancer due to the importance of integrity of the proto-oncogenes and tumour suppressor genes. This maintenance aims to eliminate spontaneous DNA damage through intrinsic errors in DNA metabolism and through DNA reactive agents (Mohaghegh and Hickson, 2001).

One form of DNA damage is double strand breaks (DSBs). These can be generated through exogenous stress and programmed recombination events (Lu *et al*., 2016). They occur when the sugar-phosphate backbone of both DNA strands are broken in a close proximity allowing the dissociation of the helix into two molecules (Aparicio *et al*., 2014). DSBs can occur accidentally during normal metabolism or because of the presence of DNA-damaging agents. It is important that these DSBs are repaired in order to maintain genome integrity and prevent chromosome rearrangements or cell death (Symington, 2014). There are two main pathways normally used to repair DSBs: homologous recombination (HR) and non-homologous end joining (NHEJ) (Aparicio *et al*., 2014). HR-dependent double strand break repair is on the most part error free. This method of repair requires either a sister or non-sister chromatid as a template and is only active during G2 and S phases (Lu *et al*., 2016). Initiation of HR-dependent double strand break repair is by the 5' end resection of DSBs, generating 3' single strand DNA (ssDNA) tails. These subsequently become coated in RPA, an ssDNA binding protein. RAD52 then recruits RAD51 to replace RPA and promote strand invasion leading to D loop formation (Bernstein *et al*., 2010). This leads to repair synthesis, ligation of the ends and the dissolution/resolution of Holliday junctions. On the other hand, NHEJ is error prone but is active during all phases of the cell cycle and DNA template-independent (Lu *et al*., 2016).

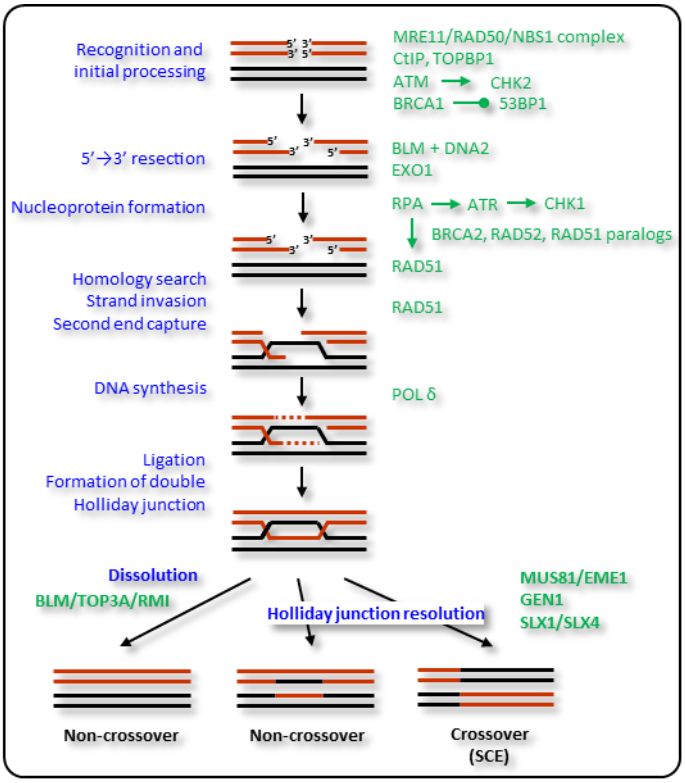

Figure 6. Homologous recombination. A simplified view of the execution step of homologous recombination repair of double-stranded DNA breaks to indicate the position and role of proteins used as functional markers (Created by Csanad Bachrati).

1.3.4 Genotoxic insult to cells

Many common clinical drugs have cytotoxic effects on cells resulting in DNA damage and can result in structural CINs. When treated with these drugs cells can normally rescue themselves from the DNA damage. If the cells are *RECQL4* deficient then end resection doesn't occur, preventing homologous recombination.

Bleomycin is an anticancer drug comprising of complex of water-soluble peptides which are extracted from *Streptomyces verticillatus*. It is considered an effective agent in the control of numerous human cancers (Adamson and Bowden, 1974). The use of bleomycin can affect many different cellular pathways, but the cause of its cytotoxic effect is through its ability to bind and cleave DNA. A number of studies also report that bleomycin produces reactive oxygen radicals, which when released can result in the expression of cytokines, subsequently inducing chromosomal aberrations, DNA strand breaks and DNA damage (Mishra *et al*., 2000).

Another cytotoxic agent is Mitomycin C, is a bifunctional DNA alkylating agent that is used in cancer treatment. Mitomycin C induces the cross-linking of complementary strands of DNA, and it is these cross-links that are considered the critical cytotoxic lesions produced from its use (Palom *et al*., 2002).

Camptothecin is a strong anti-tumour drug that inhibits DNA and RNA synthesis resulting in fragmentation of cellular DNA. Its intracellular target is topoisomerase I, an enzyme that plays a key role in DNA replication, transcription and segregation. Camptothecin binds to both the topoisomerase and the DNA complex, forming a ternary complex. This binding prevents the re-ligation step of topoisomerase action, causes S phase arrest and subsequently results in apoptosis (Ryan *et al*., 1991).

Hydroxyurea has been used clinically since 1960 and is primarily used for the treatment of chronic granulocytic leukaemia. Hydroxyurea selectively inhibits ribonucleotide reductase and consequently causes the depletion of dNTP pools, stalling of DNA synthesis and subsequent collapsing of replication forks (Bernstein *et al*., 2010).

KUO055933 is an inhibitor of the ATM kinase, which has a selectivity at least 100 fold greater than any other inhibitors for similar kinases (Li and Yang, 2010). KUO055933 usage inhibits ATM-mediated DNA repair events (Nadkarni *et al*., 2012).

PHA-767491 is a dual CDC7/CDK9 inhibitor which has shown cytotoxic activity in a range of cancers. One of the drug's primary features is its ability to downregulate the expression of the MCL1 antiapoptotic protein and its cross-reactivity with CDK9. CDC7 is a protein kinase that plays an essential role in the initiation of DNA replication and cell cycle progression. CDC7 is responsible for the phosphorylation of the minichromosome maintenance 2-7 (MCM2-7) complex, which in turn activates its intrinsic DNA helicase activity. This starts the process to establish a competent replication fork for semiconservative DNA synthesis. In non-cancerous cells, the downregulation of CDC7 by short interfering RNA results in cell cycle progression arrest (Natoni *et al*., 2011). CDK9 is a kinase that forms the catalytic core of positive transcription elongation factor b (P-TEFb). This enzyme plays an essential role in the stimulation of transcription elongation of most protein coding genes by RNA polymerase II (RNAPII) (Kryštof *et al*., 2012).

1.3.5 Associated RecQ helicase diseases

Only three of the RecQ helicases are associated with syndromes that cause premature aging and a predisposition to develop cancer. Loss of function of WRN and BLM results in the development of autosomal recessive disorders Werner syndrome and Bloom syndrome, respectively (Croteau *et al*., 2012). There are three unrelated autosomal recessive diseases that are linked with mutations in *RECQL4*; Rothmund-Thomson Syndrome (RTS), RAPADILINO syndrome and Baller-Gerold syndrome (BGS) (Bernstein *et al*., 2010, Croteau *et al*., 2012).

RTS is a rare disorder which has seen an increased tendency to develop osteosarcoma in patients, shows signs of premature aging and signs of chromosomal instability (Wang *et al*., 2003, Kitao *et al*., 1999). Other characteristics of RTS can be congenital skeletal abnormalities, short stature, sparse scalp hair, gastrointestinal disturbances and skin atrophy (Miozzo *et al*., 1998, Siitonen *et al*., 2009). The evaluation of the prominent features of RTS has led to the development of two subclasses; type I and type II. RTS type I has mutations in genes that have not yet been identified and can be defined by its characteristic poikiloderma. RTS type II patients also have poikiloderma but they have documented mutations within *RECQL4* which seems to be linked to an increase risk of osteosarcoma development (Croteau *et al*., 2012, Siitonen *et al*., 2009). Most mutations of *RECQL4* found in RTS patients are nonsense or frameshift mutations that result in a truncated polypeptide (Piard *et al*., 2015). Somatic cells that were harvested from RTS individuals showed genomic instability such as trisomy, chromosomal arrangements and aneuploidy (Der Kaloustian *et al*., 1990).

RAPADILINO is an acronym that indicates the principal signs of the syndrome: RA for radial ray defect, PA for both patellae hypoplasia or aplasia, DI for diarrhoea and dislocated joints, LI for little size and NO for long, slender nose and normal intelligence. RAPADILINO patients have many similar features to those with RTS such as growth retardation, skeletal malformations, and radial defects (Sangrithi *et al*., 2005, Siitonen *et al*., 2009). Like RTS patients, RAPADILINO patients also have an elevated risk of developing osteosarcomas and lymphomas (Croteau *et al*., 2012). Patients with the BGS phenotypes have shown to have mutations in *RECQL4, TWIST* and *FGFR2* genes. BGS can be characterised by craniosynostosis and radial aplasia. Unlike the other two *RECQL4* associated disorders, BGS patients are not predisposed to the development of osteosarcomas (Siitonen *et al*., 2009).

1.3.6 Murine models of RTS

There are several murine models that have been created to mimic RTS, focusing on mutations in *RECQL4* that map to the helicase region (Bernstein *et al*., 2010). These mice models are useful for studying which symptoms are linked with RTS. Most of the mice died within a two-week period after being born, but those that survived were smaller in size in comparison to wild-type mice. They also displayed other abnormalities such as dry skin, grey hair and also a loss of hair reminiscent of premature ageing. These mice, however, did not exhibit some of the symptoms RTS patients experience, such as osteosarcomas, poikiloderma and cataracts (Hoki *et al*., 2003).

Mann *et al*. (2005) created another mouse model in their study that mimics RTS through the disruption of the helicase domain encoded by exons 9-13 of *RECQL4*. 16% of these mice died within 24 hours of birth but the surviving mice showed an increased prevalence of skeletal defects in their limbs. However, these mice showed a normal wild-type life span, unlike RTS patients. When these mutant mice were combined with a mutant *Apc* tumour suppressor gene, there was an increased incidence of cancer development (Mann *et al*., 2005).

1.4 Aims

In this study I aim to identify how *RECQL4* depletion contributes to the development of osteosarcoma in RTS patients. To achieve this aim I will carry out a series of experiments to detect chromosomal instabilities, increased sensitivity to genotoxic agents, differentiation potential and determine the level of expression of marker genes. Throughout this study I will be working with ASC52Telo cells immortalised by hTERT expression. These results will hopefully allow for a better understanding of *RECQL4* deficient cells and provide information to help identify prevention therapies.

2. Materials and Methods

2.1 Materials

2.1.1 Cell lines

ASC52Telo, hTERT immortalised adipose derived MSCs were originally obtained from the American Type Culture Collection® at passage 13 for use in previous research studies. These were stored in liquid nitrogen and thawed out for use at the beginning of the study. These cells will be referred to as "ASC52Telo cells" during this study.

ASC52Telo cells were osteo-differentiated during a previous PhD research project to use during the study. These cells were stored in the liquid nitrogen and thawed out at the beginning of this study for use. These cells will be referred to as "OD" cells during this study.

These "OD" cells were subjected to long term 1.5µM PHA-767491 treatment in order to study the effect on OD cells. These cells were thawed out and used during this study and will be referred to as "OD+PHA" cells.

Two shRNA constructs (shRQ-9 and shRQ-10) in the pLK0.1 vector were developed during a previous research project. Fourth generation lentiviral particles were generated in 293T cells and the viral particles were used to transduce low passage as well as high passage ASC52telo cells by Dr Timea Palmai-Pallag. I continued the work with the characterisation of the resulting cell lines.

2.1.1.1 Media used

MesenPro RS™ medium was prepared by adding 10mL MesenPro RS™ growth supplement and 5mL L-Glutamine to 500mL MesenPro RS™ basal medium reduced serum (2%).

MesenPro RS™ basal medium reduced serum (2%)	Thermo Fisher Scientific
MesenPro RS™ growth supplement	Thermo Fisher Scientific
Stem Pro® adipogenesis differentiation kit	Thermo Fisher Scientific
Stem Pro® osteogenesis differentiation kit	Thermo Fisher Scientific
Stem Pro® chondrogenesis differentiation kit	Thermo Fisher Scientific

2.1.2 Plasticware and Glassware

96 well, standard, F plate (0.290cm^2)	Sarstedt
24 well, standard, F plate (1.820cm^2)	Sarstedt
12 well, standard, F plate (3.650cm^2)	Sarstedt
96 well, microtest plate, F (0290cm^2)	Sarstedt

T25 flask (canted neck, vented caps)	Sarstedt
15mL and 50mL conical centrifuge tubes	Sarstedt
1.5mL microcentrifuge tubes	Sarstedt
1.5mL cryotubes	Sarstedt
13mm glass coverslips	Thermo scientific
Haemocytometer (0.0025mm^2/0.1000mm depth)	Sigma Aldrich
5mL, 10mL and 20mL pipettes	Sarstedt
20mm Tissue culture dish	CytoOne
Ministart 0.45µl syringe filter	Sartorius

2.1.3 Chemicals

Acetic Acid	Fisher Scientific
Alizarin Red S	Santa Cruz Biotechnology
Alcian Blue 8GX	Santa Cruz Biotechnology
Amersham ECL select western blotting detecting reagent	Fisher Scientific
Bleomycin	Carbosynth
Bovine Serum Albumin (BSA)	Sigma-Aldrich
Camptothecin	Sigma Aldrich
CellTiter 96 aqueous MTS reagent powder	Promega
Demecolcine	Sigma Aldrich
Dimethyl Sulfoxide (DMSO)	Insight Biotechnology
Dithiodibutyric acid (DTT)	Sigma-Aldrich
Foetal Bovine Serum	Thermo Fisher Scientific (Gibco®)
Formaldehyde	Cell Signalling Technology®
Giemsa stain in Giemsa stain phosphate buffer pH 6.8	Gurr®, in *Stain*Rite® Wright
HEPES	Sigma Aldrich

Hydroxyurea 98% powder	Sigma-Aldrich
Isopropanol	Sigma-Aldrich
KUO055933	Tocris Bioscience
Methanol	Fisher Scientific
Mitomycin C	Sigma-Aldrich
MOPS SDS (20x)	NuPage
Oil Red O Biological Stain	Fisher Scientific
Paraformaldehyde	Sigma-Aldrich
PHA-767491	Sigma-Aldrich
Phosphate Buffered Saline (PBS) tablets	Fisher Scientific
Phenazine Methosulfate (PMS)	Sigma-Aldrich
Quick Start™ Bradford Protein assay	Bio-Rad
Spectra Multicolor Broad Range Protein Ladder	Thermo Fisher Scientific
Sodium Dodecyl Sulfate (SDS)	Fisher Scientific (Gibco®)
Potassium Chloride (KCl)	Melford Laboratories
Tris/Glycine buffer	Bio-Rad
Triton X-100	Fisher Scientific (Gibco®)
Trypan Blue	Sigma-Aldrich
Trypsin EDTA (10X)	Fisher Scientific
VECTASHIELD antifade mounting medium	Vector Laboratories
100% Ethanol	Fisher Scientific
4X Sodium Dodecyl Sulfate (SDS)	Invitrogen

2.1.4 Antibodies

Antibodies are detailed in tables when used during the methods.

2.2 Methods

2.2.1 Routine culture of cells

All methods carried out in tissue culture were performed in an appropriate laminar flow tissue culture hood (Thermo Fisher Scientific) under sterile conditions using 70% ethanol to sterile any equipment brought into the hood. Throughout all processes the cells were not allowed to remain dry for longer than 30 seconds at a time. All the cells used in this study were routinely cultured in 6 well, standard, F plates and kept in an incubator set at 5% CO_2, 95% relative humidity and 37°C. Once ~80% confluency was reached the cells were passaged. Until the cells reached the required confluency the media was changed every 2-3 days and the growth monitored using a Nikon Eclipse TS100 light microscope. The media was pre-warmed to 37°C before introduction with the cells. The cells were passaged by removing the old media, washing with 1mL PBS and then adding 3 drops of Trypsin using a P100 pipette. The plates were incubated at 5% CO_2, 95% relative humidity and 37°C with the Trypsin for ~5 minutes until all the cells detached. The plates were examined using a light microscope to ensure that all the cells had detached from the plate. Following adequate detachment, 1mL of MesenPro RS™ was added to each well and gently pipetted up and down to resuspend the cells. Depending on the confluency required during the next few days, 0.25-0.5mL of cells were added to a new well on a 6 well, standard, F plate and the required volume of prewarmed MesenPro RS™ to make a 1.5mL total volume.

2.2.2 Cryopreservation of ASC's

When confluent, the cells were detached from the culture plates using the method explained in section 2.2.1. Once detached the cells were diluted with MesenPro RS™ media and the contents transferred into a 15ml conical centrifuge tube. This was centrifuged for 3 minutes at 1500 RPM at room temperature using an Eppendorf 5702 R table top centrifuge. The supernatant was removed and then the cells resuspended in 250-500µl of MesenPro RS™ that contained 10% DMSO and 20% foetal bovine serum. This suspension was transferred to a sterile 1.5mL cryogenic tube adequately labelled with the date, cell line, passage number and then transferred to a Mr. Frosty Container in the -80°C freezer.

2.2.3 Recovery of cells

The cells were removed from the liquid nitrogen storage and kept on dry ice until all equipment and reagents were ready for use. Once ready the cells were thawed until almost defrost. The cell suspensions were then transferred from the cryogenic tube to a 15mL conical centrifuge tube and centrifuged at 1500 RPM for 3 minutes at room temperature. The supernatant was removed, and the cells resuspended in 3ml of MesenPro RS™ and centrifuged again to ensure all the DMSO was

removed. The supernatant was removed again, and the cells resuspended in 1.5mL media and plated on a 6 well, standard, F plate. The plate was then incubated at 5% CO_2, 95% relative humidity and 37°C.

2.2.4 Counting cells

When carrying out experiments that required comparable results between cell lines, it was important to plate out equal cell numbers in each well. To count cells the cells were cultured as described in section 2.2.1 until the stage where they had detached from the plate. The cells were then resuspended in 1mL MesenPro RS™ and 10µL was collected into a 1.5mL microcentrifuge tube. 10µL of Trypan blue was also added to the tube. 10µL of this solution was applied to a haemocytometer (0.0025mm^2/0.1000mm depth) and the number of live cells in each 4x4 grid were counted under a light microscope. The use of Trypan blue helps distinguish between live and dead cells as only the dead cells take up the blue dye. The total of the four grids were added up, double to allow for the Trypan blue dilution and then divided by four to obtain the average number of cells per grid. This number is equal to the number of cells in 1µL of suspension, so when $x10^3$ we know the number of cells per 1mL of suspension. This result can be used to work out diluted the suspension needs to be in order to plate the correct number of cells in every well.

2.2.5 21 day differentiation assay

The cells were cultured and detached as described in section 2.2.1. $2.5x10^4$ cells of each cell line being differentiated were counted and prepared as described in 2.2.4 then each plated into 3 separate wells on a 24 well, standard, F plate. These were left to settle overnight in the incubator at 37°C, 95% humidity and 5% CO_2. The following day the complete media was aspirated and each of the 3 wells plated for each cell type had MesenPro RS™ replaced with 500µl of either StemPro® adipogenesis, osteogenesis or chondrogenesis media. The cells were left to differentiation for 21 days with the media being changed every 2-3days. Photos of the cells differentiation progress were taken after 10 days and at the end of the 21 day period. After 21 days the differentiation media was aspirated, and the cells were gently rinsed with 1mL PBS. The PBS was then aspirated, and the cells fixed with 500µl of ice cold fixing solution (5mL 0.5M pH 7.4 HEPES, 1.06mL 33% paraformaldehyde and 3.94mL deionised water). The plate was incubated for 12 minutes in the fridge and following incubation the fixing solution was aspirated and the wells rinsed with 1mL PBS for three changes. The cells could now be stored in 1mL fresh PBS in the fridge until ready to be stained.

2.2.6 Staining of the differentiated cells

2.2.6.1 Adipocyte staining

The oil red o stock solution was prepared by weighing out 300mg of oil red o powder and mixing this with 99% isopropanol. This stock solution was stable for one year from the date which it was prepared. In a fume hood, 3 parts oil red o stock solution was mixed with 2 parts deionised water and allowed to sit at room temperature for 10 minutes. This working solution was only stable for ~2 hours. The working solution was then filtered using a filter syringe into a 50mL conical centrifuge tube.

During the staining the cells were not allowed to remain dry for longer than a period of 30 seconds at any point. The wells were rinsed gently with sterile water being careful not to disturb the monolayer. The water was removed and enough 60% isopropanol to cover the bottom of the well was added to each well. This was left to sit for 2-5 minutes. The 60% isopropanol was removed and enough of the working oil red o solution was added to completely cover the cells in each well. The dish was slowly rotated in order to spread the oil red o evenly over the cells and then left to stand for 5 minutes. Once the 5 minutes were up the wells were rinsed with tap water until the tap water ran clear. Enough haematoxylin counterstain was then added to each well to ensure all the cells were covered and left to stand for 1 minute. The haematoxylin was removed, and the plate was rinsed with warm tap water until the water ran clear. Water was left in the wells until ready to image using a Nikon Eclipse 80i Fluorescence Microscope in transmitted light where any lipids will appear red and nuclei blue.

2.2.6.2 Chondrocyte staining

The Alcian blue 8 GX staining solution was prepared by mixing 60mL Ethanol (98-100%) with 40mL Acetic Acid (98-100%). 10mg of Alcian Blue 8 GX was dissolved in this solution. The resulting working solution was stable for one year from the date it was prepared. 120mL Ethanol (98-100%) was mixed with 80mL Acetic Acid (98-100%) to prepare the destaining solution.

To stain the cells the PBS was removed, and the wells washed with distilled water. Enough Alcian staining solution was added to generously cover all the cells as some evaporation can occur. This was incubated overnight at room temperature in the dark. Once the incubation period was up the Alcian staining solution was removed and the destaining solution was added to each well and left to stand for 20 minutes. The destaining solution was removed and PBS added to each well. The cells could then be imaged on the phase microscope where any cartilage is an intense dark-blue and other tissue is at most a faint blue.

2.2.6.3 Osteocyte staining

The Alizarin Red S staining solution was prepared by dissolving 2g Alizarin Red S in 100mL distilled water, mixing it and then adjusting the pH to 4.1-4.3 with 0.1% NH_4OH. This solution was then filtered and stored in the dark.

To stain the cells the PBS was removed, and enough Alizarin Red S staining solution added to each well to cover the monolayer. This was incubated at room temperature in the dark for 3-5 hours. The Alizarin Red S staining solution was removed, and the monolayer washed four times with distilled water. The water was removed, PBS added to each well and the cells imaged. Undifferentiated MSCs were slightly reddish whereas MSC derived osteoblasts were bright orange-red.

2.2.7 Immunofluorescent staining

2.2.7.1 Preparation of the cells for staining

13mm diameter round cover slips were autoclaved and then sterilised in 70% ethanol to ensure they were completely sterile. One cover slip was then added to each well of a 24 well, standard, F, culture plate, rinsed with PBS and left to dry to ensure the removal of any residual ethanol. $3x10^4$ cells of each cell line being stained were seeded per well in MesenPro RS™ at a total of 1mL per well as described in sections 2.2.1 and 2.2.4. The plates were incubated at 5% CO_2, 95% relative humidity and 37°C until ~80% confluency was achieved. Until then the media was changed every 2-3 days, taking care not to disturb the monolayer. Once confluency was reached, the media was aspirated, and the wells rinsed with 1mL PBS. The PBS was then aspirated at 0.5mL of ice cold fixing solution (5mL 0.5M pH 7.4 HEPES, 1.06mL 33% paraformaldehyde and 3.94mL deionised water) was added to each well and incubated for 12 minutes. The fixing solution was aspirated, and the wells rinsed with 0.5mL PBS for three changes. 0.5mL of permeabilisation solution (10µl Triton X-100, 9.99mL PBS) was added to each well and incubated on ice for 20 minutes. This solution was then aspirated, and the cells were rinsed with 0.5mL PBS for a further 3-5 changes whilst gently rocking the plate. 0.5mL of blocking solution (10% Foetal Bovine Serum, 0.1% Triton X-100 in PBS) was added to each well and the plate incubated at 37°C for one hour. This solution was aspirated, and the cells stored in 0.5mL PBS until ready to be stained.

2.2.7.2 Staining of the cover slips: Ki67, RUNX2, Osterix and 53BP1.

The cells were prepared as explained in 2.2.7.1. Enough of the primary antibody for each stain was prepared to the correct dilution and volume to allow for 20µl per cover slip.

Table 2. Primary antibodies used in Immunofluorescent staining.

Stain	Company	Product code	Animal	Dilution
Ki67	Abcam	Ab15580-100	Rabbit	1:200
Osterix	R&D systems	MAB7547	Mouse	1:200
53BP1	Bethyl laboratories	A300-272A	Rabbit	1:500
RUNX2	Santa cruz	SC10758	Rabbit	1:200

20µl of the primary was dropped onto a clean glass slide and the cover slip removed from the 24 well plate, standard, F and placed cell side down onto the antibody. The edges of the coverslip were then fixed with Fixogum (Marabu) to retain moisture. Once the Fixogum had dried, the slide was placed into a clean petri dish with a damp piece of tissue and sealed with parafilm. These petri dishes were incubated overnight at 4°C. The following day, the Fixogum was removed from the slides and the cover slips replaced, cell side up, back into the 24 well, Standard, F, culture plate. The cover slips were then washed with 0.5mL PBS for 5 changes whilst rocking, each for a period of 5 minutes. A final wash was done with deionised water to remove any residual salt from the PBS. The secondary antibodies were then prepared according to table 3.

Table 3. Secondary antibodies used in fluorescent staining.

Stain	Company	Alexa Fluor	Cat. No.	Animal	Dilution
Ki67, RUNX2, 53BP1	ThermoFisher Scientific	AF488	A11055	Donkey anti-rabbit	1:800
Osterix	ThermoFisher Scientific	AF555	A21422	Goat anti-mouse	1:800

150µl of the diluted secondary antibody was added to each well. The plate was sealed with parafilm and incubated in the dark at 5% CO_2, 95% relative humidity and 37°C for one hour. After an hour the antibody was aspirated, and the coverslips were washed with 0.5mL PBS for 5 changes and a final wash was done with deionised water. The coverslips were then removed and placed cell side up on Whatman® 3M filter paper to air dry. It is important that they remain in the dark whilst air drying. 10µl of VECTASHIELD antifade mounting medium with DAPI was applied to each cover slip. Each coverslip was mounted onto a clean glass slide. Light pressure was applied to the coverslips using Whatman® 3M filter paper to remove any excess VECTASHIELD. The slides were then sealed with clear nail varnish and stored at 4°C until ready to be imaged using the Leica confocal microscope.

2.2.7 Western blotting

Prior to starting the western blot, the cells should be counted, as described in 2.2.4, and seeded into a standard 96 well, standard, F plate with a cell number of $1x10^4$. The cells were incubated overnight to ensure they've settled.

2.2.7.1 Lysing the cell

Reagents used:

2x lysis solution: 25mM Tris-HCl (pH7.6) + 150mM NaCl + 1% NP-40 + 1% sodium-deoxycholate + 0.1% SDS.

Protein lysis buffer stock: 5ml 2x lysis stock solution + 3ml 18MΩ H_20 + 500µl 5mM NaPPi + 100µl 10 mM NaF.

Protease inhibitor: 1 mini complete tablet + 1ml 18MΩ H_20 (7x solution).

Western blotting lysis buffer: 420 µl Protein lysis buffer stock + 71.4 µl protease inhibitor cocktail.

PBS: 1 phosphate buffered saline tablet per 100 ml 18MΩ H_20 (1x).

To lyse the cells ready for western blotting the media was aspirated from the wells and then the wells were rinsed twice in0 .5mL PBS. The PBS was removed, replaced with 30µl of lysis buffer containing protease inhibitor and then left the plate to stand on ice for three minutes. The lysates were then collected into 1.5mL microcentrifuge tubes and kept on ice whilst processing the rest of the samples. The samples were then sonicated four times for three seconds bursts each time using Soniprep 150 Ultrasonic Disinegrator at full power. These lysates were then centrifuged at 13,000 RPM, 4°C for 20 minutes.

2.2.7.2 Protein content quantification

The protein concentration of each sample was quantified using Quick Start™ Bradford Protein Assay. 5µl of each of the bovine serum albumin protein standards of known concentrations were added to a fresh 96 well, microtes plate, F (BSA: 0.1 mg/ml, 0.25 mg/ml, 0.5 mg/ml, 1.0 mg/ml, 1.5 mg/ml, 2.0 mg/ml) including a blank of lysis buffer. Each of the samples were diluted 1:5 in H_20 and 5µl of each sample was added to the 96 well, microtest, F plate. 250µl of Quick Start™ Bradford Reagent was added to each well and the plate incubated for 5 minutes in the dark. Using SoftMax Pro software, the plate could be read at an absorbance of 595nm using the Hidex Chameleon plate reader and SoftMax Pro 5.2 software. and the results used to calculate the appropriate dilutions for the western; the sample with the lowest protein sample was set as 100% and the high concentrations were diluted in lysis buffer in comparison to this concentration, ensuring a maximum loading volume of 20µl.

2.2.7.3 Running samples

5µl of 4X Sodium Dodecyl Sulfate (SDS) Sample buffer supplemented with DTT was added to each of the samples in 200µl PCR tubes and then denatured at 98°C for 5 minutes using the C100 Touch™ Thermal Cycler (BioRad). The samples were left on ice for two minutes and then centrifuged to reduce any condensation.

2.2.7.3.1 10 well precast gradient polyacrylamide gels (Novex NuPage)

These were running in Criterion™ running tanks (BioRad) using 500ml MOPS running buffer (25ml MOPS SDS (20X) + 475ml 18MΩ H_20). A maximum of 20µl was loaded per well and 7µl of Spectra Multicolor Broad Range Protein Ladder was loaded either side of the sample. The gel was run at 150V for ~1.5hours.

2.2.7.3.2 18 well precast gradient polyacrylamide gels

These were also running in Criterion™ running tanks (BioRad) using 500ml 1xTris-Glycine-SDS running buffer (30g Tris base, 144g Glycine 10g SDS + 1 litre H_20). A maximum of 30µl was loaded per well and 7µl of Spectra Multicolor Broad Range Protein Ladder was loaded either side of the sample. The gel was run at 120V for ~1 hour or 200#v for ~45 minutes.

2.2.7.4 Blotting

Once the gel had finished running the gel was transferred to Hybond ECL nitrocellulose membrane a blotting chamber filled with transfer buffer 1x Tris Glycine with 10% MetOH (100ml 10x Tris-Glycine buffer + 700ml H_20 + 200ml MetOH). Run at 100V for 50 minutes.

2.2.7.5 Blocking, incubation with antibodies and imaging

The membrane was blocked in the appropriate solution; either 5% milk in PBS-Tween (0.1%) or 5% BSA in PBS-Tween (0.1%) for 30 minutes on a rocker. Primary antibodies were diluted using the same blocking buffer to the appropriate dilution.

Table 4. Primary antibodies used in Western Btotting.

Band	Company	Product code	Animal	Dilution
RECQL4	Cell signalling	28145	Rabbit	1:500 in BSA
Tubulin alpha	Bio-Rad	MCA78G	Mouse	$1:10^4$ in milk

The membrane was sealed in plastic pockets along with the diluted primary antibodies and incubated rotating at 4°C overnight. The membrane was then removed from the plastic pocket and washed in an excess of PBS-0.1% Tween-20 buffer for 10 minutes whilst rocking. This step

was repeated three times. Secondary antibodies were diluted in the same blocking buffer to the appropriate dilution and incubated with the membrane for 1 hour at room temperature.

Table 5. Secondary antibodies used in western blotting.

Band	Company	Product code	Animal	Dilution
RECQL4	Promega	F00108	Anti-rabbit IgG (FC) AP conj.	1:5000 in BSA
Tubulin	Promega	F00109	Anti-mouse IgG (H+L) AP conj.	1:10000 in milk

After an hour the membrane was washed in PBS-0.1% Tween-20 buffer for 10 minutes whilst rocking. This was repeated four times. Amersham ECL Select Wester Blotting Detection Reagent was used with a 1:1 ratio of the luminol and peroxide solutions. The membranes were incubated in the dark and then developed using x50 Autoradiography film (GE Healthcare Amersham).

2.2.8 Growth assay

$1.5x10^3$ cells of each cell line being analysed were seeded into 96 well, standard, tissue culture plates as described in sections 2.2.1 and 2.2.4. One plate was analysed each day for 7 days using MTS/PMS solution to analyse the number of metabolically active cells. Both the MTS solution and the Phenazine methosulfate (PMS) solution were made up as per the manufacturer's instructions and aliquoted before needed then stored at -20°C. Immediately before use the solutions were thawed and 50µl of PMS solution was added to 1.0ml of MTS solution (MTS:PMA 1:20). 20µl of the combined MTS/PMS solution was pipetted into each well of the 96 well, standard, F plate. The plate was incubated for 1-4 hours at 37°C in a 95% humidified and 5% CO_2 atmosphere. The absorbance was read at 490nm using the Hidex Chameleon plate reader. This was repeated every 24hours for 7 days.

2.2.9 Drug sensitivity assay

To determine the sensitivity of each cell line to a variety of drugs, the cells were grown and $2x10^3$ were seeded into 96 well, standard, F, tissue culture plates as described in sections 2.2.1 and 2.2.4. The cells were left to settle overnight in 100µl of complete MesenPro RS^{TM}. The following day the MesenPro RS^{TM} was removed and were the treated with different concentrations of the chosen drug over a 6 day period. The drugs were diluted in MesenPro RS^{TM}. The media containing the drug was changed after 2-3 days. After 6 days an MTS assay was carried out on each plate as described in section 2.2.8.

2.2.10 Chromosome preparation

$3x10^5$ cells were seeded in 90cm petri dishes in 8mL of complete MesenPro RS™ and left to grow until around 70% confluent as described in 2.2.1 and 2.2.4. Once the appropriate confluency was reached, 80µl of 10µg/mL Demecolcine was added to each petri dish to arrest the cells in metaphase. The cells were incubated for 8 hours at 95% humidity, 37°C and 5% $C0_2$. During this time 75mM Potassium Chloride and Caranoy's fixative (Methanol and Glacial Acetic acid at a ratio of 3:1) was prepared ready for use in the following steps. After 8 hours the media was removed and collected into a 15mL conical centrifuge tube. The cells were then rinsed in 3mL pre-warmed PBS which was subsequently removed and put into the same conical centrifuge tube. 1mL of trypsin was added to each petri dish and incubated until the cells detached. The cells were collected from the petri dish using the media collected in the 15mL conical centrifuge tube. The plate was then rinsed one final time with PBS to collect any remaining cells and also put in the same 15mL conical centrifuge tube. Each conical centrifuge tube was centrifuged at 1.0K RPM for 5 minutes. Once centrifuged the supernatant was carefully removed and the cells washed with PBS. Each time a new solution was added the 15mL conical centrifuge tube was flicked to agitate the cells and re-suspend them. The tubes were centrifuged once more at 1.0K RPM for 5 minutes. The supernatant was removed once again and 7mL of warm 75mM Potassium Chloride solution was added dropwise to each tube to hypotonise cells. The tubes were incubated for 8 minutes in a 37°C water bath and then centrifuged at 1.0K RPM for 5 minutes. The supernatant was removed and 7mL of Caranoy's fixative mixed with PBS (1:1 ratio) was added dropwise to each tube. The tubes were further centrifuged at 1.2K RPM for 5 minutes. The cells were then fixed by the dropwise addition of 7mL Caranoy's fixative. The tubes were centrifuged at 1.2K RPM for 5 minutes. This addition of Caranoy's fixative was repeated once more and after a final centrifuge most of the supernatant was removed leaving only 0.5mL. The cells were re-suspended and stored at -20°C overnight. The following day the fixed cells were dropped onto slides and left to sit overnight.

2.2.10.1 Giemsa staining

The slides were rinsed for 5 minutes in PBS using a Coplin jar. These slides were then transferred into a Coplin jar containing 10% Giemsa staining solution (Gurr®, in *Stain*Rite® Wright-Giemsa stain phosphate buffer pH 6.8) for ~1 hour. The slides were then transferred to a final Coplin jar and washed three times with distilled water. The slides could then be imaged under a Nikon Eclipse 80i Fluorescence Microscope in transmitted light. Images were taken of the chromosomes and the number of chromosomes present were counted.

3 Results

The following section presents the data and images collected from the experiments carried out during this project.

3.1 Verification of RECQL4 depletion by western blot

In order to study the effect of RECQL4 depletion in ASC cells, two shRNA constructs (shRQ-9 and shRQ-10) were previously built in the pLKO.1 vector in our laboratory as part of a PhD project. Fourth generation lentiviral particles were generated in 293T cells and the viral particles were used to transduce low passage as well as high passage ASC52telo cells by Dr Timea Palmai-Pallag. I continued the work with the characterisation of the resulting cell lines.

A western blot was performed to determine whether RECQL4 was adequately depleted by the Lentiviral shRNA construct. The RECQL4 protein is 150kDa in size and a band at this mark is only expected to be seen for P14 pLKO.1 and p44 pLKO.1

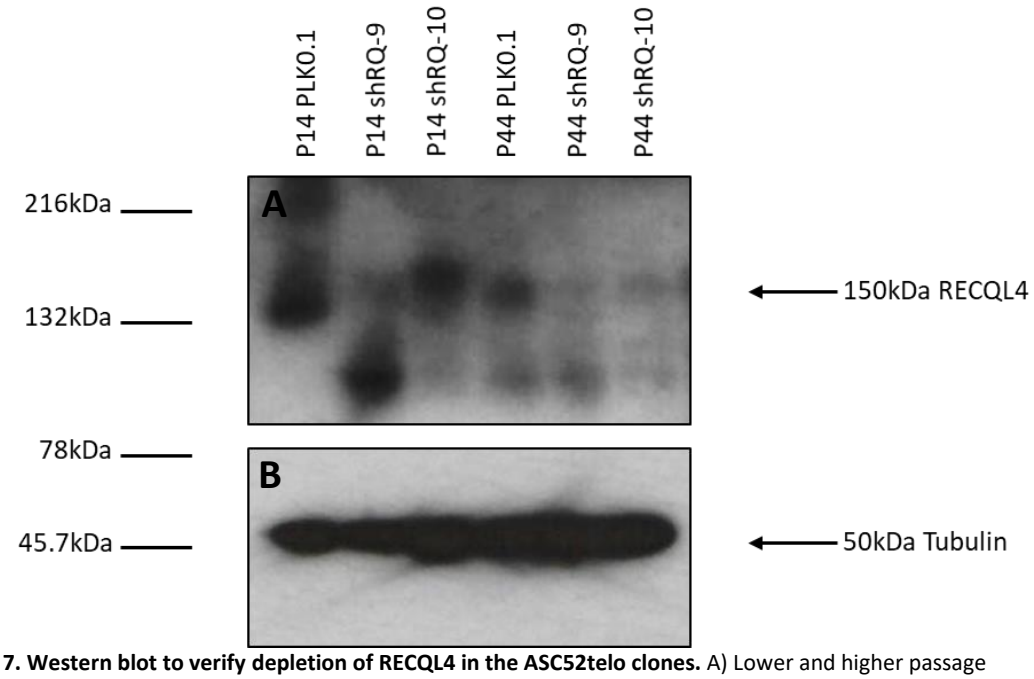

Figure 7. Western blot to verify depletion of RECQL4 in the ASC52telo clones. A) Lower and higher passage knockdowns and their pLKO.1 controls probed for RECQL4 protein levels. B) Tubulin controls of each sample to control equal loading.

A clear western blot was not obtained, and a high background can be seen. However, the band for P44 shRQ-9 and P44 shRQ-10 is a lot weaker in intensity than for any of the other cell lines. The control samples have a visibly stronger band. β-Tubulin was used as loading control to give a visualisation of whether equal amounts of protein from each sample were loaded.

3.2 Assaying Differentiation capability

In order to assess if suppression of *RECQL4* expression impacts differentiation capability of our adipose-derived stem cells their trilineage differentiation capacity was tested with standard methods.

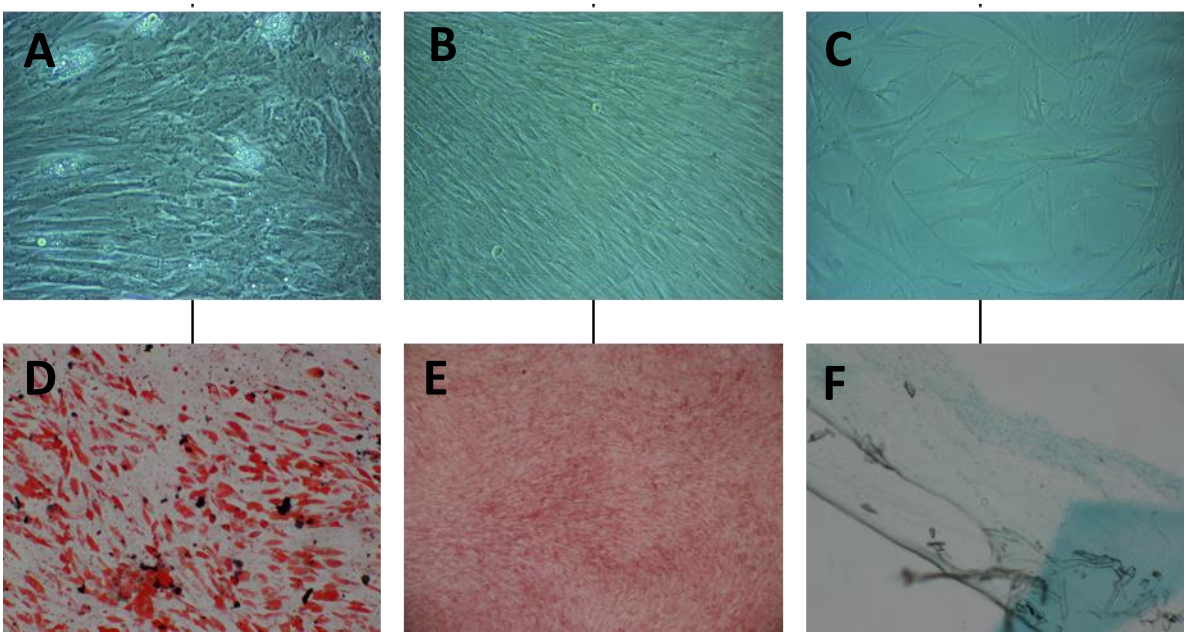

Figure 8. Trilineage potential of ASC52telo cells. Differentiation capability of ASC52telo cells into adipocytes, osteocytes and chondrocytes after 10 and 21 days. A) adipocyte differentiation after 10 days (x40), B) osteocyte differentiation after 10 days (x40), C) chondrocyte differentiation after 10 days (x40), D) adipocyte differentiation stained with oil red O after 21 days (x40), E) osteocyte differentiation stained with Alizarin Red after 21 days (x100) and F) chondrocyte differentiation stained with Alcian Blue after 21 days (x40).

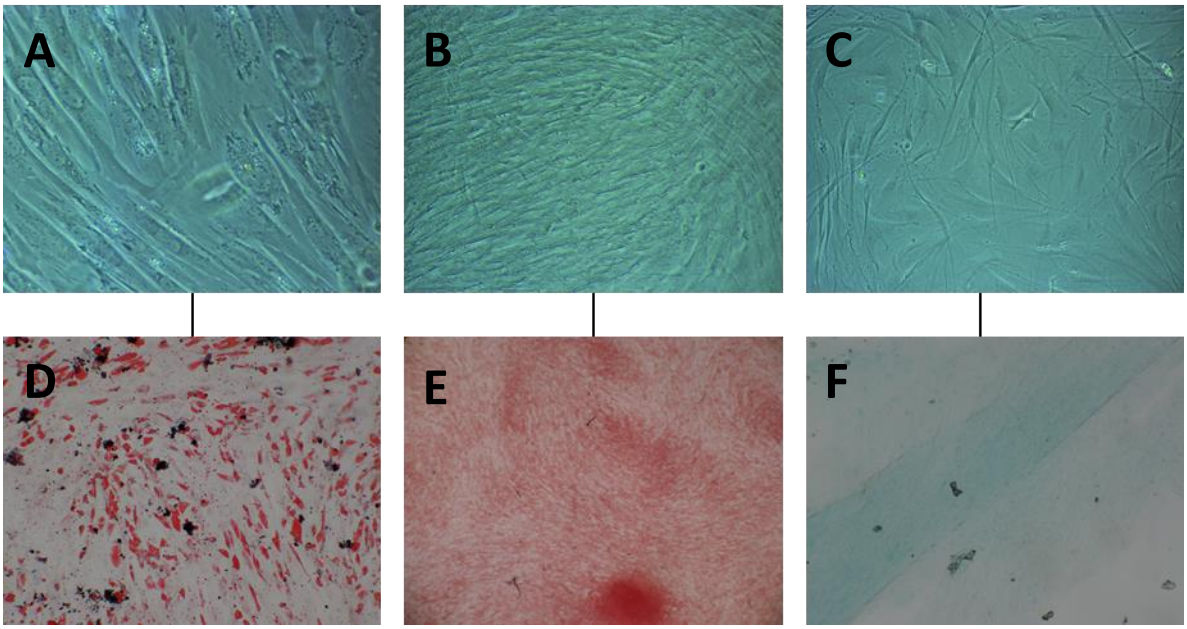

Figure 9. Trilineage potential of P14 pLK0.1. Differentiation capability of P14 pLK0.1 cells into adipocytes, osteocytes and chondrocytes after 10 and 21 days. A) adipocyte differentiation after 10 days (x40), B) osteocyte differentiation after 10 days (x40), C) chondrocyte differentiation after 10 days (x40), D) adipocyte differentiation stained with oil red O after 21 days (x40), E) osteocyte differentiation stained with Alizarin Red after 21 days (x100) and F) chondrocyte differentiation stained with Alcian Blue after 21 days (x40).

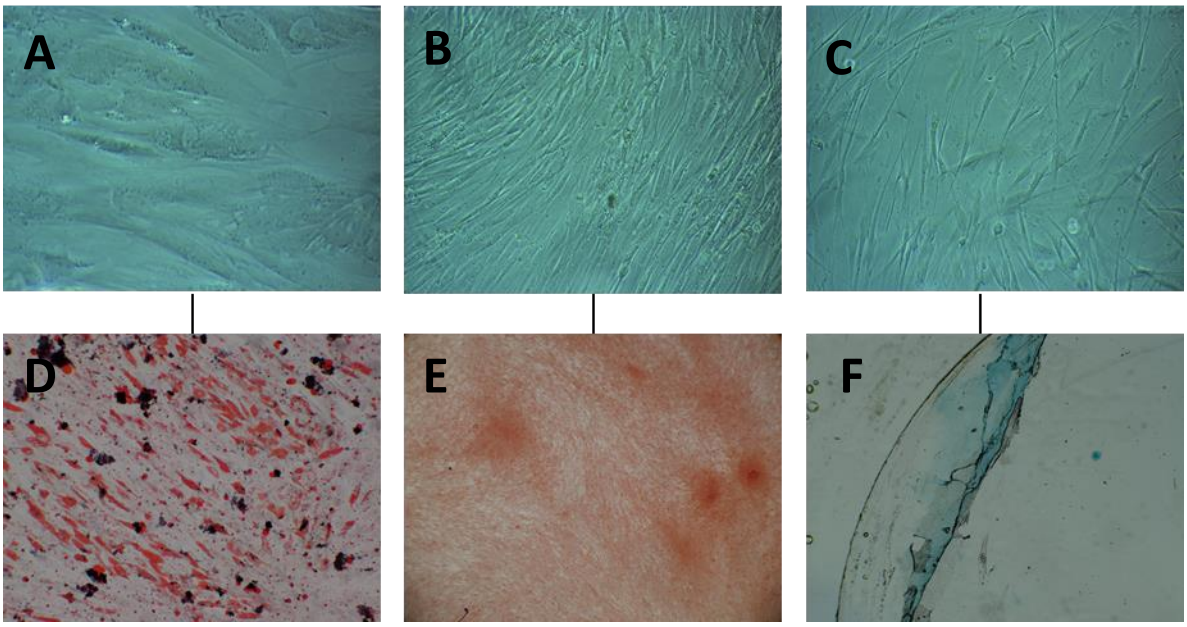

Figure 10. Trilineage potential of P14 shRQ-9. Differentiation capability of P14 shRQ-9 into adipocytes, osteocytes and chondrocytes after 10 and 21 days. A) adipocyte differentiation after 10 days (x40), B) osteocyte differentiation after 10 days (x40), C) chondrocyte differentiation after 10 days (x40), D) adipocyte differentiation stained with oil red O after 21 days (x40), E) osteocyte differentiation stained with Alizarin Red after 21 days (x100) and F) chondrocyte differentiation stained with Alcian Blue after 21 days (x40).

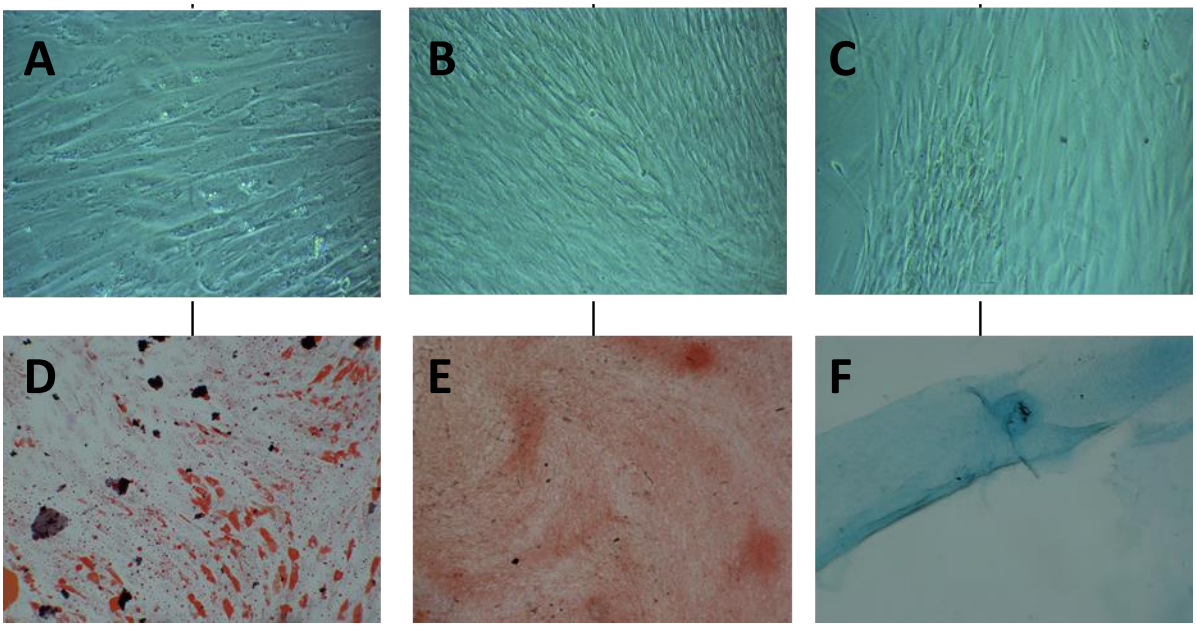

Figure 11. Trilineage potential of P14 shRQ-10. Differentiation capability of P14 shRQ-10 into adipocytes, osteocytes and chondrocytes after 10 and 21 days. A) adipocyte differentiation after 10 days (x40), B) osteocyte differentiation after 10 days (x40), C) chondrocyte differentiation after 10 days (x40), D) adipocyte differentiation stained with oil red O after 21 days (x40), E) osteocyte differentiation stained with Alizarin Red after 21 days (x100) and F) chondrocyte differentiation stained with Alcian Blue after 21 days (x40).

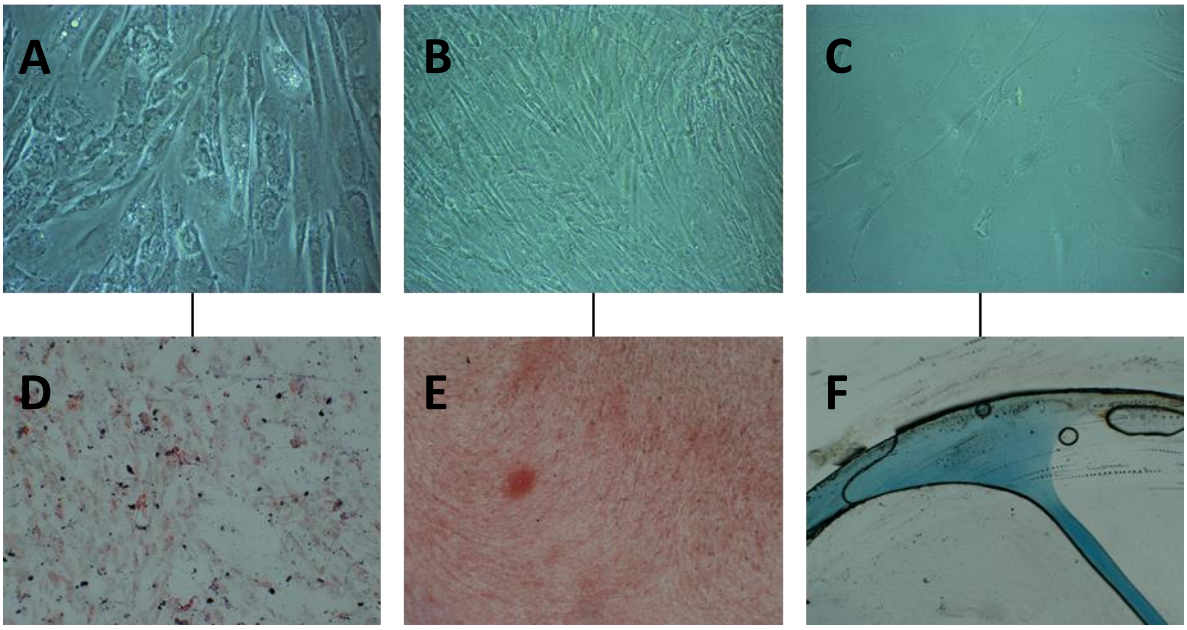

Figure 12. Trilineage potential of P44 pLK0.1. Differentiation capability of P44 pLK0.1 into adipocytes, osteocytes and chondrocytes after 10 and 21 days. A) adipocyte differentiation after 10 days (x40), B) osteocyte differentiation after 10 days (x40), C) chondrocyte differentiation after 10 days (x40), D) adipocyte differentiation stained with oil red O after 21 days (x40), E) osteocyte differentiation stained with Alizarin Red after 21 days (x100) and F) chondrocyte differentiation stained with Alcian Blue after 21 days (x40).

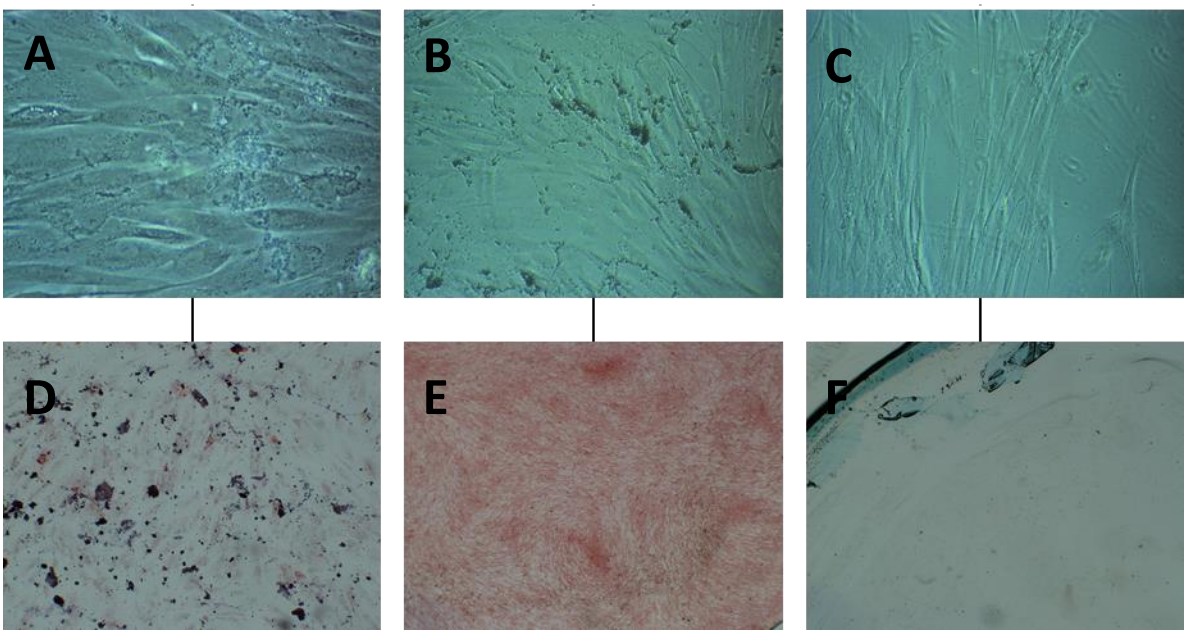

Figure 13. Trilineage potential of P44 shRQ-9. Differentiation capability of P44 shRQ-9 into adipocytes, osteocytes and chondrocytes after 10 and 21 days. A) adipocyte differentiation after 10 days (x40), B) osteocyte differentiation after 10 days (x40), C) chondrocyte differentiation after 10 days (x40), D) adipocyte differentiation stained with oil red O after 21 days (x40), E) osteocyte differentiation stained with Alizarin Red after 21 days (x100) and F) chondrocyte differentiation stained with Alcian Blue after 21 days (x40).

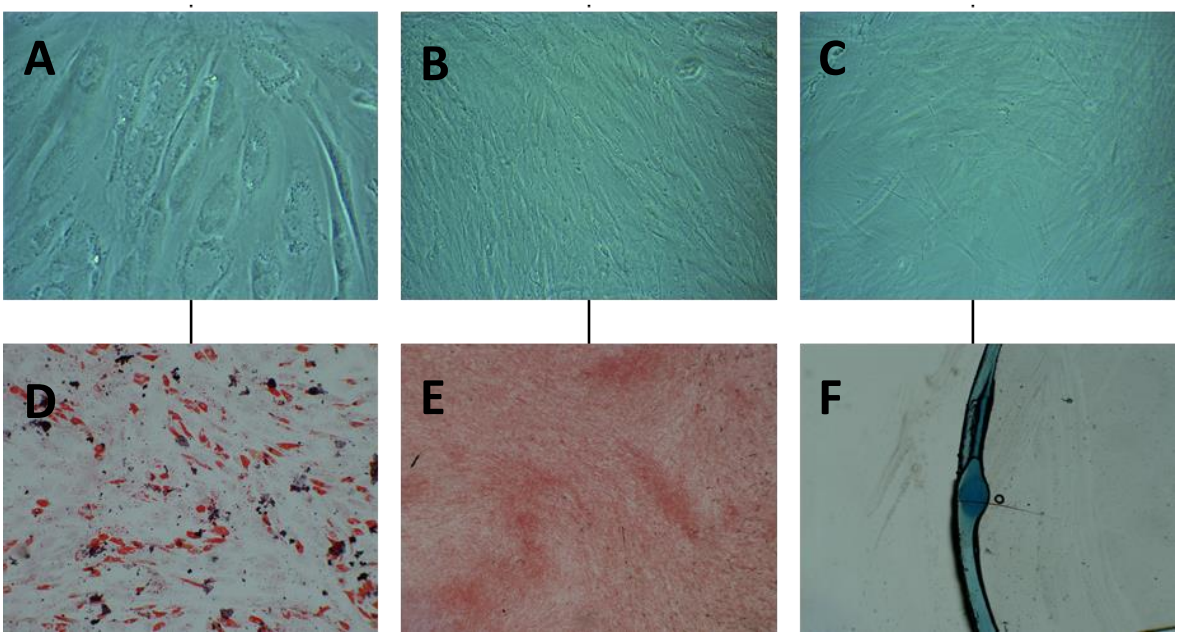

Figure 14. Trilineage potential of P44 shRQ-10. Differentiation capability of P44 shRQ-10 into adipocytes, osteocytes and chondrocytes after 10 and 21 days. A) adipocyte differentiation after 10 days (x40), B) osteocyte differentiation after 10 days (x40), C) chondrocyte differentiation after 10 days (x40), D) adipocyte differentiation stained with oil red O after 21 days (x40), E) osteocyte differentiation stained with Alizarin Red after 21 days (x100) and F) chondrocyte differentiation stained with Alcian Blue after 21 days (x40).

The ASC52Telo cells, *RECQL4* knockdowns and their controls were treated for 21 days with adipogenesis, osteogenesis and chondrogenesis media, to establish whether all the cell lines still have the trilineage differentiation potential found in normal MSCs. All cell lines differentiated into adipocytes, shown by the presence of lipid vacuoles, and osteoblasts, shown by the presence of Alizarin red stained calcified extracellular matrix, but we had difficulties with chondrogenic differentiation due to the loss of cells and detachment of the monolayer. The higher passage PLK0.1 and shRQ-9 cells appear to have a decreased adipocyte differentiation in comparison to the lower passage cells.

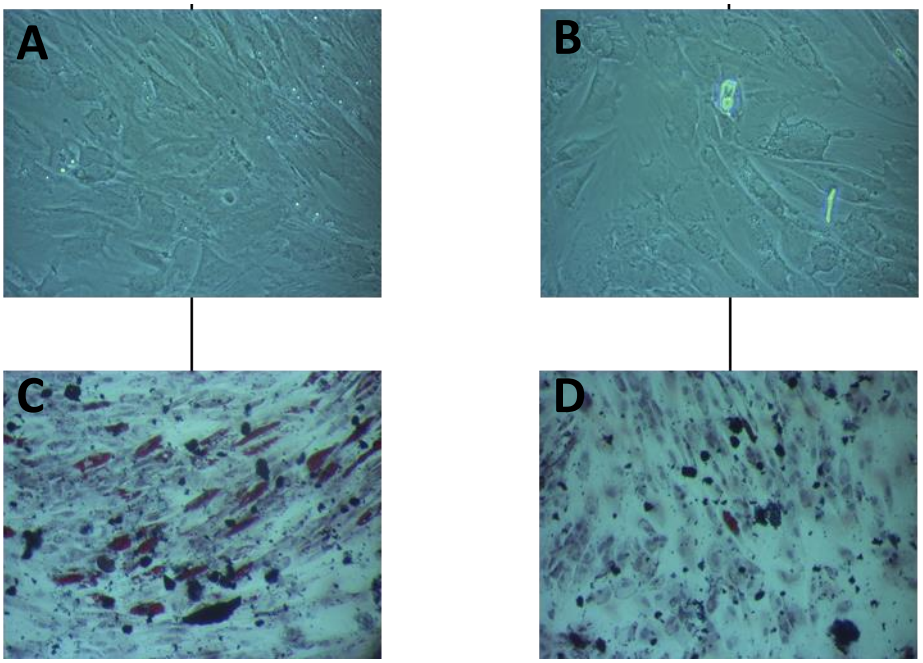

Figure 15. Adipogenesis potential of OD and OD+PHA cell lines. OD and OD+PHA cells after 10 days and 21 days culturing with adipogenesis media. A) OD cells after 10 days culturing in adipogenesis media (x40), B) OD+PHA cells after 10 days culturing in adipogenesis media (x40), C) OD cells after 21 days culturing in adipogenesis media (x40), D) OD+PHA cells after 21 days culturing in adipogenesis media (x40).

As the first step to characterise the cultures that were recovered from long term osteogenic differentiation, we wanted to show if this culture still contains cells that are capable to differentiated into directions other than osteoblasts. OD and OD+PHA cells were treated for 21 days with adipogenesis media to see if any differentiation occurs. Both cell lines show the presence of lipid vacuoles, with the PHA-767491 treated OD cells displaying a lower number in comparison to the untreated OD cells. However, their overall morphology and the extent of adipogenic differentiation is different to what was observed using ASC52telo cells.

3.3 Growth assay

We also wanted to assess whether there was a difference in the growth characteristics of cells in which RECQL4 was depleted, or replication initiation was disturbed during osteogenic differentiation. Seven plates were set up for each cell line and an MTT assay carried out on a plate each day. This allowed us to plot the growth of the cell lines over a period of 7 days.

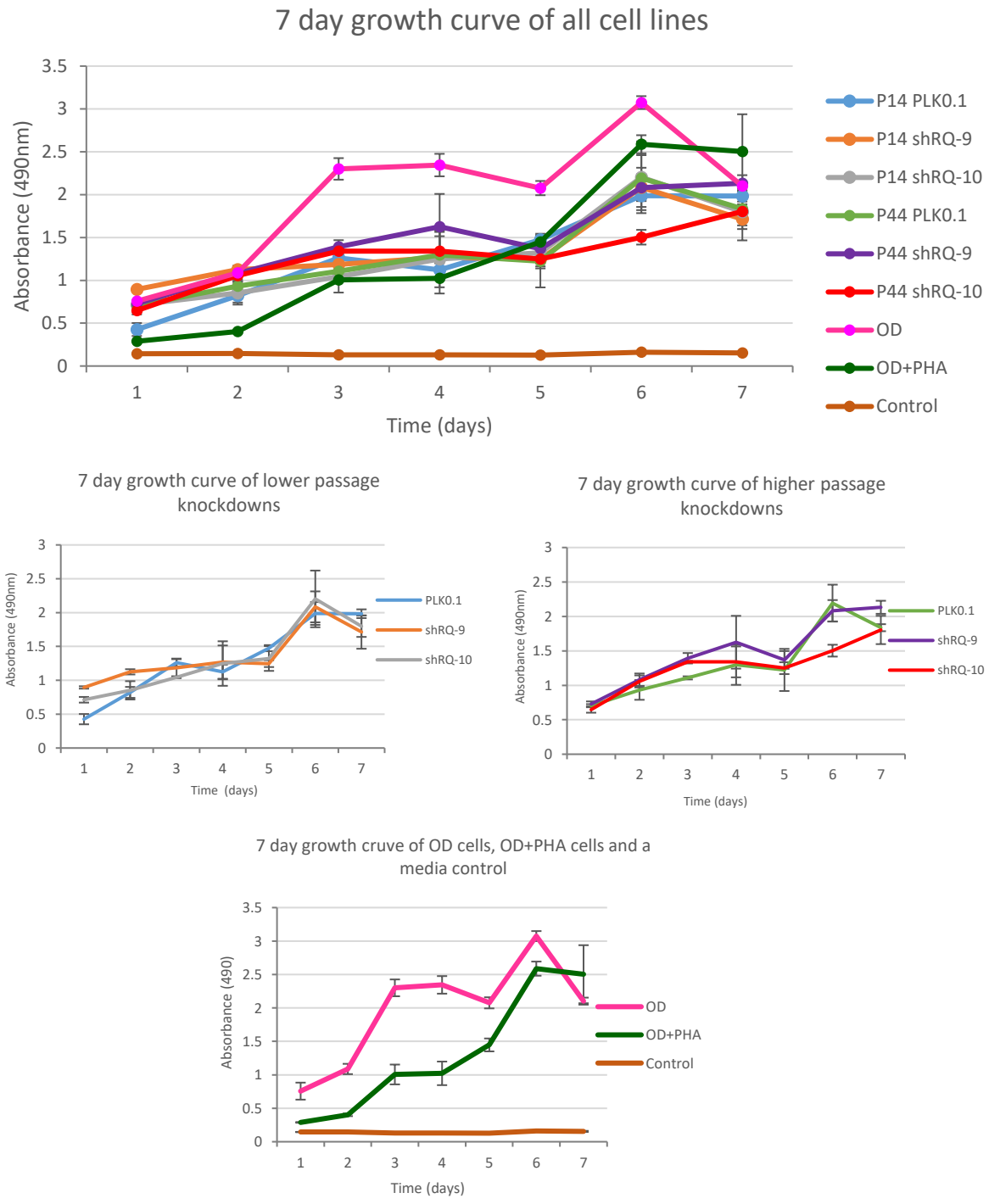

Figure 16. Growth curves of all the knockdowns, their controls, OD cells and OD+PHA cells.

No significant difference was observed between the cells in which RECQL4 was knocked down and their controls. Cells that were recovered from osteoblastic differentiation (OD cells) have the quickest cell proliferation rate and for the first four days, the OD cells treated with PHA-767491, to interfere with replication initiation, proliferate at half the rate of the untreated OD cells.

3.4 Immunofluorescence staining

Immunofluorescence staining was carried out on the knockdowns, OD cells and OD+PHA cells to identify any differences in 53BP1, Ki67, RUNX2 and Osterix expression.

3.4.1 53BP1 staining

53BP1 is essential in maintaining genome stability and is an important mediator of DNA damage checkpoint. Abnormal expressions of 53BP1 have been linked with tumour prevalence and development (Bi *et al*., 2015).

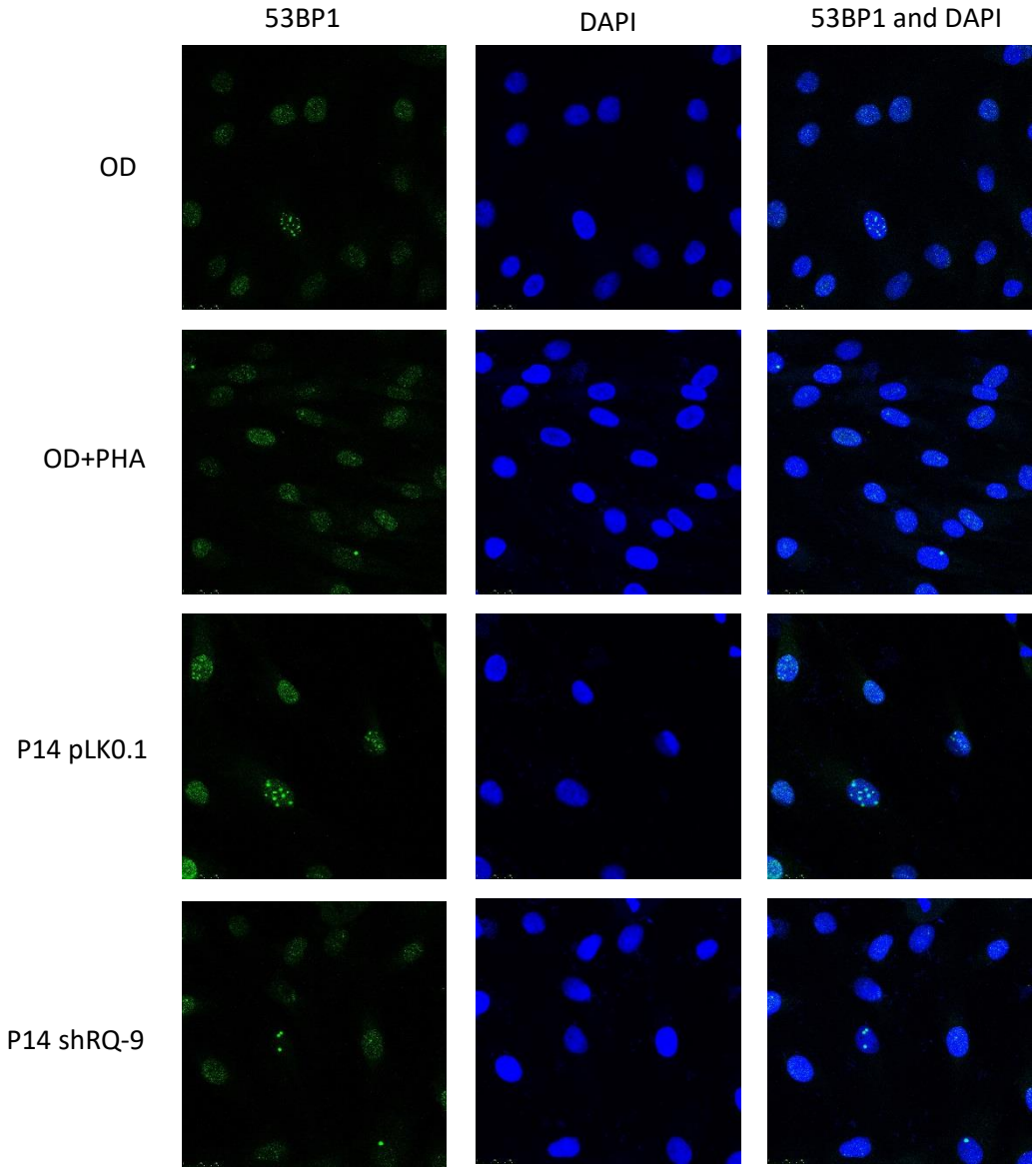

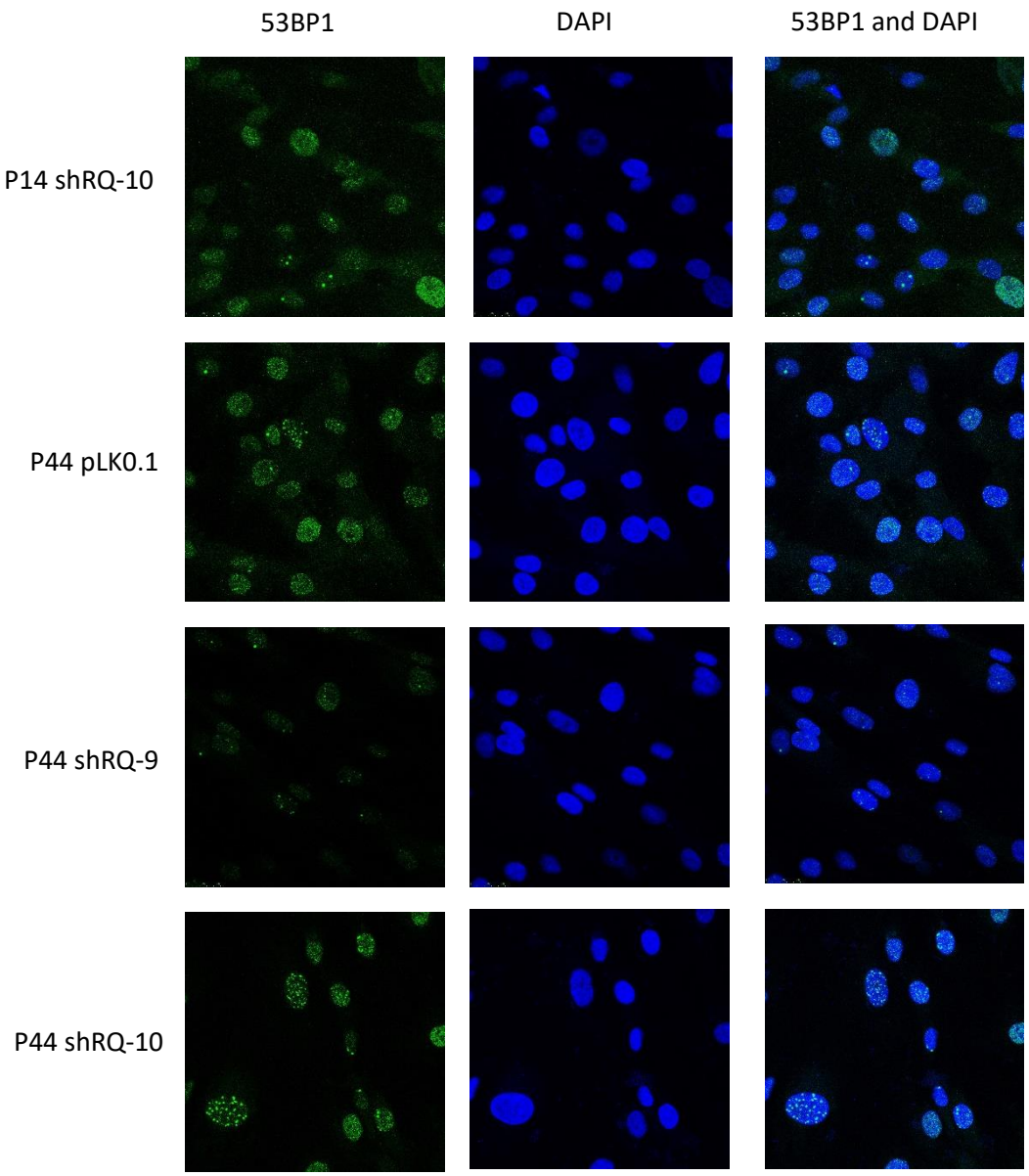

Figure 17. Immunofluorescence images of each cell line stained with DAPi (blue) and 53BP1 (green).

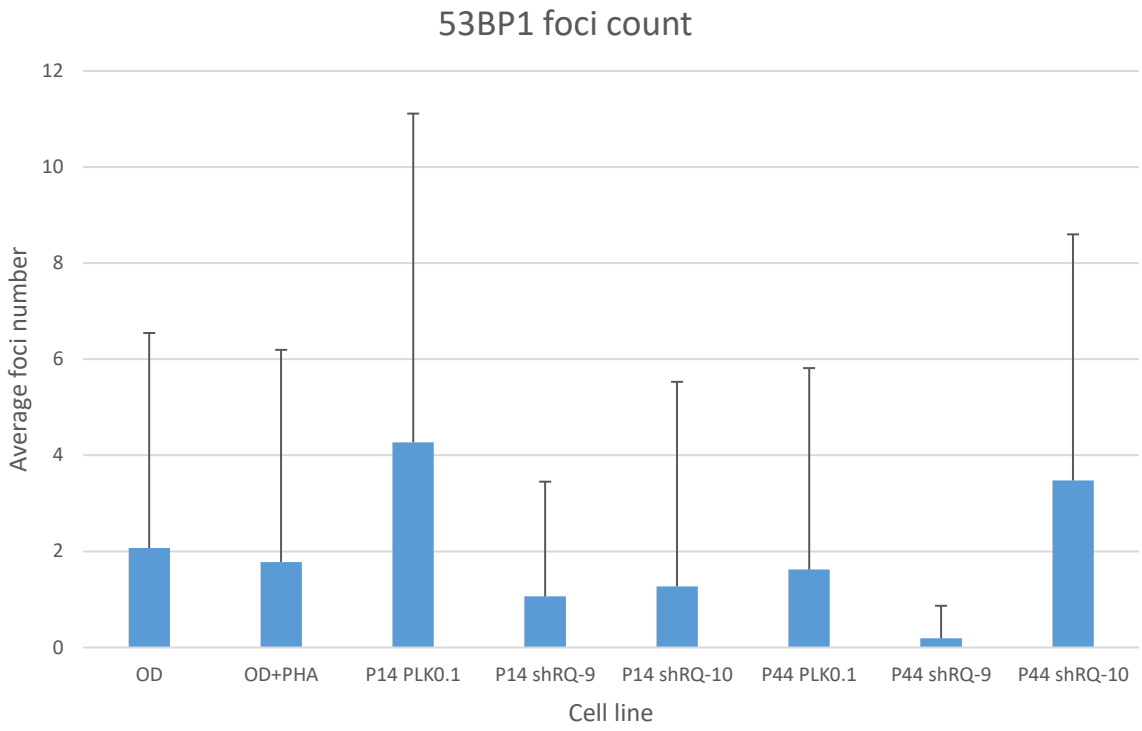

Figure 18. The average foci count of each cell line when stained to show 53BP1 expression. The confocal images were analysed using cell profiler which provided the number of foci counted per cell. The average could then be calculated.

The results show a lower average foci number in P44 shRQ-9 cells particularly in comparison to the rest, and P14 PLK0.1 and P44 shRQ-10 show a higher count. There are no significant differences between the cell lines.

3.4.2 Ki67 staining

Ki67 protein expression is associated with cell proliferation. It can be detected during all active phases of the cell cycle, but is absent in G0 phase (resting cells) (Scholzen and Gerdes, 2000).

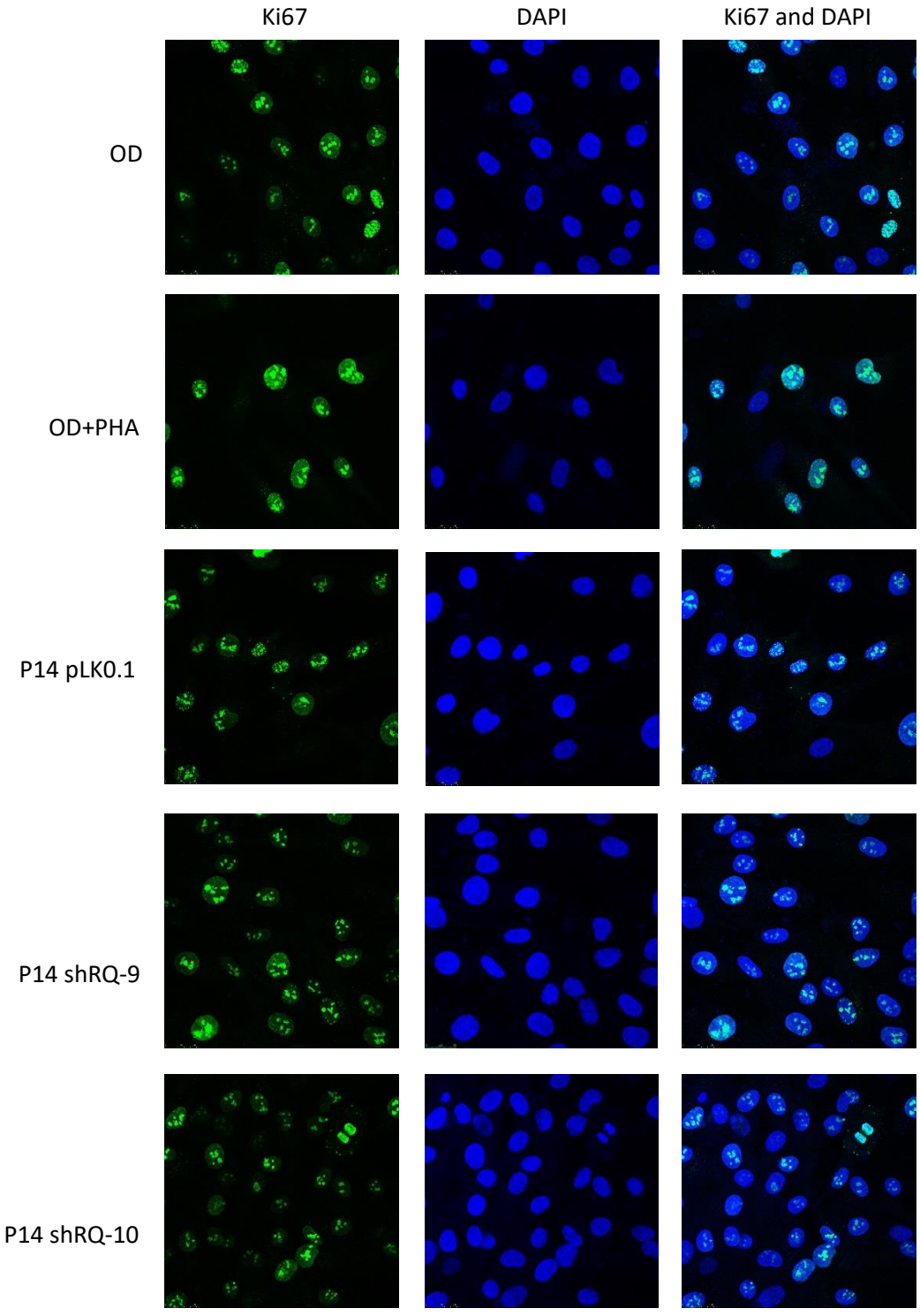

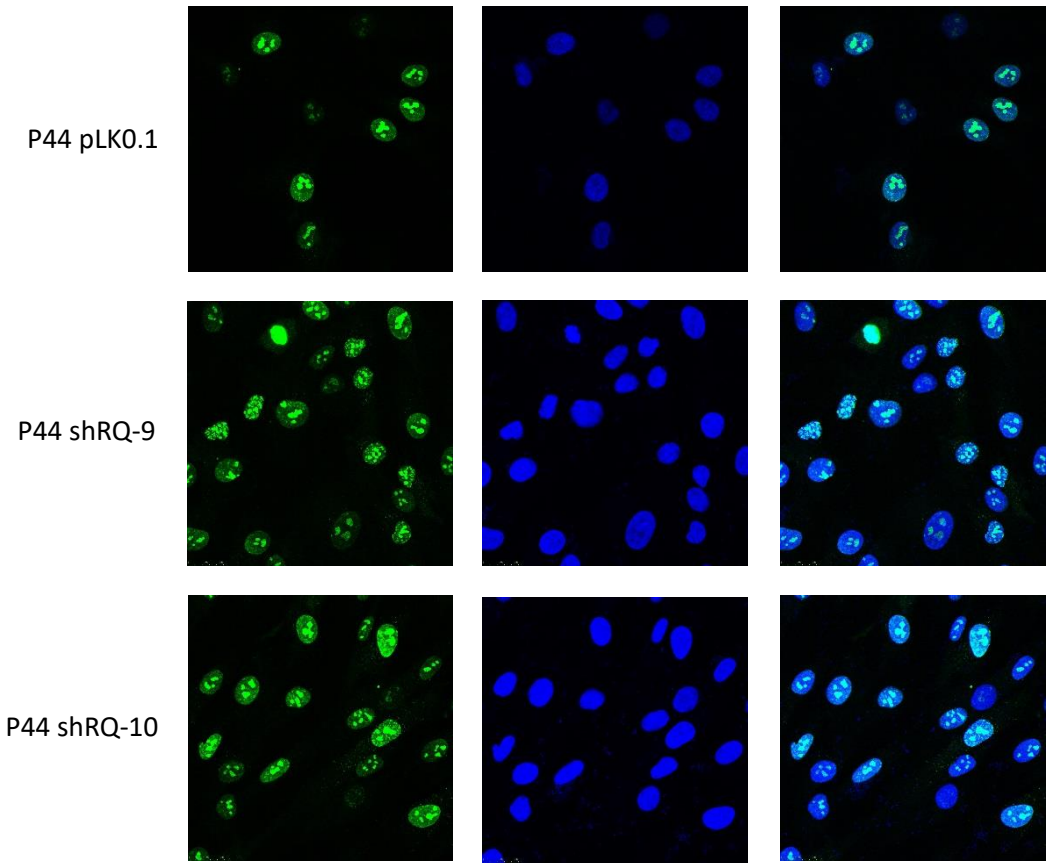

Figure 19. Immunofluorescence images of each cell line stained with DAPI (blue) and Ki67 (green).

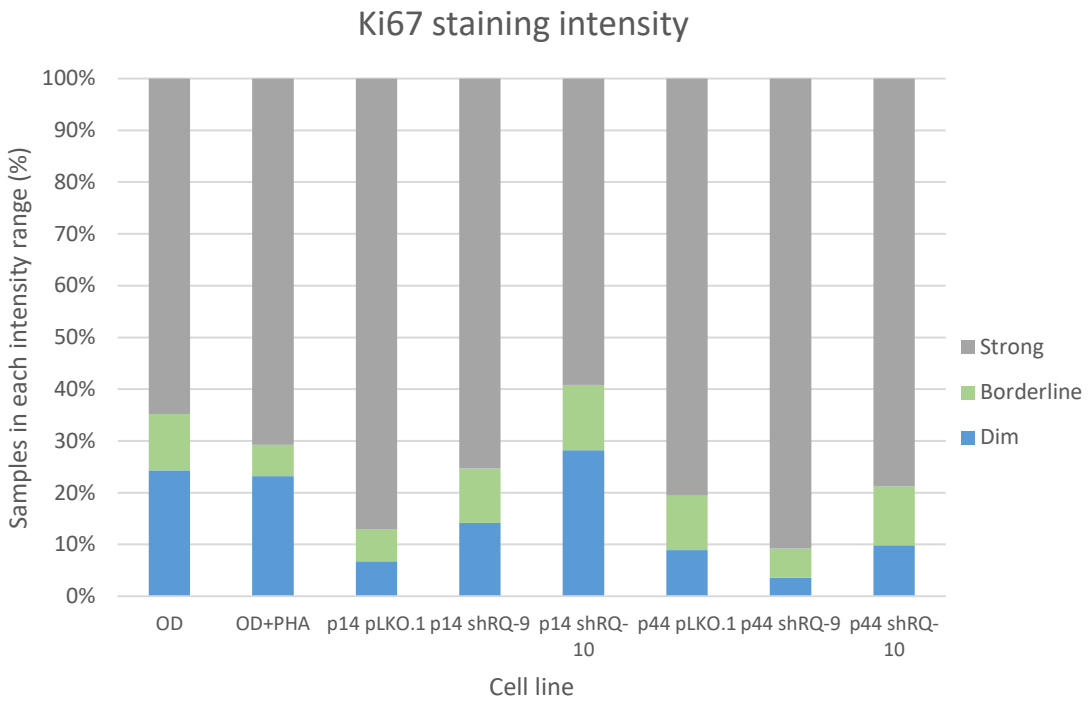

Figure 20. The Ki67 staining intensity of each cell line group into dim, borderline and strong intensities. The confocal images were analysed using cell profiler which provided the number of foci counted per cell. The average could then be calculated.

Intensity of the KI67 signal was quantified with CellProfiler and cells were categorised as 'strong' and actively proliferating, and 'dim' as resting cells. A third category was established and characterised by a small number of cells which cannot be convincingly put in either of the two categories; these cells are likely in the process of exiting cycling. At least 60% of the intensity results for each cell line are in the strong category, suggesting all the cell lines contain a considerable proportion of proliferating cells. The P14 shRQ-10 cells have the lowest proportion of intensities in the strong category out of all the cell lines, suggesting that this cell line is the least actively proliferating.

3.4.3 RUNX2 and Osterix staining

RUNX2 and Osterix are transcription factors that play an essential role in bone formation and osteoblast differentiation (Martin *et al*., 2011). RUNX2 is expressed in mesenchymal stem cells and during early osteoblast differentiation (Martin *et al*., 2011), while Osterix expression is characteristic to osteoblasts.

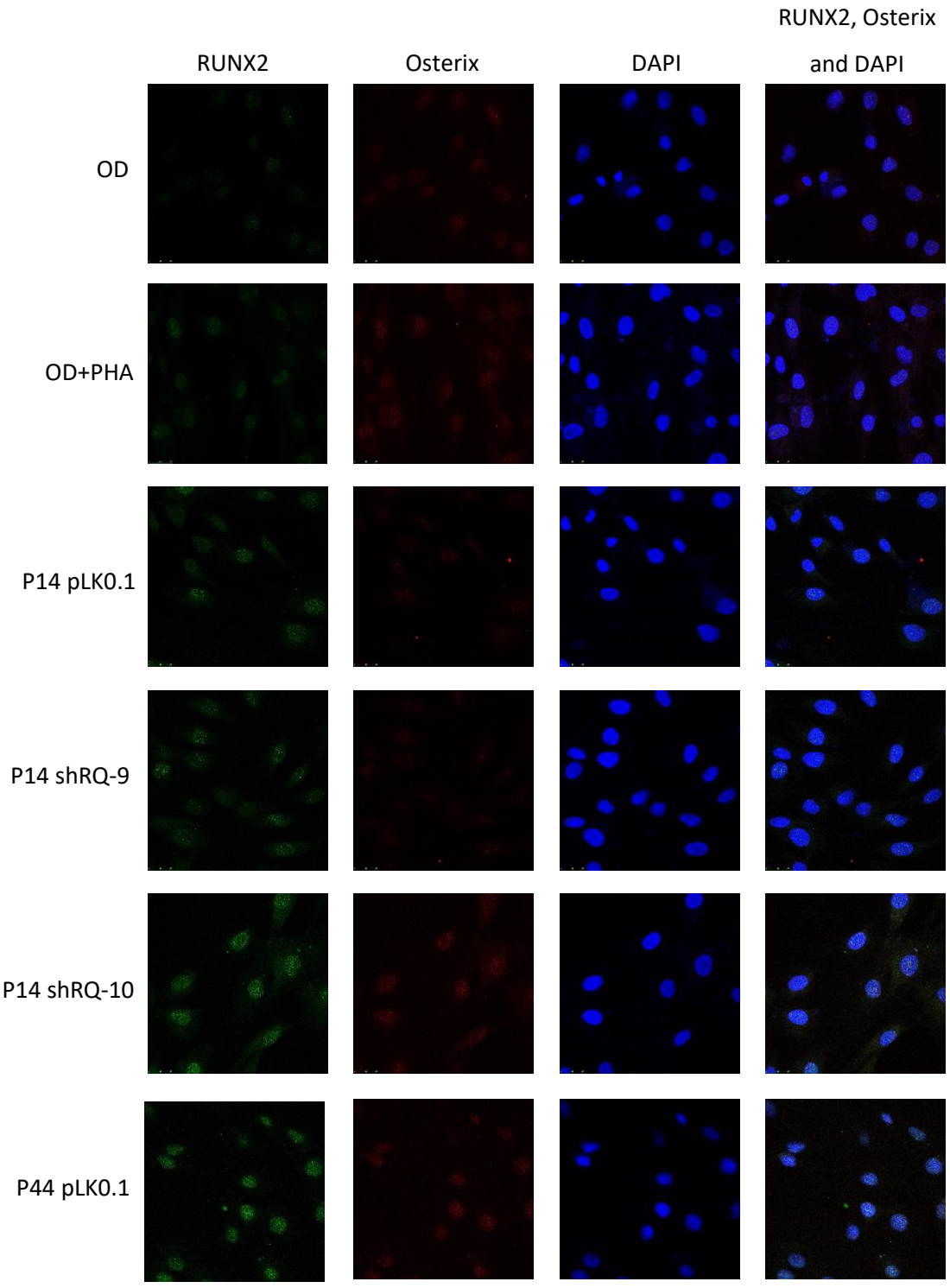

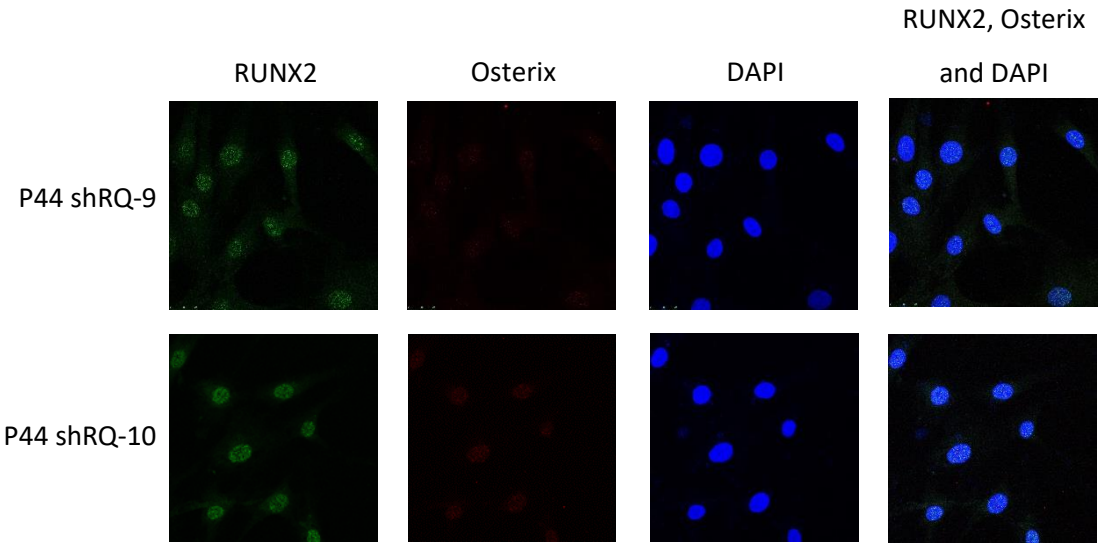

Figure 22. Immunofluorescence staining of each cell line with DAPI (blue), RUNX2 (green) and Osterix (red).

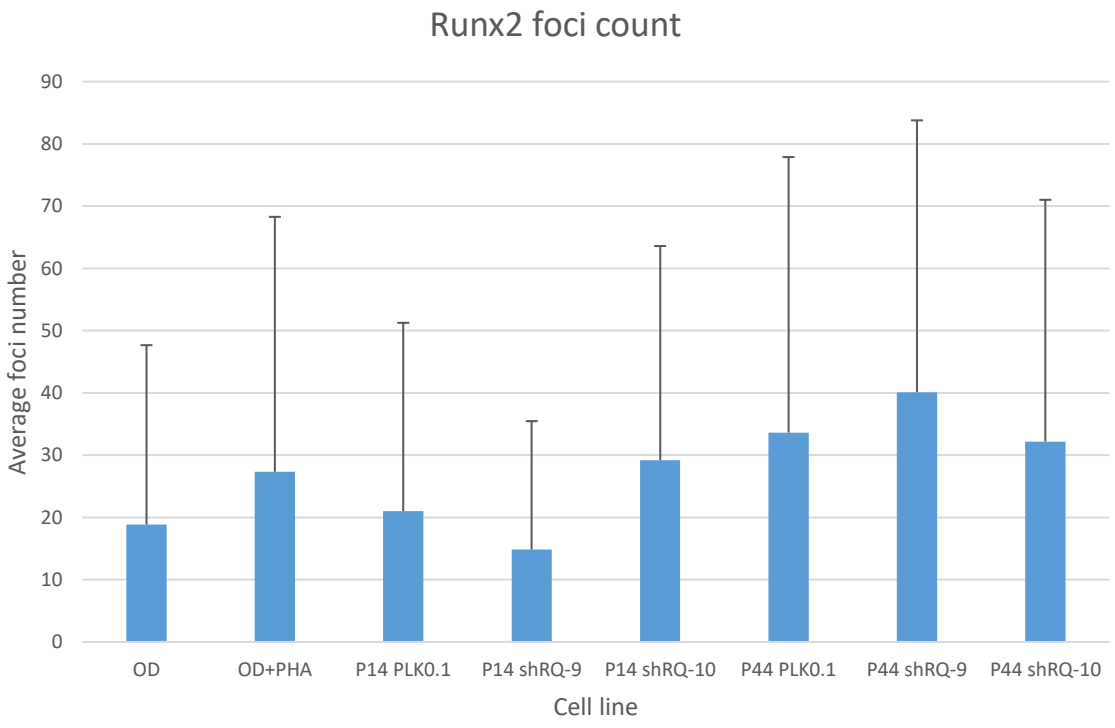

Figure 21. A graph to show the average foci count of each cell line when stained to show RUNX2 expression. The confocal images were analysed using cell profiler which provided the number of foci counted per cell. The average could then be calculated.

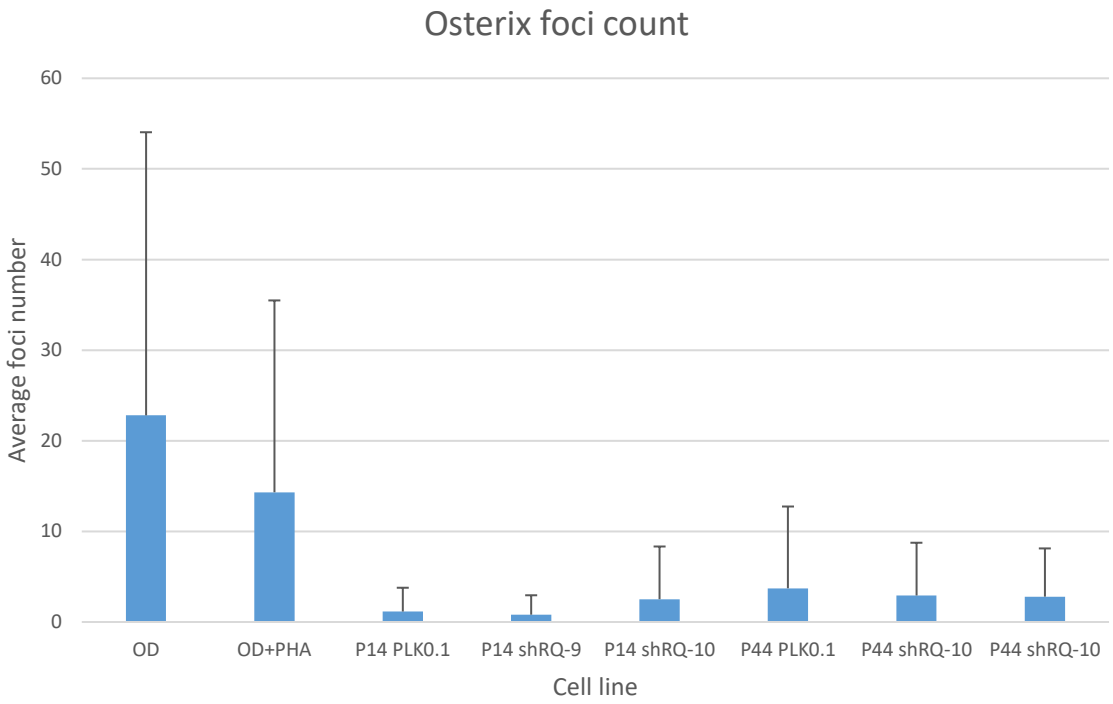

Figure 23. A graph to show the average foci count of each cell line when stained to show Osterix expression. The confocal images were analysed using cell profiler which provided the number of foci counted per cell. The average could then be calculated.

The RUNX2 average foci count results show a higher count in the p44 knockdowns than the rest of the cell lines. The OD cells have the second lowest count which is expected as these cells contain a large proportion of fully differentiated osteoblasts, and a population of undifferentiated MSCs that are still RUNX2 positive. The Osterix foci count shows results that we would expect to see from these cell lines. The average foci count is much higher in the two osteo-differentiated cell lines compared to the six knockdowns. The osteo-differentiated cells treated with PHA-767491 display a lower Osterix expression, suggesting a slower osteoblast differentiation rate.

3.5 Drug sensitivity assays

The literature reports contradictory results of sensitivity of cells mutated in RECQL4. We wanted to know how depletion of RECQL4 in ASC cells affects their sensitivity to drugs that induce DNA damage.

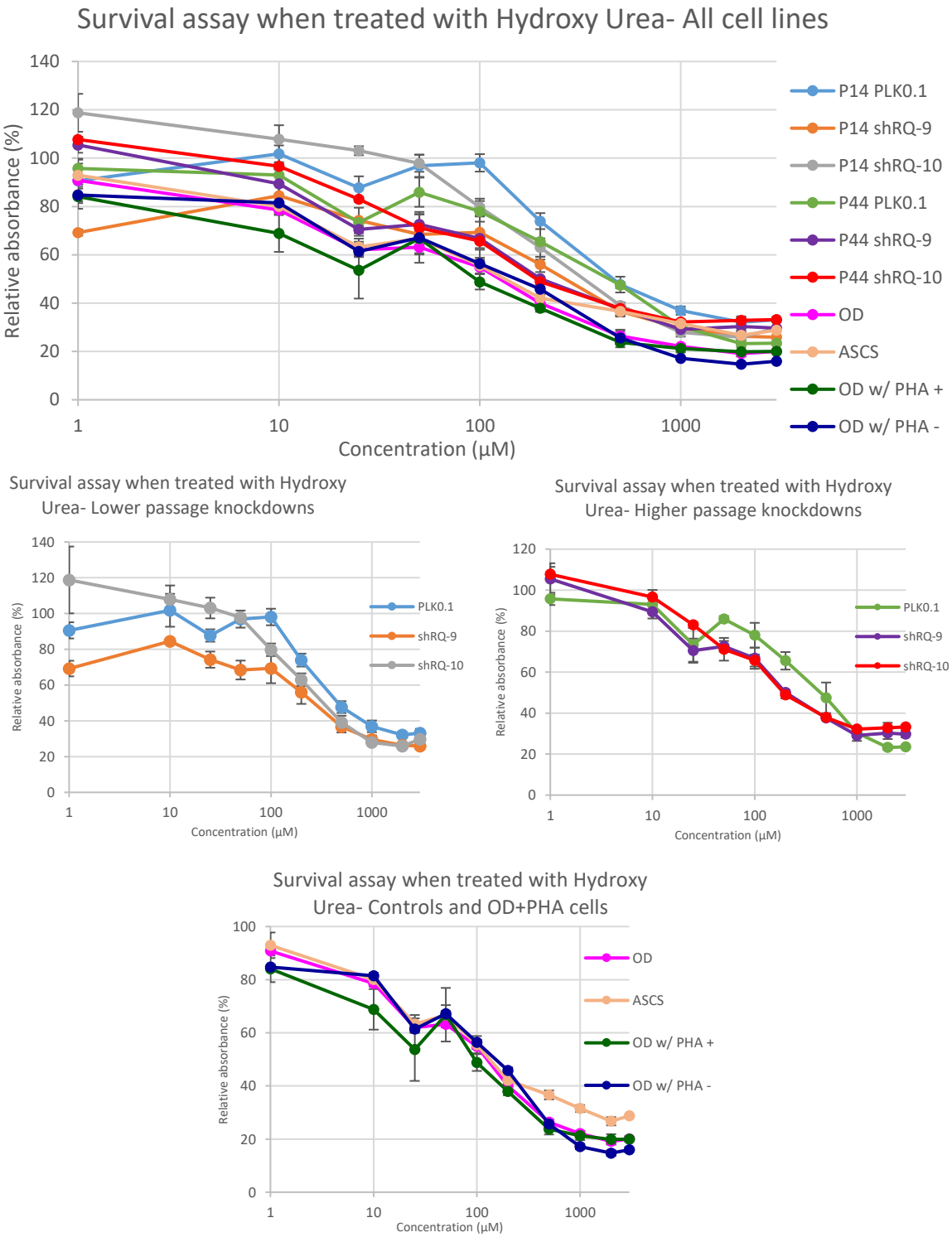

Figure 24. Survival assays for the treatment of the knockdowns, their controls, ASC52Telo cells, OD cells, OD+PHA cells+ (PHA present) and OD+PHA cells- (PHA not present) with Hydroxy Urea for a period of 7 days. Logarithmic scale, base 10.

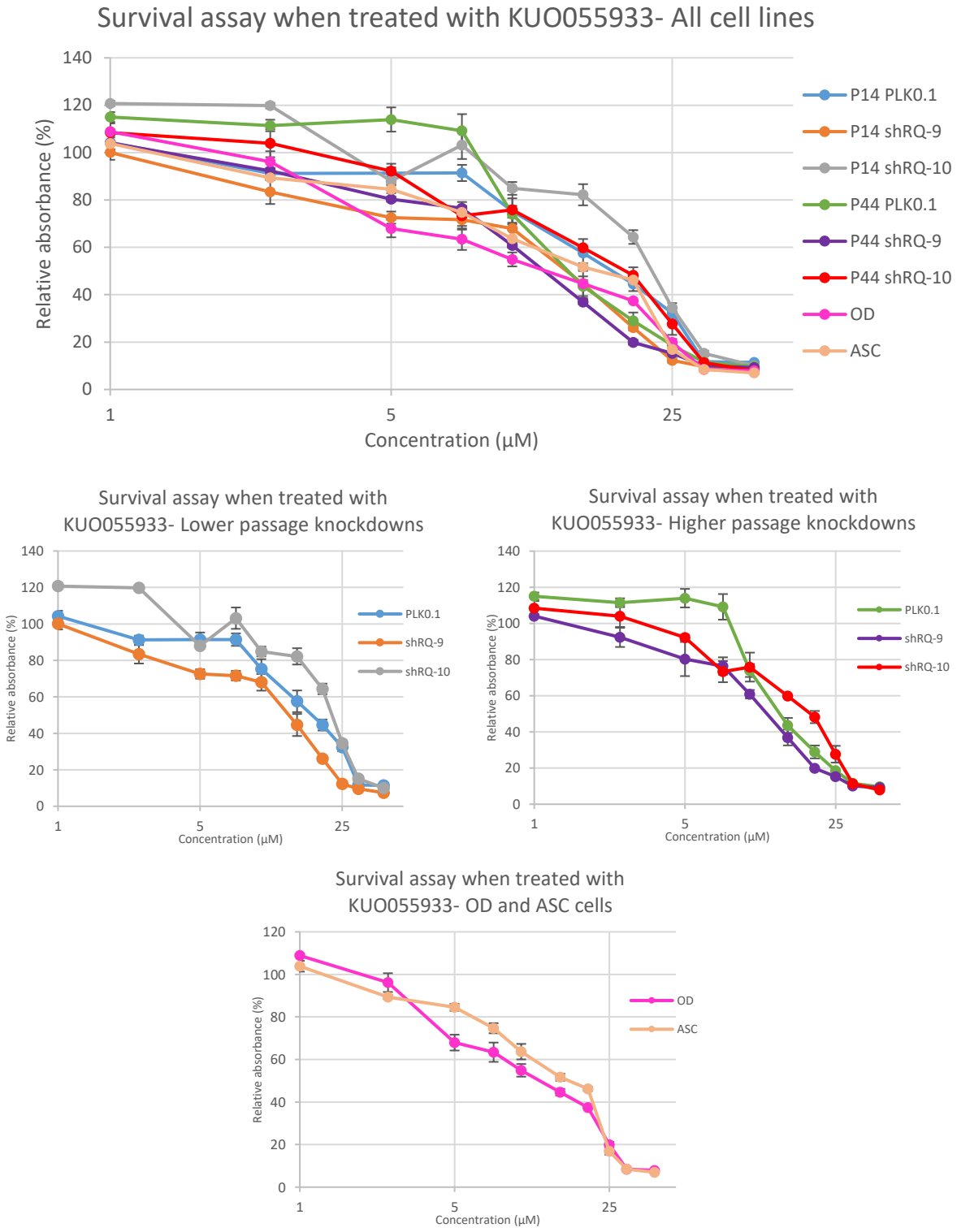

Figure 25. Survival assays for the treatment of the knockdowns, their controls, ASC52Telo cells and OD cells with KUO055933 for a period of 7 days. Logarithmic scale, base 5.

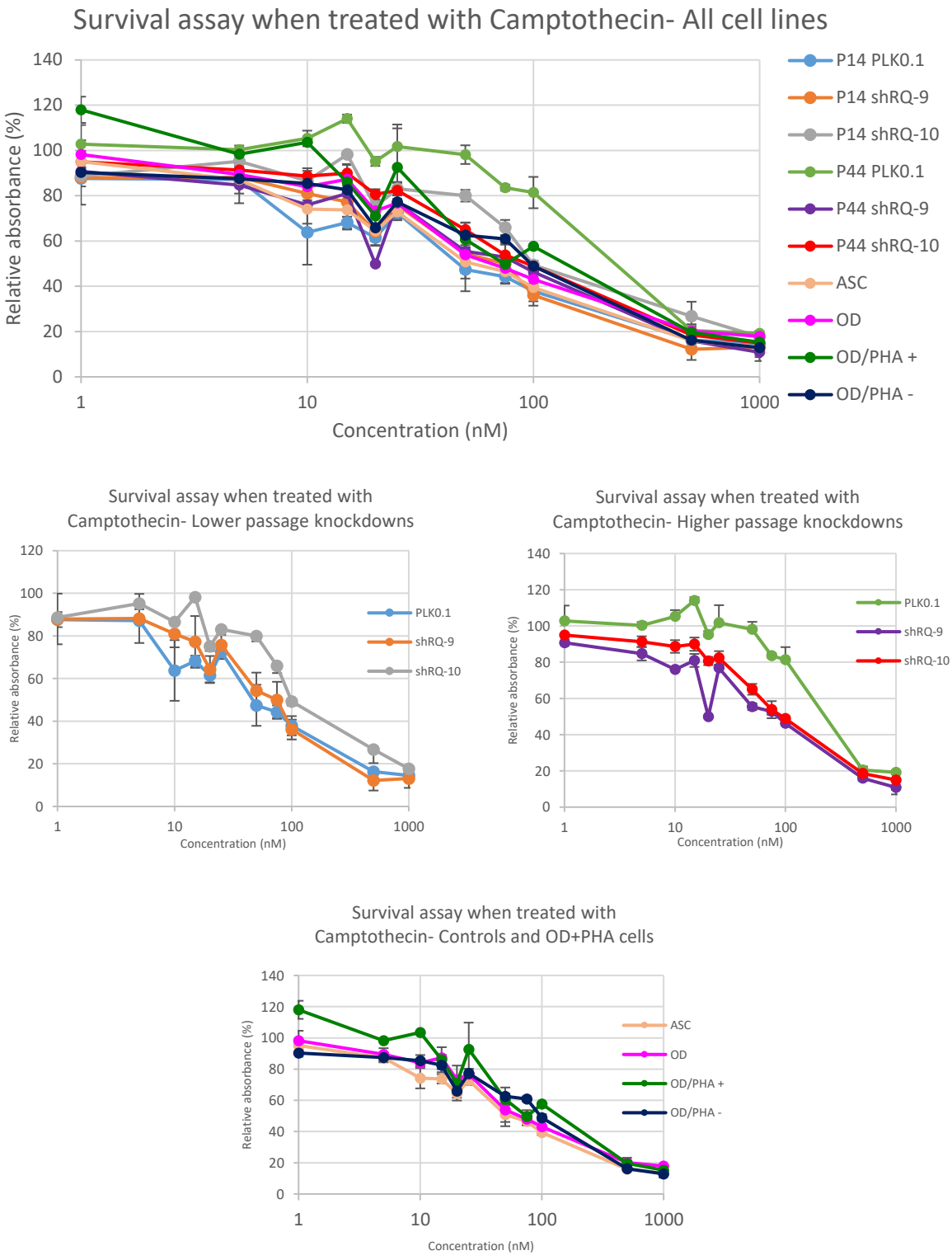

Figure 26. Survival assays for the treatment of the knockdowns, their controls, ASC52Telo cells, OD cells, OD+PHA+ cells (PHA present) and OD+PHA- cells (PHA not present) with Camptothecin for a period of 7 days. Logarithmic scale, base 10.

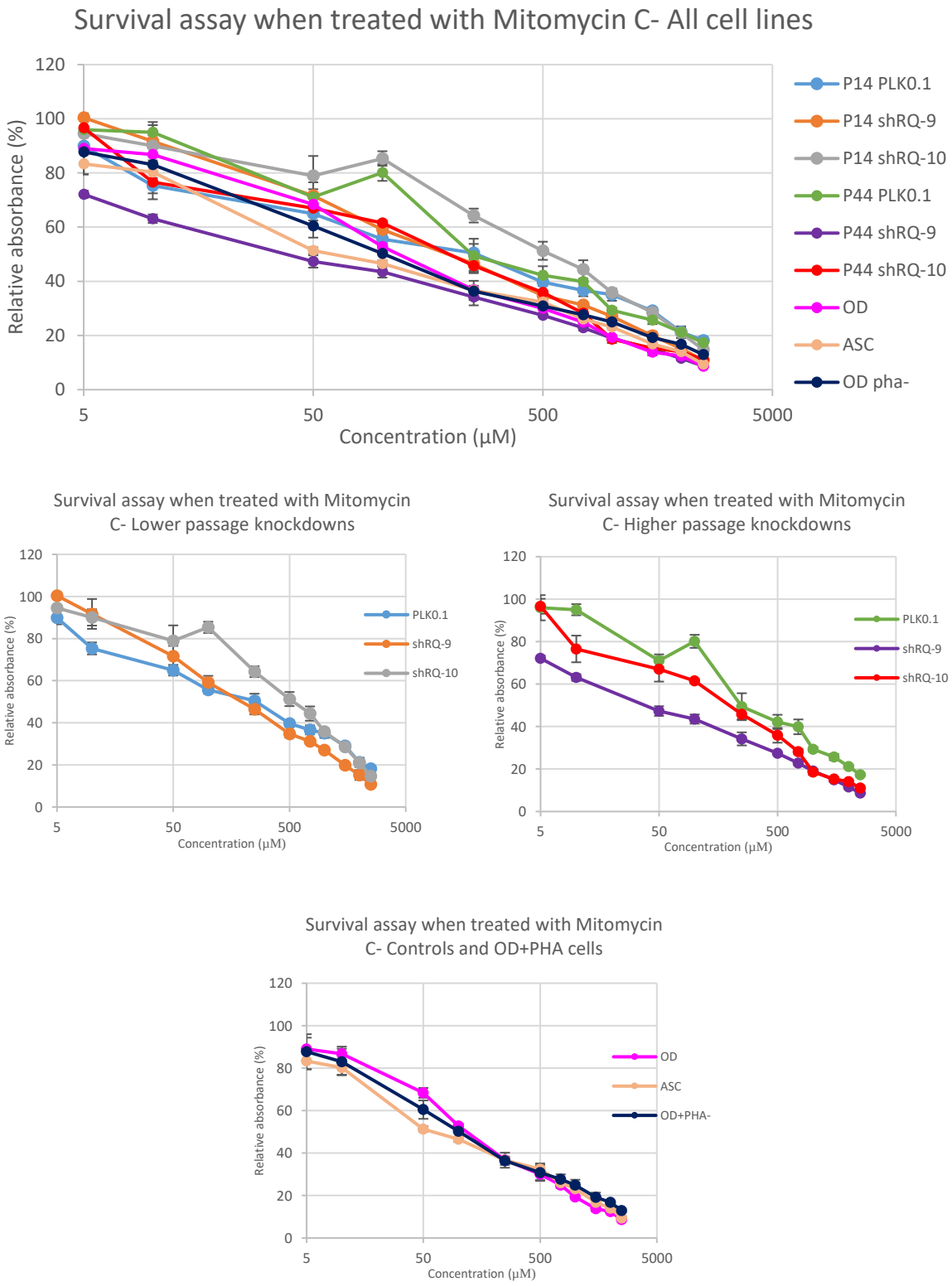

Figure 27. Survival assays for the treatment of the knockdowns, their controls, ASC52Telo cells, OD cells,) and OD+PHA- cells (PHA not present) with Mitomycin C for a period of 7 days. Logarithmic scale, base 10.

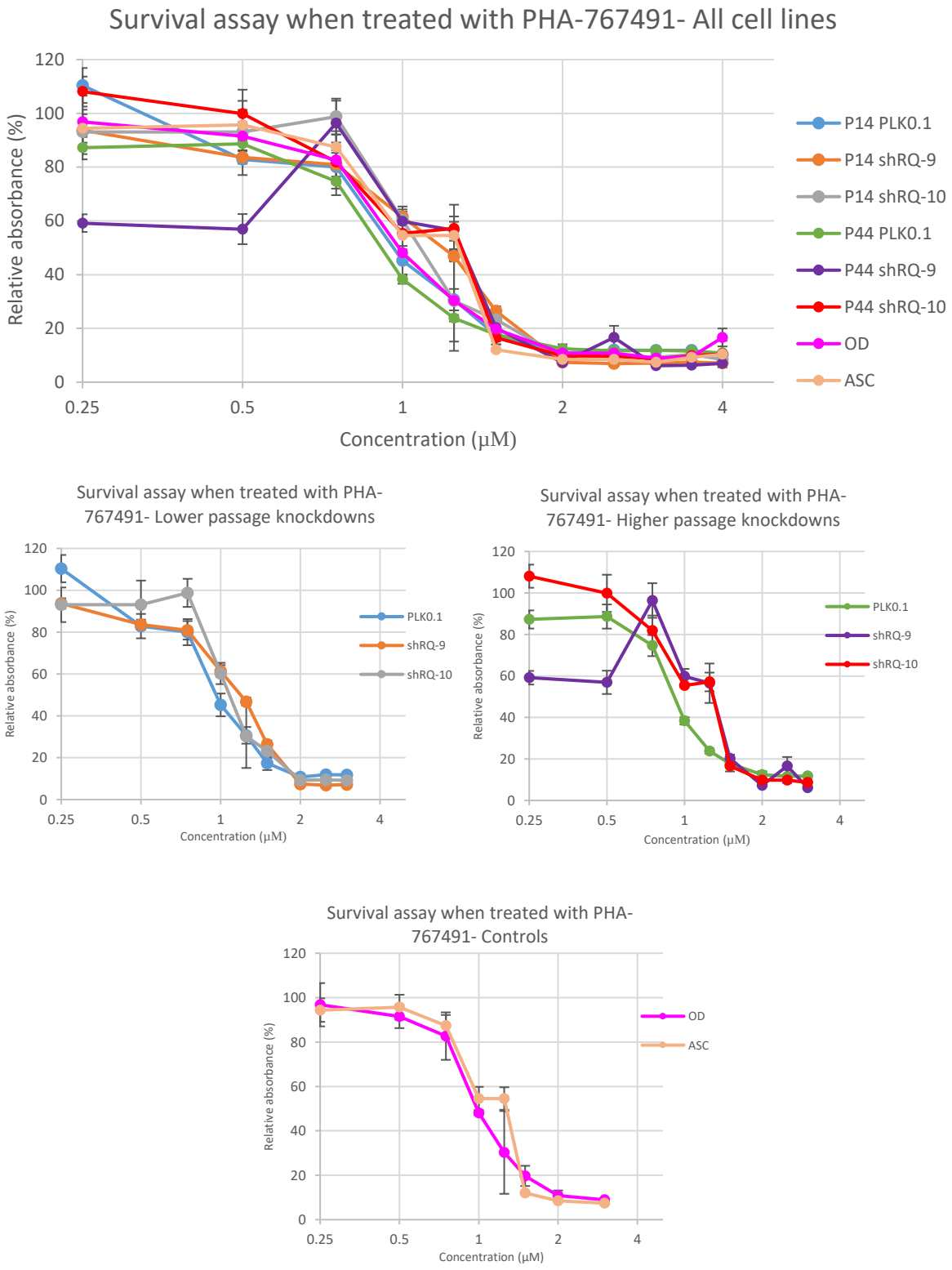

Figure 28. Survival assays for the treatment of the knockdowns, their controls, ASC52Telo cells and OD cells with PHA-767491 for a period of 7 days. Logarithmic scale, base 2.

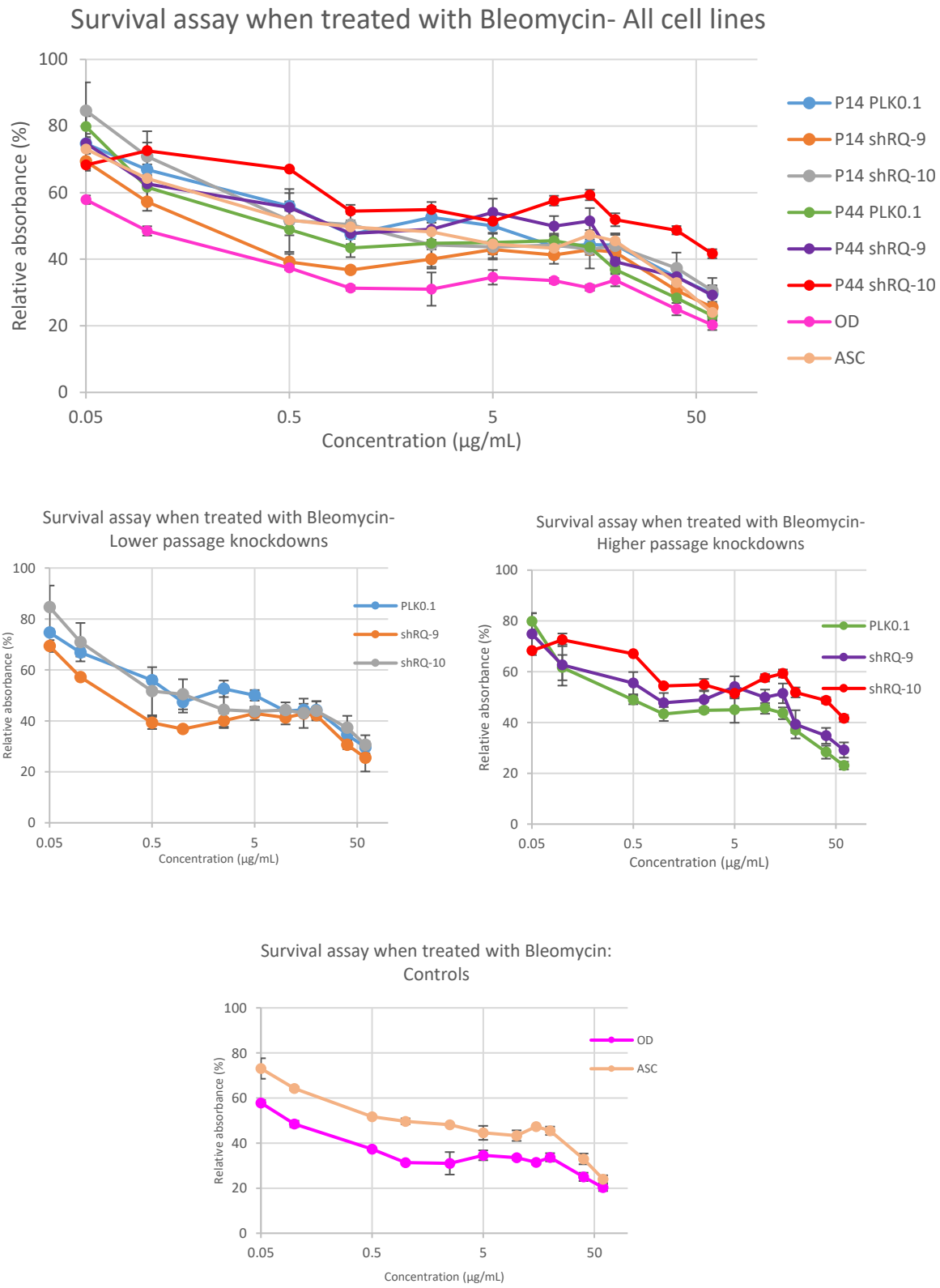

Figure 29. Survival assays for the treatment of the knockdowns, their controls, ASC52Telo cells and OD cells with Bleomycin for a period of 7 days. Logarithmic scale, base 10.

Survival assays were carried out on all of the cell lines testing for sensitivity when treated with Bleomycin, Mitomycin C, PHA-767491, Camptothecin, KU0055933 and Hydroxy urea. The cells were treated for a period of seven days with each drug and an MTT assay carried out at the end of the seven days to test the number of viable cells left. These results are plotted on graphs to show the decrease in viability as drug concentration increases (see figures 24-29). The assays are plotted on a logarithmic scale to better the spread of the results. The results show no significant difference in sensitivity between the controls and the *RECQL4* deficient cells. However, we can see from some of the sensitivity assays that p14 shRQ-10 and p44 shRQ-10 appear to be less sensitive in the mid-range concentrations in comparison to the control ASC52Telo cells and OD cells.

3.6 Evaluation of chromosomal instability

Mutations of RECQL4 and interference with replication initiation may cause chromosomal instabilities (Maire *et al*., 2009). Chromosomes were prepared from each cell line and analysed to identify any chromosome alterations.

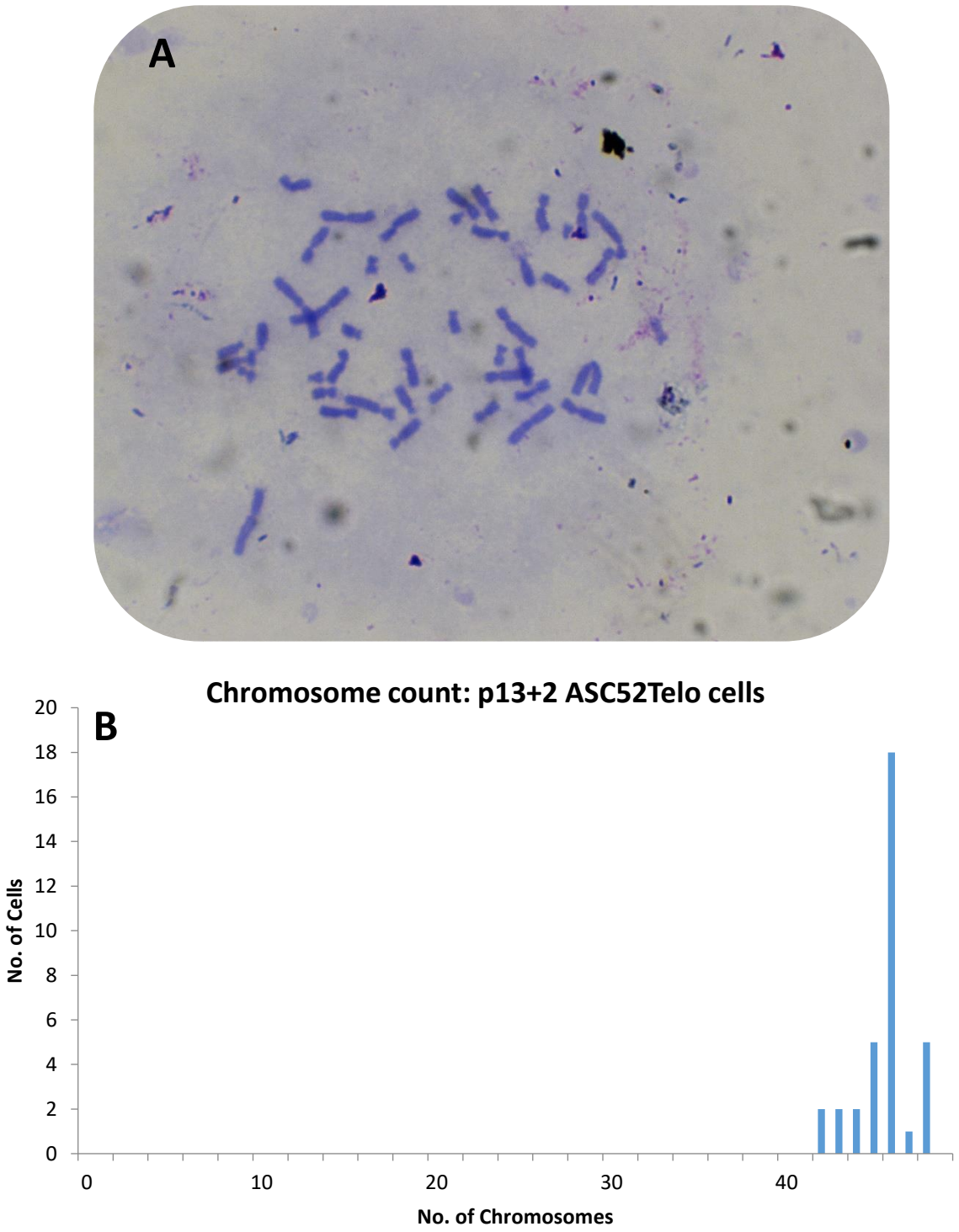

Figure 30. Preparation and count of chromosomes in ASC52Telo cells. ~35 sets of chromosomes were imaged, counted and analysed for any alterations. A) giemsa stained chromosomes (x100), B) a graph showing the number of chromosomes in each cell counted.

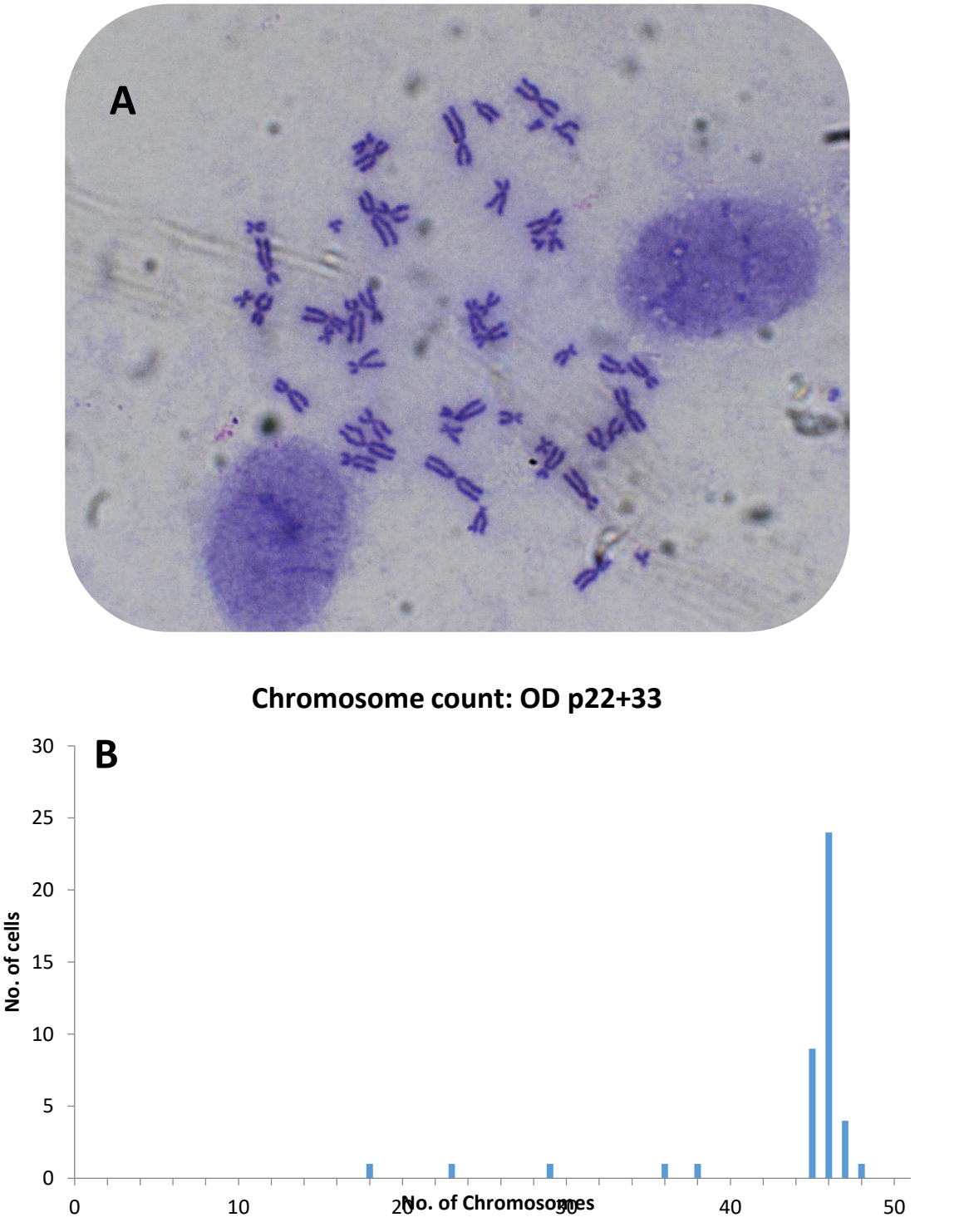

Figure 31. Preparation and count of chromosomes in OD cells. ~35 sets of chromosomes were imaged, counted and analysed for any alterations. A) giemsa stained chromosomes (x100), B) a graph showing the number of chromosomes in each cell counted.

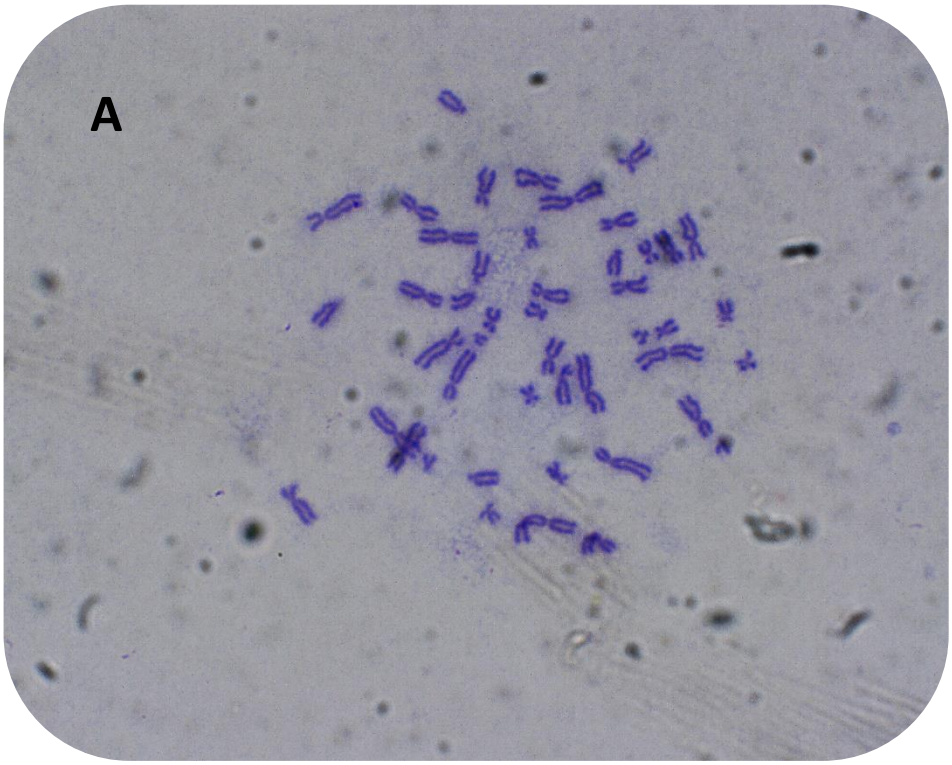

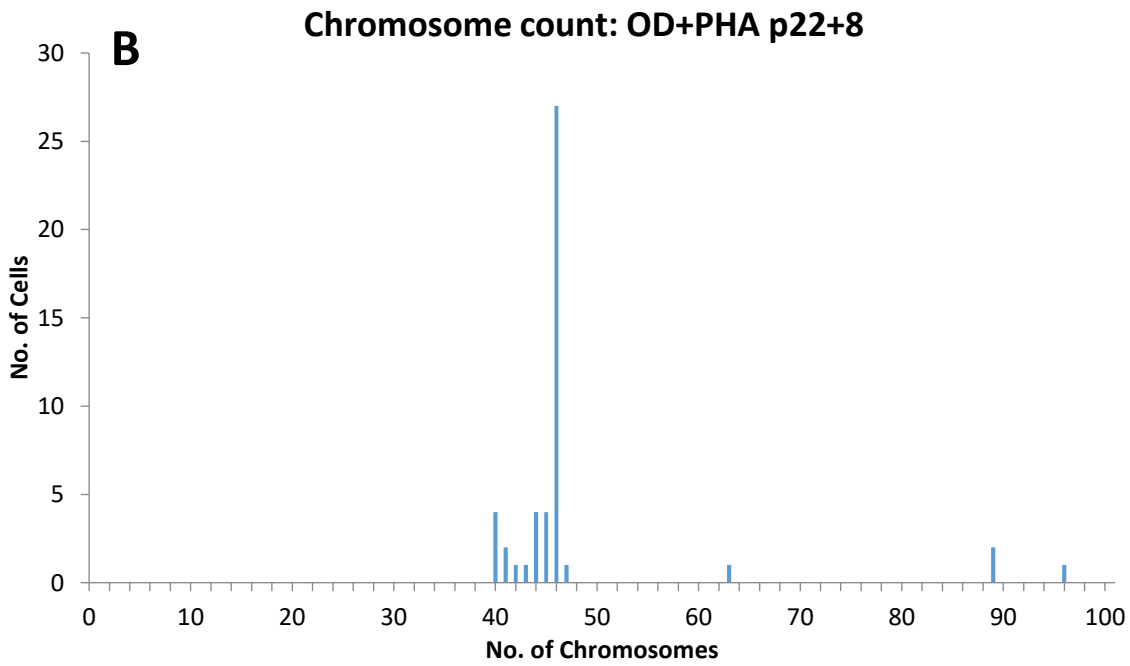

Figure 32. Preparation and count of chromosomes in OD+PHA cells. ~35 sets of chromosomes were imaged, counted and analysed for any alterations. A) giemsa stained chromosomes (x100), B) a graph showing the number of chromosomes in each cell counted.

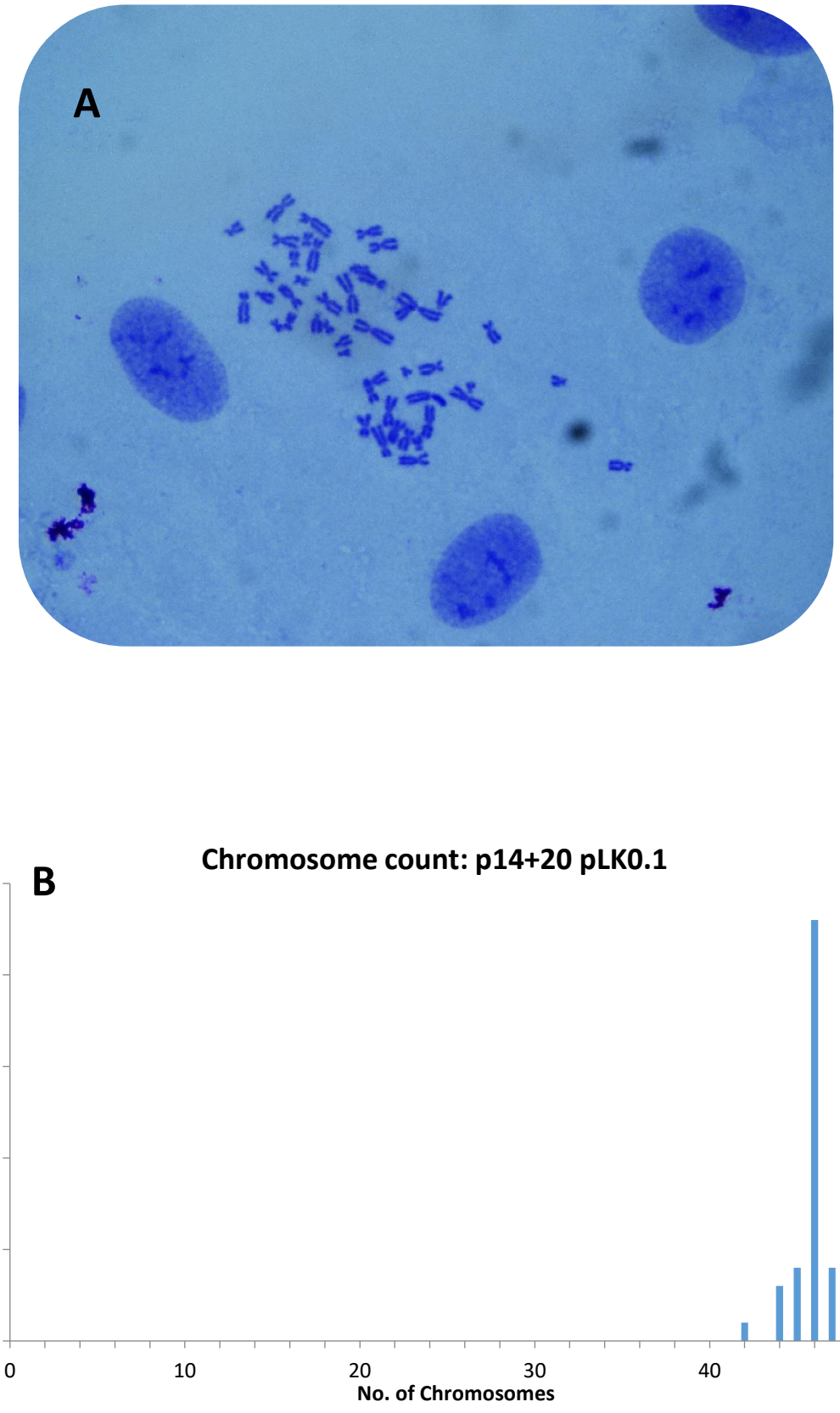

Figure 33. Preparation and count of chromosomes in P14 pLK0.1 cells. ~35 sets of chromosomes were imaged, counted and analysed for any alterations. A) giemsa stained chromosomes (x100), B) a graph showing the number of chromosomes in each cell counted.

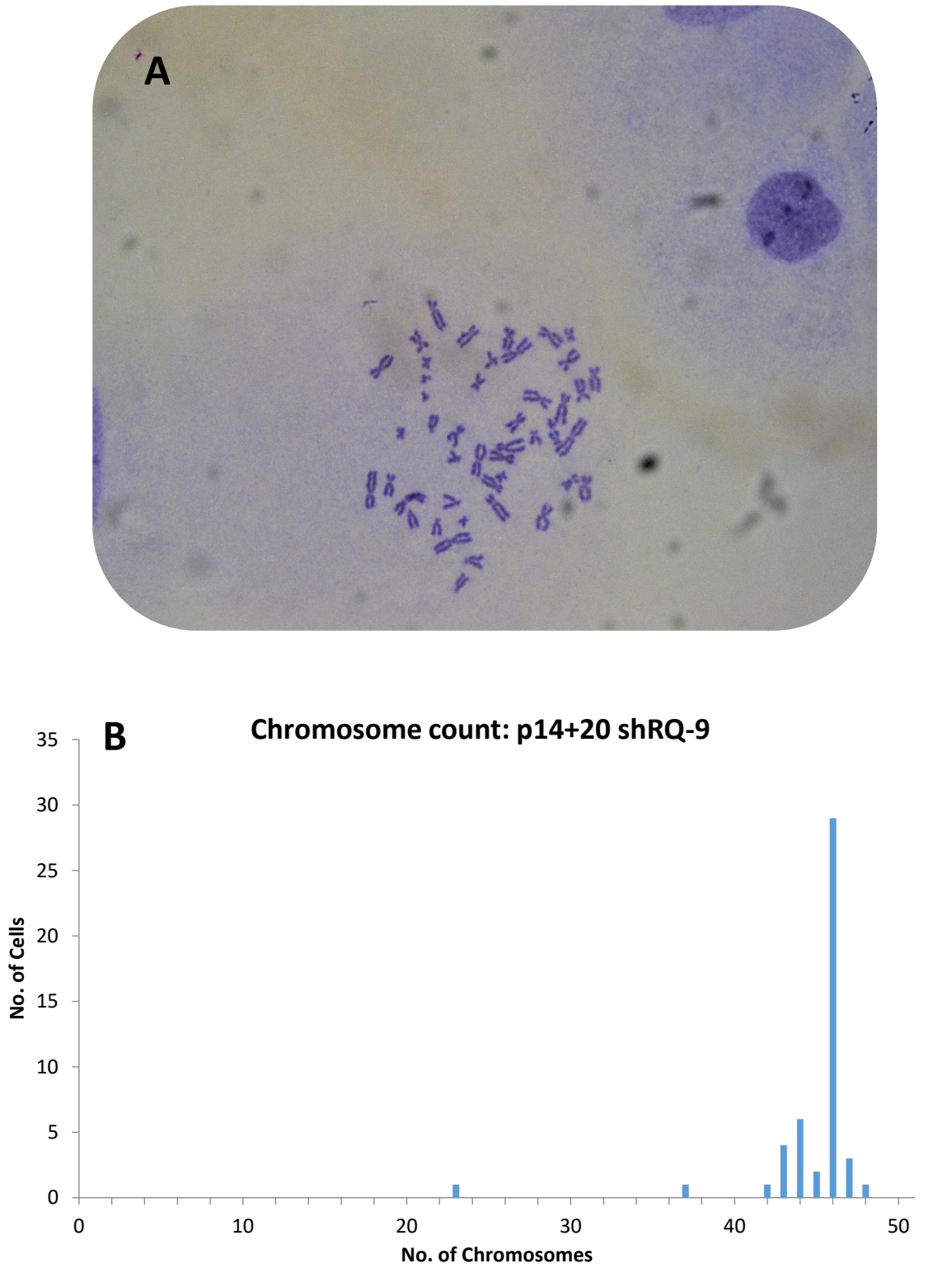

Figure 34. Preparation and count of chromosomes in P14 shRQ-9 cells. ~35 sets of chromosomes were imaged, counted and analysed for any alterations. A) giemsa stained chromosomes (x100), B) a graph showing the number of chromosomes in each cell counted.

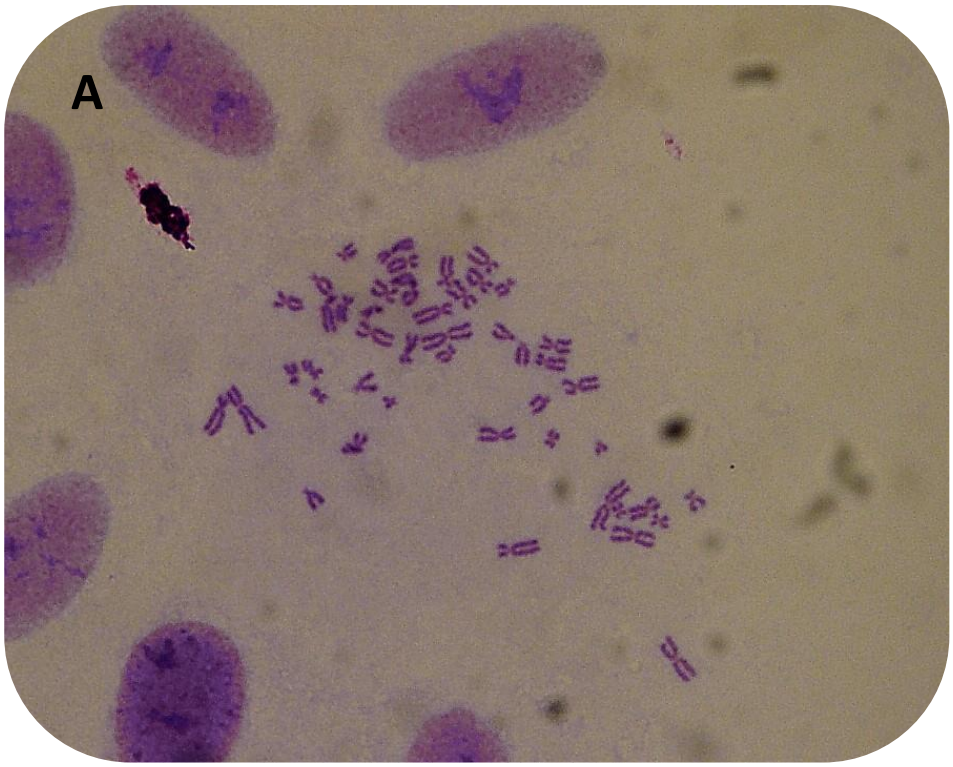

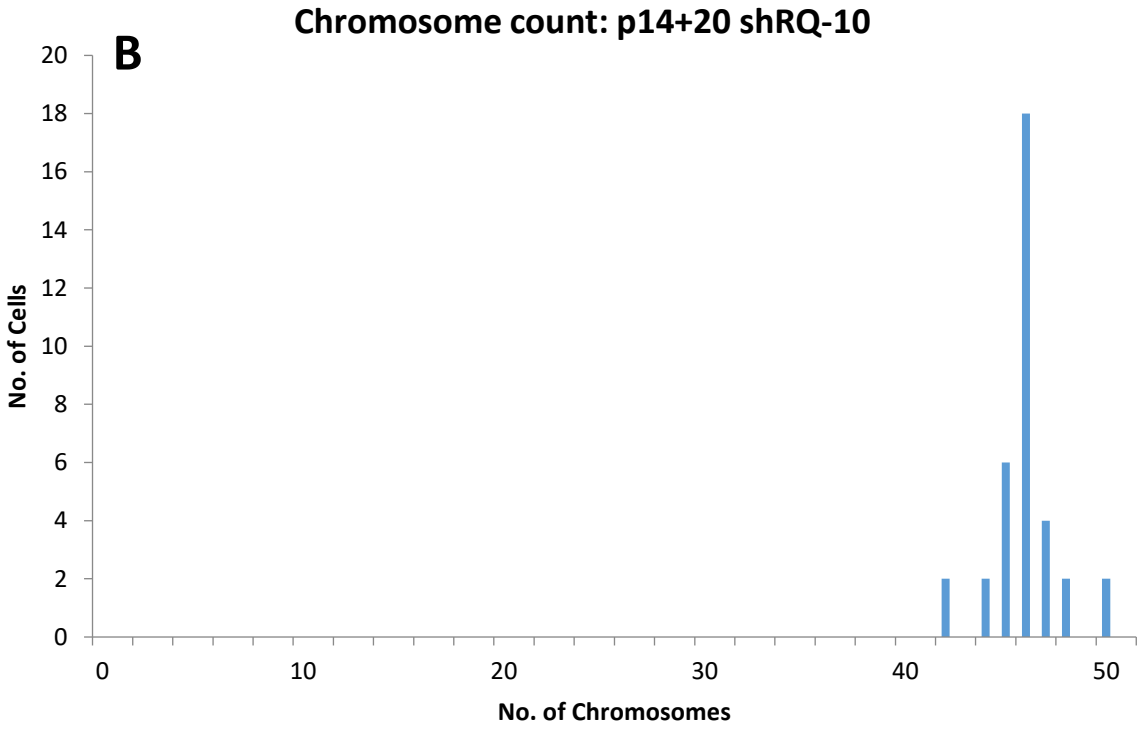

Figure 35. Preparation and count of chromosomes in P14 shRQ-10 cells. ~35 sets of chromosomes were imaged, counted and analysed for any alterations. A) giemsa stained chromosomes (x100), B) a graph showing the number of chromosomes in each cell counted.

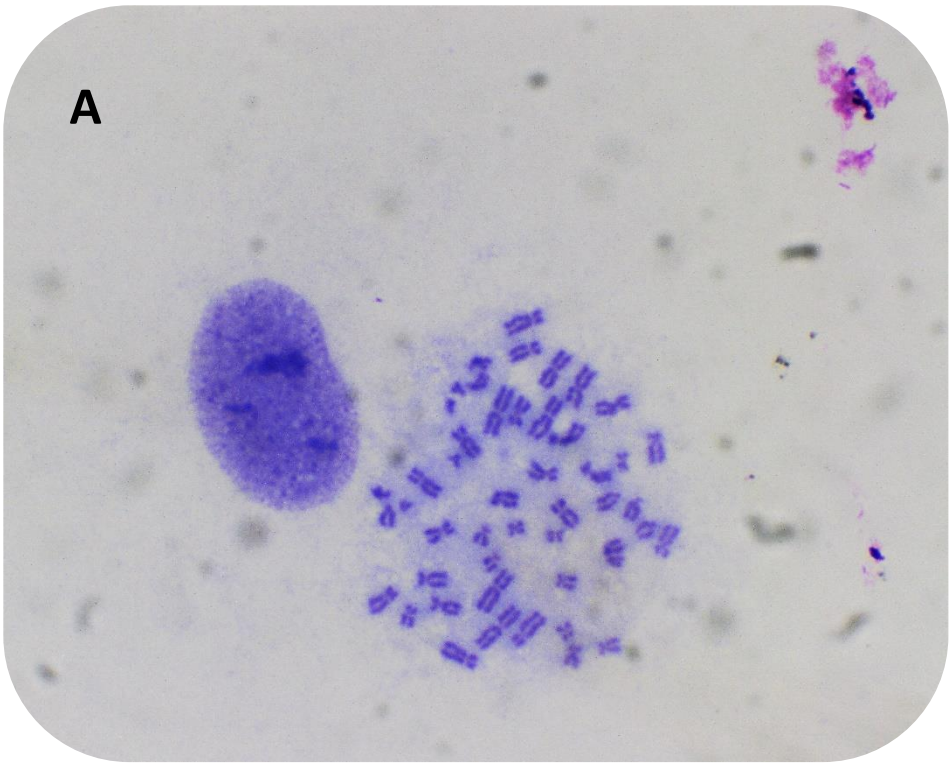

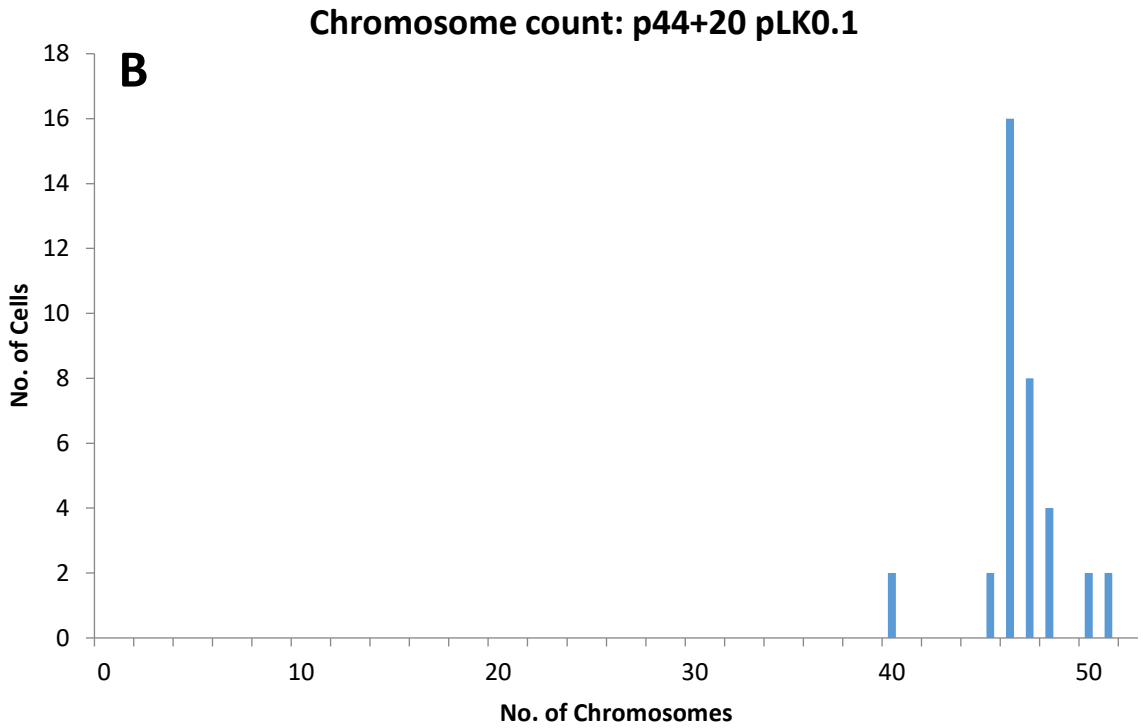

Figure 36. Preparation and count of chromosomes in P44 pLK0.1 cells. ~35 sets of chromosomes were imaged, counted and analysed for any alterations. A) giemsa stained chromosomes (x100), B) a graph showing the number of chromosomes in each cell counted.

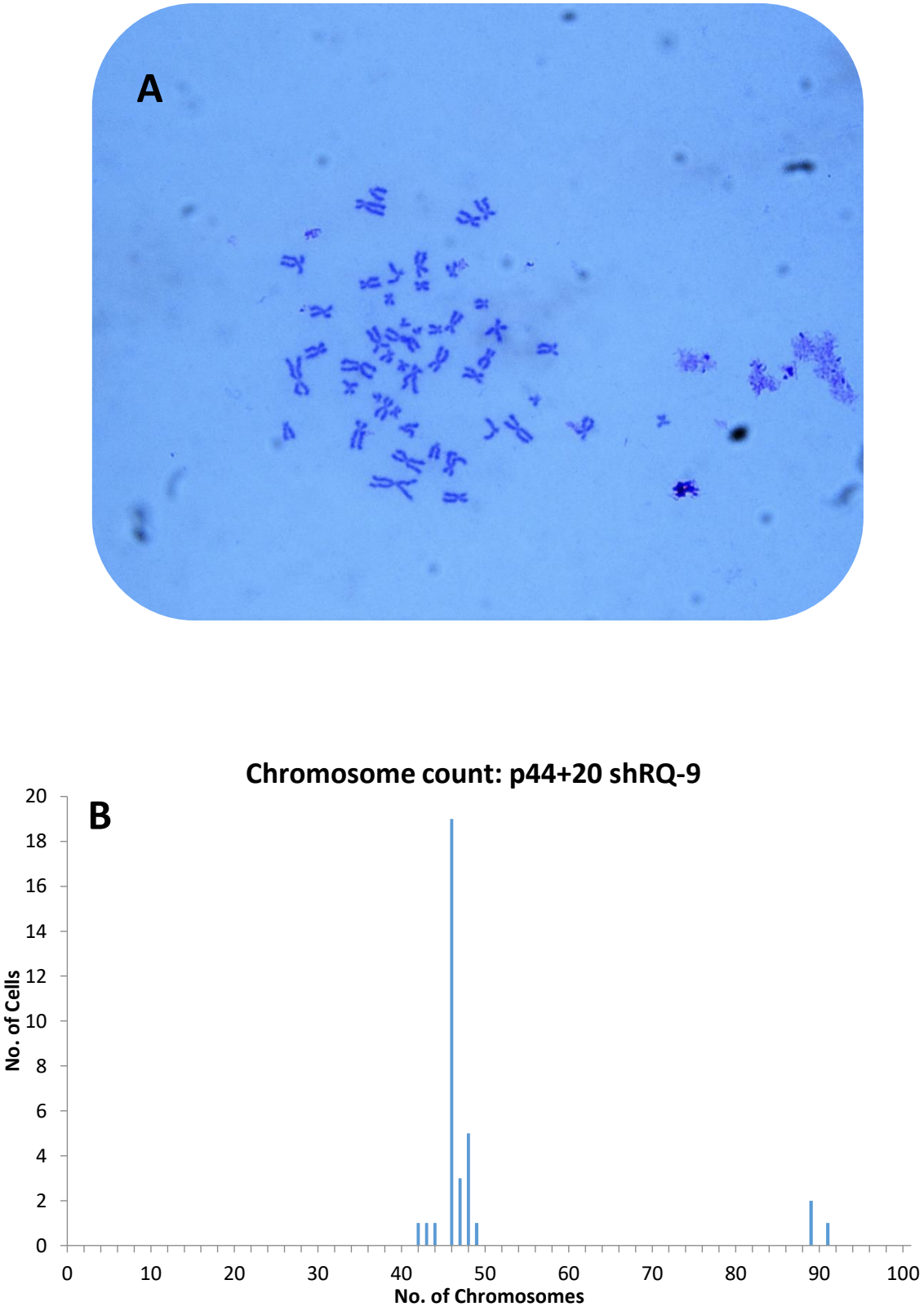

Figure 37. Preparation and count of chromosomes in P44 shRQ-9 cells. ~35 sets of chromosomes were imaged, counted and analysed for any alterations. A) giemsa stained chromosomes (x100), B) a graph showing the number of chromosomes in each cell counted.

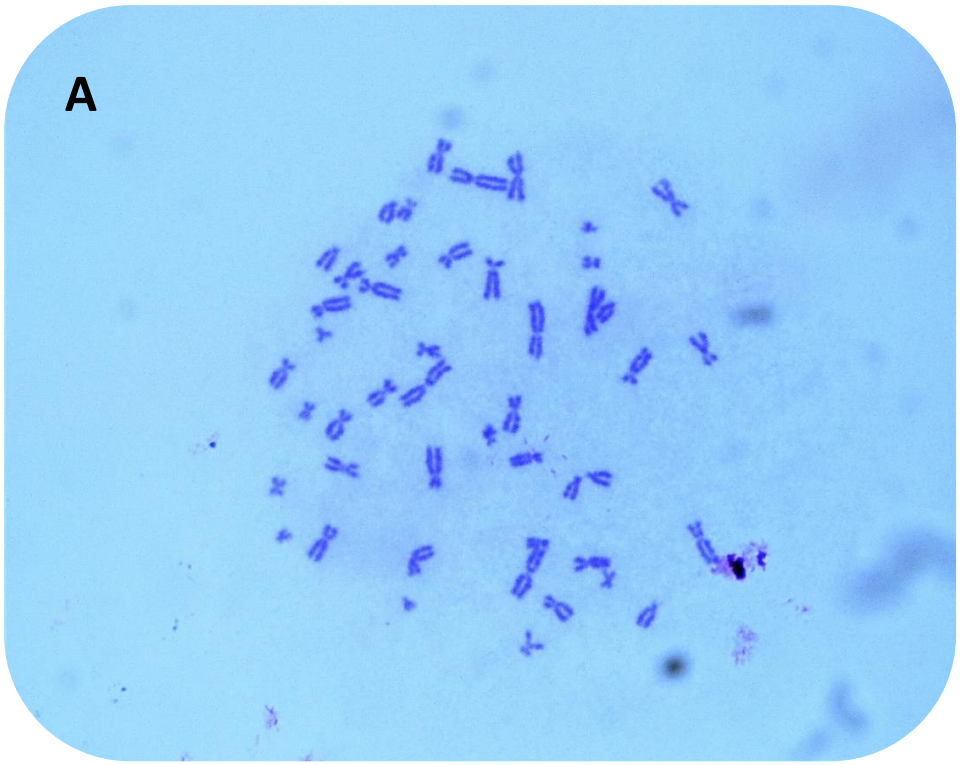

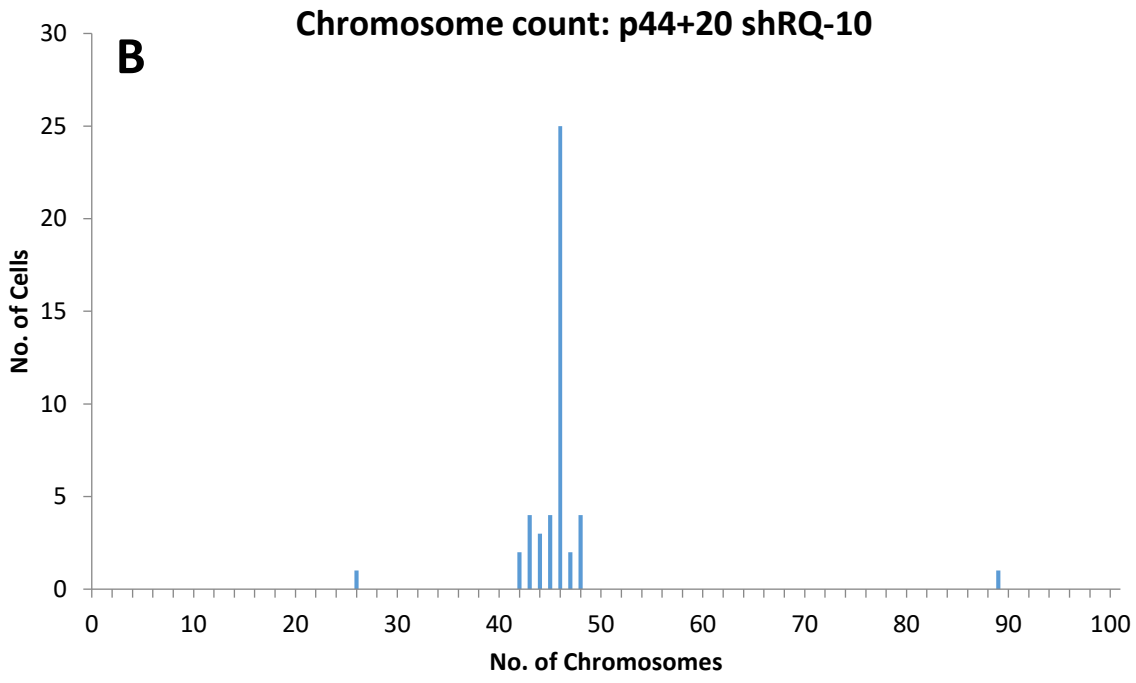

Figure 38. Preparation and count of chromosomes in P44 shRQ-10 cells. ~35 sets of chromosomes were imaged, counted and analysed for any alterations. A) giemsa stained chromosomes (x100), B) a graph showing the number of chromosomes in each cell counted.

Cells were arrested in metaphase and chromosomes were prepared from all of the cell lines and then dropped onto glass slides. These slides were then stained with Giemsa and ~35 metaphase nuclei were imaged. The chromosomes were counted for each cell that was imaged and analysed to identify any signs of chromosomal alterations. None of the cells lines show any signs of structural chromosomal alterations that were observable with this technique. The chromosome counts show a modal count of 46, which is the normal number of chromosomes expected to be seen. Each cell line has cells that display aneuploidy, missing or gaining only one or two chromosomes. Importantly however, cells with a modal chromosome number of 92, (tetraploid cells) and cells with an increased degree of aneuploidy can be seen in the OD+PHA, P44 shRQ-9 and P44 shRQ-10 cell lines.

4. Discussion

This study set out to identify how RECQL4 depletion in ASC52Telo cells contributes to the development of osteosarcoma in RTS patients using long term *in vitro* culturing of hTert immortalised ASC52Telo cells.

Verification of *RECQL4* knockdown

The tubulin control confirms that a comparable amount of each protein sample was loaded. Although bands are seen at 150kDa on the western as expected, there are also non-specific bands present at other molecular weights on the western. The band at around 100kDa is likely a degradation product. The western blot results suggest the knockdown is working at a good efficiency in the higher passage clones, both shRQ-9 and shRQ-10, whereas the knockdown in the lower passage clones is less convincing.

The RECQL4 antibody used in this experiment has caused difficulties in the past due to its quick loss of activity when in storage. It has also proven sensitive to the blocking agent used and so after some experimentation BSA was identified as the most efficient blocking agent. The levels of RECQL4 expression is also cell cycle-dependent and so cells that are slow cycling or unhappy show very low expression. When loading the samples, they are normalised for total protein concentration and as ASC cells are very large and there is a possibility of under loading the gel for the detection of RECQL4; a nuclear protein. To try and solve this issue of under loading the cell extracts were fractionated to enrich any nuclear proteins present. Unfortunately, this extra process did not produce any results that were more successful. Nevertheless, the western results confidently show that the knockdown of RECQL4 has worked at least in high passage cells and perhaps in low passage cells with shRQ-9.

Differentiation capability of *RECQL4* containing ASCs and *RECQL4* deficient ASCs.

Adipogenesis and osteogenesis can be seen in all the cell lines to some degree. A study by Ng *et al*. (2015) showed a decrease in osteogenic differentiation in conditional *Recql4* mutant mice, which supports the low bone mass and short stature symptoms seen in RTS patients. Our *RECQL4* deficient cells lines appeared to carry out osteogenic differentiation equally as well as the control cell lines. The higher passage cell lines seemed to show a lower number of cells that successfully differentiated into adipocytes as a lower number of vacuoles are present both at day 10 and day 21. Higher passage numbers can sometimes see alterations in the ability of the cells to differentiate and proliferate efficiently which could explain the difference in our results for each

cell line induced to carry out adipogenesis. Our chondrogenic differentiation does not show the results we were expecting to see, as there is a distinct lack of cells growing on the coverslip. The sparse number of cells present may be due a faster rate of proliferation that caused the cells to become over-confluent and lift off the cover slip. This results in the cells being washed away during a media change. This occurred during every repeat of this experiment.

The OD and OD+PHA cells were only treated with adipogenesis media to see if the recovered populations contain cells with mesenchymal stem cell characteristics, or whether they are differentiated osteoblasts. The results suggest that some cells may be able to differentiate into adipocytes. However, given that the number of cells that differentiated to adipocytes was considerably lower than in parallel control cultures, it suggests that these cultures contain a high percentage of committed osteogenic cells. The presence of PHA-767491 doesn't seem to affect the differentiation capability of these cultures.

Expression of marker genes: *Ki67, RUNX2*, *Osterix* and *53BP1*

The differentiation capability results of the OD and OD+PHA cells is further supported through the immunostaining for the expression of marker genes. Osterix and RUNX2 are transcription factors involved in bone formation and osteoblast differentiation (Martin *et al*., 2011). Osterix is a more accurate marker of osteoblast differentiation as RUNX2 is expressed in MSCs, as well as early osteoblasts (Zou *et al*.). The RUNX2 results show no significant difference whereas our average Osterix foci number is much higher in OD and OD+PHA cells, confirming that there is a higher percentage of committed osteogenic cells. Lu *et al*. (2008) reported that when quantitative reverse transcription-PCR analysis of RUNX2 in osteosarcoma patient's samples was carried out, overexpression of RUNX2 was seen. Our results show that when treated with PHA-767491 a higher level of RUNX2 expression was seen, suggesting that PHA-767491 treatment may induce transformation and osteosarcoma in these treated cultures. A link could be possible in p44 pLK0.1 and p44 shRQ-9 cells between a high RUNX2 expression and a reduced capability in differentiating.

53BP1 is an important mediator of DNA damage check points and abnormal quantities can be linked with tumour development (Bi *et al*., 2015). It is a key regulator of DSB repair pathway choice and promotes NHEJ during G_1 by antagonising DNA end-resection (Panier and Boulton, 2013). A study by Singh *et al*. (2010) showed that when exposed to gamma-irradiation, RECQL4 deficient fibroblasts displayed an increased number of 53BP1 foci. This suggested that defects in efficient DSB repair were present in the RECQL4 deficient fibroblasts. Our results show no statistically significant differences between the levels of 53BP1 expression in each cell line.

Contrary to the results found by Singh *et al*. (2010), the p14 shRQ-9, p14 shRQ-10 and p44 shRQ-9 cells show a lower average foci count in comparison to the other cell lines. These results could suggest that there is no abnormal DNA damage to any of the cell lines.

Ki67 protein expression is associated with cell proliferation (Scholzen and Gerdes, 2000). Studies of breast cancer patients have shown that a high level of Ki67 expression is associated with a worse prognosis (Inwald *et al*., 2013). This suggests that any development of osteosarcoma will result in an increased expression of Ki67 being present. Our results show no significant differences in the expression of Ki67 between the knockdowns and the controls.

Differences in growth

RECQL4 plays an important role in DNA replication initiation and so without this gene it is assumed that the efficiency of cell proliferation would be decreased as DNA replication would occur at a reduced rate. _ENREF_76Sangrithi *et al*. (2005) obtained evidence that RECQL4 depletion results in cell proliferation failure. The results from this study do not complement this evidence as no significant difference can be seen between the *RECQL4* deficient cells and the controls. This is, although unexpected, not inexplicable. There might be some residual RECQL4 expression in these clones, as suggested by Figure 7. It is not uncommon to achieve only around 95% knockdown with siRNA / shRNA, and this residual activity can be sufficient enough to carry out some functions meaning the cells that are more sensitive to expression levels might be affected (Fakhr *et al*., 2016). Patient-derived *RECQL4* mutant cell lines can also display different degrees of activity, which may explain the differences they show in proliferation capacity. Full knockout of *Recql4* in the mouse is embryonic lethal, other mouse mutant alleles are hypomorphic with residual expression that retains some activity of the protein (Xu and Liu, 2009).

Sensitivity to genotoxic stress

There are a number of studies available that provide data and information on the sensitivity of RTS cells to different genotoxic agents, and the data that is available is contradictory. These inconsistent findings could indicate genetic heterogeneity in RTS (Jin *et al*., 2008). As *RECQL4* plays a key role in DNA replication initiation, sensitivity is expected to be seen in *RECQL4* deficient cells when treated with DNA damaging agents that inhibit replication. This is because stalled replication forks can be rescued by the firing of dormant origins (Petermann *et al*., 2010), and if this firing is inhibited it results in sensitivity to replication inhibition in general. To test if our *RECQL4* deficient cells were more sensitive in comparison to their controls, we treated them for a seven day period with Camptothecin, Mitomycin C, Hydroxy Urea, PHA-767491, Bleomycin and KU0055933 and then evaluated the cytotoxic effect using an MTT assay. Mitomycin C and Hydroxy

Urea both cause replication fork arrest directly as Mitomycin C creates DNA inter-strand crosslinks and Hydroxy Urea inhibits ribonucleotide reductase, which depletes the dNTP pool. Camptothecin is an inhibitor of DNA topoisomerase I; it arrests TOPO1 in its transient state when the single-stranded break is created by the enzyme and it induces collapse of the replication fork. PHA-767491 inhibits replication initiation by inhibiting CDC7/DBF4. Bleomycin induces double-stranded DNA breaks, while KU0055933 is an ATM inhibitor and it interferes with the DNA damage response.

Our results show no increase in sensitivity in the *RECQL4* deficient cells in comparison to the control cell lines. These results support the results obtained by Cabral *et al*. (2008) that there was no significant increase in sensitivity of the *RECQL4* deficient cells in comparison to the controls when treated with Mitomycin C and Hydroxy Urea. When treated with Hydroxy Urea and Camptothecin, the lower passage shRQ-10 knockdown appears to have a slightly decreased sensitivity in comparison to the healthy OD and ASC cells. These results are contrary to those obtained in a study by Jin *et al*. (2008) that showed RTS fibroblasts were more sensitive to Hydroxy Urea and Camptothecin in comparison to their controls. Differences in results could be due to the different systems and models used to mimic RTS *RECQL4* deficient cells. However, as seen above in sections 3.1 and 4.1, the most likely cause for the inconsistencies is the nature of the mutations and residual expression. The PHA-767491 sensitivity assay shows a dip at 0.25µM and 0.5µM for P44 shRQ-9. This result may be promising if real; in earlier studies in our laboratory increased sensitivity of the *RECQL4* deficient RTS fibroblast cell line AG05013 to PHA-767491 was demonstrated (Tammy Wiltshire, personal communication). However, this sudden decrease could also be due to pipetting errors in those wells meaning there were not enough cells to pick up cell proliferation again, rather than the effects of the PHA-767491 itself.

Chromosomal analysis

Osteosarcomas normally see a number of chromosome alterations and genomic instability with aneuploidy being a common feature within cells in osteosarcoma patients (Nishijo *et al*., 2004). Chromosome instability is also a characteristic of RTS cell lines. Chromosomes were prepared from all nine of the cell lines used in this study and their chromosome number counted from around 35 cells. The chromosomes were also thoroughly examined for any obvious structural defects. As most previous studies show, aneuploidy exists in all *RECQL4* deficient cells lines, but it is also seen in control cell lines. However, the degree of aneuploidy in both of the higher passage *RECQL4* deficient cell lines and the OD+PHA cell line is greater, and contain cells with a tetraploid modal number of chromosomes. A study by Muff *et al*. (2015) reported that the gene expression

signature osteosarcoma cells is difficult to determine with stochastic chromosomal instability playing a key role in altered gene expressions. None of the cell lines show signs of chromosomal defects detectable by the techniques we used. Breakage analysis conducted by Smida *et al*. (2017) shows unstable regions in osteosarcoma in tumour suppressor genes such as *TP53* and *RB1*. Comparative analysis of osteosarcoma-derived cell lines suggests that chromosomal instability arises from chromatin modifications at specific genomic locations in the osteosarcoma. Further tests would need to be conducted to evaluate whether our results support any of these findings.

5. Conclusion and further research

Multiple experiments were carried out in this study to determine whether there are any differences in chromosomal instabilities, sensitivity to genotoxic agents, differentiation potential and level of expression of marker genes between RECQL4 deficient ASC52Telo and control cells. Although we found no significant differences in growth characteristics, marker expression and drug sensitivity, the degree of numerical chromosomal instabilities was found to be greater in RECQL4 deficient cells. Slight differences could be seen in some of the results, but without confirmation that there is no residual RECQL4 expression in the knockdowns, it cannot be confirmed that the results are due to RECQL4 depletion.

There are some improvements and variations that could be considered for future development of this experiment. These could benefit both the accuracy of the experiment, and the depth of information obtained.

To better clarify RECQL4 expression in the shRNA knockdowns, a repeat of the western with a better RECQL4 antibody needs to be carried out. Patient derived cell lines from RTS patients with confirmed RECQL4 depletion could also be used to ensure RECQL4 depleted cells are being used.

A popular method of analysing chromosomes is using spectral karyotyping (SKY). If a collaborator could be found, the samples obtained from these cells lines could be sent to be analysed to gain more accurate results and see if any chromosomal alterations can be identified. SKY staining of these chromosomal preparations would unravel structural chromosomal rearrangements at much higher sensitivity and resolution, and would also increase confidence in analysing numerical abnormalities. Chromosomes could also be prepared from *RECQL4* depleted cells treated with the genotoxic agents to see if any obvious abnormalities can be seen when DNA damage is stimulated. Immunofluorescence staining could also be repeated on *RECQL4* depleted cells treated with the genotoxic agents to evaluate the expression DNA damage response markers.

References

ADAMSON, I. Y. R. & BOWDEN, D. H. 1974. The Pathogenesis of Bleomycin-Induced Pulmonary Fibrosis in Mice. *The American Journal of Pathology,* 77**,** 185-198.

AL-ROMAIH, K., BAYANI, J., VOROBYOVA, J., KARASKOVA, J., PARK, P. C., ZIELENSKA, M. & SQUIRE, J. A. 2003. Chromosomal instability in osteosarcoma and its association with centrosome abnormalities. *Cancer Genetics and Cytogenetics,* 144**,** 91-99.

APARICIO, T., BAER, R. & GAUTIER, J. 2014. DNA double-strand break repair pathway choice and cancer. *DNA repair,* 19**,** 169-175.

AUGELLO, A. & DE BARI, C. 2010. The regulation of differentiation in mesenchymal stem cells. *Human gene therapy,* 21**,** 1226-1238.

BACHRATI, C. Z. & HICKSON, I. D. 2003. RecQ helicases: suppressors of tumorigenesis and premature aging. *Biochemical Journal,* 374**,** 577-606.

BERNADOTTE, A., MIKHELSON, V. M. & SPIVAK, I. M. 2016. Markers of cellular senescence. Telomere shortening as a marker of cellular senescence. *Aging (Albany NY),* 8**,** 3-11.

BERNSTEIN, K. A., GANGLOFF, S. & ROTHSTEIN, R. 2010. The RecQ DNA helicases in DNA repair. *Annual review of genetics,* 44**,** 393-417.

BI, J., HUANG, A., LIU, T., ZHANG, T. & MA, H. 2015. Expression of DNA damage checkpoint 53BP1 is correlated with prognosis, cell proliferation and apoptosis in colorectal cancer. *International Journal of Clinical and Experimental Pathology,* 8**,** 6070-6082.

BOLAND, G. M., PERKINS, G., HALL, D. J. & TUAN, R. S. 2004. Wnt 3a promotes proliferation and suppresses osteogenic differentiation of adult human mesenchymal stem cells. *Journal of cellular biochemistry,* 93**,** 1210-1230.

BUNNELL, B. A., FLAAT, M., GAGLIARDI, C., PATEL, B. & RIPOLL, C. 2008. Adipose-derived stem cells: isolation, expansion and differentiation. *Methods,* 45**,** 115-120.

CABRAL, R. E. C., QUEILLE, S., BODEMER, C., DE PROST, Y., NETO, J. B. C., SARASIN, A. & DAYA-GROSJEAN, L. 2008. Identification of new RECQL4 mutations in Caucasian Rothmund–Thomson patients and analysis of sensitivity to a wide range of genotoxic agents. *Mutation Research/Fundamental and Molecular Mechanisms of Mutagenesis,* 643**,** 41-47.

CAO, Y., ZHOU, Z., DE CROMBRUGGHE, B., NAKASHIMA, K., GUAN, H., DUAN, X., JIA, S.-F. & KLEINERMAN, E. S. 2005. Osterix, a transcription factor for osteoblast differentiation, mediates antitumor activity in murine osteosarcoma. *Cancer research,* 65**,** 1124-1128.

CHAMBERLAIN, G., FOX, J., ASHTON, B. & MIDDLETON, J. 2007. Concise Review: Mesenchymal Stem Cells: Their Phenotype, Differentiation Capacity, Immunological Features, and Potential for Homing. *STEM CELLS,* 25**,** 2739-2749.

CLARK, J. C. M., DASS, C. R. & CHOONG, P. F. M. 2008. A review of clinical and molecular prognostic factors in osteosarcoma. *Journal of Cancer Research and Clinical Oncology,* 134**,** 281-297.

COSCHI, C. H., MARTENS, A. L., RITCHIE, K., FRANCIS, S. M., CHAKRABARTI, S., BERUBE, N. G. & DICK, F. A. 2010. Mitotic chromosome condensation mediated by the retinoblastoma protein is tumor-suppressive. *Genes & Development,* 24**,** 1351-1363.

CROTEAU, D. L., SINGH, D. K., HOH FERRARELLI, L., LU, H. & BOHR, V. A. 2012. RECQL4 in genomic instability and aging. *Trends in Genetics,* 28**,** 624-631.

DER KALOUSTIAN, V. M., MCGILL, J. J., VEKEMANS, M. & KOPELMAN, H. R. 1990. Clonal lines of aneuploid cells in Rothmund-Thomson syndrome. *American Journal of Medical Genetics,* 37**,** 336-339.

DIFFLEY, J. F. 2004. Regulation of early events in chromosome replication. *Current Biology,* 14**,** R778-R786.

DING, D.-C., SHYU, W.-C. & LIN, S.-Z. 2011. Mesenchymal stem cells. *Cell transplantation,* 20**,** 5-14.

DOLLEY-SONNEVILLE, P. J., ROMEO, L. E. & MELKOUMIAN, Z. K. 2013. Synthetic surface for expansion of human mesenchymal stem cells in xeno-free, chemically defined culture conditions. *PloS one,* 8**,** e70263.

DUCHMAN, K. R., GAO, Y. & MILLER, B. J. 2015. Prognostic factors for survival in patients with high-grade osteosarcoma using the Surveillance, Epidemiology, and End Results (SEER) Program database. *Cancer epidemiology,* 39**,** 593-599.

ETHERIDGE, S. L., SPENCER, G. J., HEATH, D. J. & GENEVER, P. G. 2004. Expression profiling and functional analysis of wnt signaling mechanisms in mesenchymal stem cells. *Stem cells,* 22**,** 849-860.

FAKHR, E., ZARE, F. & TEIMOORI-TOOLABI, L. 2016. Precise and efficient siRNA design: a key point in competent gene silencing. *Cancer gene therapy,* 23**,** 73-82.

FENG, J. Q., WARD, L. M., LIU, S., LU, Y., XIE, Y., YUAN, B., YU, X., RAUCH, F., DAVIS, S. I., ZHANG, S., RIOS, H., DREZNER, M. K., QUARLES, L. D., BONEWALD, L. F. & WHITE, K. E. 2006. Loss of DMP1 causes rickets and osteomalacia and identifies a role for osteocytes in mineral metabolism. *Nature Genetics,* 38**,** 1310.

FLORENCIO-SILVA, R., SASSO, G. R. D. S., SASSO-CERRI, E., SIMÕES, M. J. & CERRI, P. S. 2015. Biology of Bone Tissue: Structure, Function, and Factors That Influence Bone Cells. *BioMed Research International,* 2015**,** 421746.

FRANZ-ODENDAAL, T. A., HALL, B. K. & WITTEN, P. E. 2006. Buried alive: How osteoblasts become osteocytes. *Developmental Dynamics,* 235**,** 176-190.

FRIEDENSTEIN, A., CHAILAKHJAN, R. & LALYKINA, K. 1970. The development of fibroblast colonies in monolayer cultures of guinea-pig bone marrow and spleen cells. *Cell Proliferation,* 3**,** 393-403.

GAUR, T., LENGNER, C. J., HOVHANNISYAN, H., BHAT, R. A., BODINE, P. V., KOMM, B. S., JAVED, A., VAN WIJNEN, A. J., STEIN, J. L. & STEIN, G. S. 2005. Canonical WNT signaling promotes osteogenesis by directly stimulating Runx2 gene expression. *Journal of Biological Chemistry,* 280**,** 33132-33140.

HOKI, Y., ARAKI, R., FUJIMORI, A., OHHATA, T., KOSEKI, H., FUKUMURA, R., NAKAMURA, M., TAKAHASHI, H., NODA, Y., KITO, S. & ABE, M. 2003. Growth retardation and skin abnormalities of the Recql4 -deficient mouse. *Human Molecular Genetics,* 12**,** 2293-2299.

IM, J.-S., PARK, S.-Y., CHO, W.-H., BAE, S.-H., HURWITZ, J. & LEE, J.-K. 2015. RecQL4 is required for the association of Mcm10 and Ctf4 with replication origins in human cells. *Cell Cycle,* 14**,** 1001-1009.

INWALD, E. C., KLINKHAMMER-SCHALKE, M., HOFSTÄDTER, F., ZEMAN, F., KOLLER, M., GERSTENHAUER, M. & ORTMANN, O. 2013. Ki-67 is a prognostic parameter in breast cancer patients: results of a large population-based cohort of a cancer registry. *Breast Cancer Research and Treatment,* 139**,** 539-552.

JAVAZON, E. H., BEGGS, K. J. & FLAKE, A. W. 2004. Mesenchymal stem cells: paradoxes of passaging. *Experimental hematology,* 32**,** 414-425.

JIN, W., LIU, H., ZHANG, Y., OTTA, S. K., PLON, S. E. & WANG, L. L. 2008. Sensitivity of RECQL4-deficient fibroblasts from Rothmund–Thomson syndrome patients to genotoxic agents. *Human genetics,* 123**,** 643-653.

KERN, S., EICHLER, H., STOEVE, J., KLÜTER, H. & BIEBACK, K. 2006. Comparative analysis of mesenchymal stem cells from bone marrow, umbilical cord blood, or adipose tissue. *Stem cells,* 24**,** 1294-1301.

KIM, W.-S., PARK, B.-S., SUNG, J.-H., YANG, J.-M., PARK, S.-B., KWAK, S.-J. & PARK, J.-S. 2007. Wound healing effect of adipose-derived stem cells: a critical role of secretory factors on human dermal fibroblasts. *Journal of dermatological science,* 48**,** 15-24.

KITAO, S., LINDOR, N. M., SHIRATORI, M., FURUICHI, Y. & SHIMAMOTO, A. 1999. Rothmund–Thomson syndrome responsible gene, RECQL4: genomic structure and products. *Genomics,* 61**,** 268-276.

KOMORI, T. 2008. Regulation of bone development and maintenance by Runx2. *Frontiers in bioscience: a journal and virtual library,* 13**,** 898-903.

KRYŠTOF, V., BAUMLI, S. & FÜRST, R. 2012. Perspective of Cyclin-dependent kinase 9 (CDK9) as a Drug Target. *Current Pharmaceutical Design,* 18**,** 2883-2890.

LABIB, K. 2010. How do Cdc7 and cyclin-dependent kinases trigger the initiation of chromosome replication in eukaryotic cells? *Genes & development,* 24**,** 1208-1219.

LEE, K. M., CHOI, K. H. & OUELLETTE, M. M. 2004. Use of exogenous hTERT to immortalize primary human cells. *Cytotechnology,* 45**,** 33-38.

LI, Y. & YANG, D.-Q. 2010. The ATM Inhibitor KU-55933 Suppresses Cell Proliferation and Induces Apoptosis by Blocking Akt In Cancer Cells with Overactivated Akt. *Molecular Cancer Therapeutics,* 9**,** 113-125.

LOHMAN, T. M. 1993. Helicase-catalyzed DNA unwinding. *Journal of Biological Chemistry,* 268**,** 2269-72.

LU, H., SHAMANNA, RAGHAVENDRA A., KEIJZERS, G., ANAND, R., RASMUSSEN, LENE J., CEJKA, P., CROTEAU, DEBORAH L. & BOHR, VILHELM A. 2016. RECQL4 Promotes DNA End Resection in Repair of DNA Double-Strand Breaks. *Cell Reports,* 16**,** 161-173.

LU, X.-Y., LU, Y., ZHAO, Y.-J., JAEWEON, K., KANG, J., XIAO-NAN, L., GE, G., MEYER, R., PERLAKY, L., HICKS, J., CHINTAGUMPALA, M., CAI, W.-W., LADANYI, M., GORLICK, R., LAU, C. C., PATI, D., SHELDON, M. & RAO, P. H. 2008. Cell Cycle Regulator Gene CDC5L, a Potential Target for 6p12-p21 Amplicon in Osteosarcoma. *Molecular cancer research : MCR,* 6**,** 937-946.

LUETKE, A., MEYERS, P. A., LEWIS, I. & JUERGENS, H. 2014. Osteosarcoma treatment – Where do we stand? A state of the art review. *Cancer Treatment Reviews,* 40**,** 523-532.

MAIRE, G., YOSHIMOTO, M., CHILTON-MACNEILL, S., THORNER, P. S., ZIELENSKA, M. & SQUIRE, J. A. 2009. Recurrent RECQL4 Imbalance and Increased Gene Expression Levels Are Associated with Structural Chromosomal Instability in Sporadic Osteosarcoma. *Neoplasia,* 11**,** 260-IN6.

MANN, M. B., HODGES, C. A., BARNES, E., VOGEL, H., HASSOLD, T. J. & LUO, G. 2005. Defective sister-chromatid cohesion, aneuploidy and cancer predisposition in a mouse model of type II Rothmund–Thomson syndrome. *Human Molecular Genetics,* 14**,** 813-825.

MARTIN, J. W., SQUIRE, J. A. & ZIELENSKA, M. 2012. The Genetics of Osteosarcoma. *Sarcoma,* 2012**,** 11.

MARTIN, J. W., ZIELENSKA, M., STEIN, G. S., VAN WIJNEN, A. J. & SQUIRE, J. A. 2011. The Role of RUNX2 in Osteosarcoma Oncogenesis. *Sarcoma,* 2011**,** 13.

MIOZZO, M., CASTORINA, P., RIVA, P., DALPRA, L., FUHRMAN CONTI, A. M., VOLPI, L., HOE, T. S., KHOO, A., WIEGANT, J. & ROSENBERG, C. 1998. Chromosomal instability in fibroblasts and mesenchymal tumors from 2 sibs with Rothmund-Thomson syndrome. *International journal of cancer,* 77**,** 504-510.

MISHRA, A., DOYLE, N. A. & MARTIN, W. J. 2000. Bleomycin-mediated pulmonary toxicity: evidence for a p53-mediated response. *American journal of respiratory cell and molecular biology,* 22**,** 543-549.

MITCHELL, K. E., WEISS, M. L., MITCHELL, B. M., MARTIN, P., DAVIS, D., MORALES, L., HELWIG, B., BEERENSTRAUCH, M., ABOU-EASA, K. & HILDRETH, T. 2003. Matrix cells from Wharton's jelly form neurons and glia. *Stem cells,* 21**,** 50-60.

MOHAGHEGH, P. & HICKSON, I. D. 2001. DNA helicase deficiencies associated with cancer predisposition and premature ageing disorders. *Human Molecular Genetics,* 10**,** 741-746.

MUFF, R., RATH, P., KUMAR, R. M. R., HUSMANN, K., BORN, W., BAUDIS, M. & FUCHS, B. 2015. Genomic instability of osteosarcoma cell lines in culture: impact on the prediction of metastasis relevant genes. *PloS one,* 10**,** e0125611.

NADKARNI, A., SHRIVASTAV, M., MLADEK, A. C., SCHWINGLER, P. M., GROGAN, P. T., CHEN, J. & SARKARIA, J. N. 2012. ATM inhibitor KU-55933 increases the TMZ responsiveness of only inherently TMZ sensitive GBM cells. *Journal of neuro-oncology,* 110**,** 349-357.

NATONI, A., MURILLO, L. S., KLISZCZAK, A. E., CATHERWOOD, M. A., MONTAGNOLI, A., SAMALI, A., O'DWYER, M. & SANTOCANALE, C. 2011. Mechanisms of Action of a Dual Cdc7/Cdk9 Kinase Inhibitor against Quiescent and Proliferating CLL Cells. *Molecular Cancer Therapeutics,* 10**,** 1624-1634.

NG, A. J. M., WALIA, M. K., SMEETS, M. F., MUTSAERS, A. J., SIMS, N. A., PURTON, L. E., WALSH, N. C., MARTIN, T. J. & WALKLEY, C. R. 2015. The DNA Helicase Recql4 Is Required for Normal Osteoblast Expansion and Osteosarcoma Formation. *PLoS Genetics,* 11**,** e1005160.

NG, F., BOUCHER, S., KOH, S., SASTRY, K. S. R., CHASE, L., LAKSHMIPATHY, U., CHOONG, C., YANG, Z., VEMURI, M. C., RAO, M. S. & TANAVDE, V. 2008. PDGF, TGF-β, and FGF signaling is important for differentiation and growth of mesenchymal stem cells (MSCs): transcriptional profiling can identify markers and signaling pathways important in differentiation of MSCs into adipogenic, chondrogenic, and osteogenic lineages. *Blood,* 112**,** 295-307.

NISHIJO, K., NAKAYAMA, T., AOYAMA, T., OKAMOTO, T., ISHIBE, T., YASURA, K., SHIMA, Y., SHIBATA, K. R., TSUBOYAMA, T. & NAKAMURA, T. 2004. Mutation analysis of the RECQL4 gene in sporadic osteosarcomas. *International journal of cancer,* 111**,** 367-372.

NISHIO, Y., DONG, Y., PARIS, M., O'KEEFE, R. J., SCHWARZ, E. M. & DRISSI, H. 2006. Runx2-mediated regulation of the zinc finger Osterix/Sp7 gene. *Gene,* 372**,** 62-70.

NOMBELA-ARRIETA, C., RITZ, J. & SILBERSTEIN, L. E. 2011. The elusive nature and function of mesenchymal stem cells. *Nature reviews. Molecular cell biology,* 12**,** 126.

OTTAVIANI, G. & JAFFE, N. 2010. The Epidemiology of Osteosarcoma. *In:* JAFFE, N., BRULAND, O. S. & BIELACK, S. (eds.) *Pediatric and Adolescent Osteosarcoma.* Boston, MA: Springer US.

OVERHOLTZER, M., RAO, P. H., FAVIS, R., LU, X.-Y., ELOWITZ, M. B., BARANY, F., LADANYI, M., GORLICK, R. & LEVINE, A. J. 2003. The presence of p53 mutations in human osteosarcomas correlates with high levels of genomic instability. *Proceedings of the National Academy of Sciences of the United States of America,* 100**,** 11547-11552.

PALOM, Y., SURESH KUMAR, G., TANG, L.-Q., PAZ, M. M., MUSSER, S. M., ROCKWELL, S. & TOMASZ, M. 2002. Relative toxicities of DNA cross-links and monoadducts: new insights from studies of decarbamoyl mitomycin C and mitomycin C. *Chemical research in toxicology,* 15**,** 1398-1406.

PALUMBO, C., PALAZZINI, S., ZAFFE, D. & MAROTTI, G. 1990. *Osteocyte Differentiation in the Tibia of Newborn Rabbit: An Ultrastructural Study of the Formation of Cytoplasmic Processes*.

PANIER, S. & BOULTON, S. J. 2013. Double-strand break repair: 53BP1 comes into focus. *Nature Reviews Molecular Cell Biology,* 15**,** 7.

PARFITT, A. 1990. Bone forming cells in clinical conditions. *Bone: A Treatise, The Osteoblast and Osteocyte.,* 1**,** 351-429.

PETERMANN, E., ORTA, M. L., ISSAEVA, N., SCHULTZ, N. & HELLEDAY, T. 2010. Hydroxyurea-Stalled Replication Forks Become Progressively Inactivated and Require Two Different RAD51-Mediated Pathways for Restart and Repair. *Molecular Cell,* 37**,** 492-502.

PETKOVIC, M., DIETSCHY, T., FREIRE, R., JIAO, R. & STAGLJAR, I. 2005. The human Rothmund-Thomson syndrome gene product, RECQL4, localizes to distinct nuclear foci that coincide with proteins involved in the maintenance of genome stability. *Journal of Cell Science,* 118**,** 4261-4269.

PIARD, J., ARAL, B., VABRES, P., HOLDER-ESPINASSE, M., MEGARBANE, A., GAUTHIER, S., CAPRA, V., PIERQUIN, G., CALLIER, P. & BAUMANN, C. 2015. Search for ReCQL4 mutations in 39 patients genotyped for suspected Rothmund–Thomson/Baller-Gerold syndromes. *Clinical genetics,* 87**,** 244-251.

PITTENGER, M. F., MACKAY, A. M., BECK, S. C., JAISWAL, R. K., DOUGLAS, R., MOSCA, J. D., MOORMAN, M. A., SIMONETTI, D. W., CRAIG, S. & MARSHAK, D. R. 1999. Multilineage potential of adult human mesenchymal stem cells. *science,* 284**,** 143-147.

POOS, K., SMIDA, J., MAUGG, D., ECKSTEIN, G., BAUMHOER, D., NATHRATH, M. & KORSCHING, E. 2015. Genomic heterogeneity of osteosarcoma - shift from single candidates to functional modules. *PloS one,* 10.

ROBERTS, I. 2004. Mesenchymal stem cells. *Vox Sanguinis,* 87**,** 38-41.

ROMANOV, Y. A., SVINTSITSKAYA, V. A. & SMIRNOV, V. N. 2003. Searching for Alternative Sources of Postnatal Human Mesenchymal Stem Cells: Candidate MSC-Like Cells from Umbilical Cord. *STEM CELLS,* 21**,** 105-110.

RYAN, A. J., SQUIRES, S., STRUTT, H. L. & JOHNSON, R. T. 1991. Camptothecin cytotoxicity in mammalian cells is associated with the induction of persistent double strand breaks in replicating DNA. *Nucleic Acids Research,* 19**,** 3295-3300.

SANGRITHI, M. N., BERNAL, J. A., MADINE, M., PHILPOTT, A., LEE, J., DUNPHY, W. G. & VENKITARAMAN, A. R. 2005. Initiation of DNA Replication Requires the RECQL4 Protein Mutated in Rothmund-Thomson Syndrome. *Cell,* 121**,** 887-898.

SCHOLZEN, T. & GERDES, J. 2000. The Ki-67 protein: from the known and the unknown. *Journal of cellular physiology,* 182**,** 311-322.

SIITONEN, H. A., SOTKASIIRA, J., BIERVLIET, M., BENMANSOUR, A., CAPRI, Y., CORMIER-DAIRE, V., CRANDALL, B., HANNULA-JOUPPI, K., HENNEKAM, R. & HERZOG, D. 2009. The mutation spectrum in RECQL4 diseases. *European journal of human genetics,* 17**,** 151.

SINGH, D. K., KARMAKAR, P., AAMANN, M., SCHURMAN, S. H., MAY, A., CROTEAU, D. L., BURKS, L., PLON, S. E. & BOHR, V. A. 2010. The involvement of human RECQL4 in DNA double-strand break repair. *Aging cell,* 9**,** 358-371.

SMIDA, J., XU, H., ZHANG, Y., BAUMHOER, D., RIBI, S., KOVAC, M., VON LUETTICHAU, I., BIELACK, S., O'LEARY, V. B., LEIB-MÖSCH, C., FRISHMAN, D. & NATHRATH, M. 2017. Genome-wide analysis of somatic copy number alterations and chromosomal breakages in osteosarcoma. *International Journal of Cancer,* 141**,** 816-828.

SYMEONIDOU, I.-E., TARAVIRAS, S. & LYGEROU, Z. 2012. Control over DNA replication in time and space. *FEBS letters,* 586**,** 2803-2812.

SYMINGTON, L. S. 2014. End resection at double-strand breaks: mechanism and regulation. *Cold Spring Harbor perspectives in biology,* 6**,** a016436.

TOYODA, M., CUI, C. & UMEZAWA, A. 2007. Myogenic transdifferentiation of menstrual blood-derived cells. *Acta Myologica,* 26**,** 176.

WAGNER, W., WEIN, F., SECKINGER, A., FRANKHAUSER, M., WIRKNER, U., KRAUSE, U., BLAKE, J., SCHWAGER, C., ECKSTEIN, V. & ANSORGE, W. 2005. Comparative characteristics of mesenchymal stem cells from human bone marrow, adipose tissue, and umbilical cord blood. *Experimental hematology,* 33**,** 1402-1416.

WAKITANI, S., SAITO, T. & CAPLAN, A. I. 1995. Myogenic cells derived from rat bone marrow mesenchymal stem cells exposed to 5-azacytidine. *Muscle & nerve,* 18**,** 1417-1426.

WANG, L. L., GANNAVARAPU, A., KOZINETZ, C. A., LEVY, M. L., LEWIS, R. A., CHINTAGUMPALA, M. M., RUIZ-MALDANADO, R., CONTRERAS-RUIZ, J., CUNNIFF, C. & ERICKSON, R. P. 2003. Association between osteosarcoma and deleterious mutations in the RECQL4 gene in Rothmund–Thomson syndrome. *Journal of the National Cancer Institute,* 95**,** 669-674.

WESTENDORF, J. J., KAHLER, R. A. & SCHROEDER, T. M. 2004. Wnt signaling in osteoblasts and bone diseases. *Gene,* 341**,** 19-39.

WILLIAMS, A. R. & HARE, J. M. 2011. Mesenchymal stem cells. *Circulation research,* 109**,** 923-940.

XIAO, W., MOHSENY, A. B., HOGENDOORN, P. C. W. & CLETON-JANSEN, A.-M. 2013. Mesenchymal stem cell transformation and sarcoma genesis. *Clinical Sarcoma Research,* 3**,** 10-10.

XU, X. & LIU, Y. 2009. Dual DNA unwinding activities of the Rothmund–Thomson syndrome protein, RECQ4. *The EMBO Journal,* 28**,** 568-577.

ZEDDOU, M., BRIQUET, A., RELIC, B., JOSSE, C., MALAISE, M. G., GOTHOT, A., LECHANTEUR, C. & BEGUIN, Y. 2010. The umbilical cord matrix is a better source of mesenchymal stem cells (MSC) than the umbilical cord blood. *Cell biology international,* 34**,** 693-701.

ZOU, L., KIDWAI, FAHAD K., KOPHER, ROSS A., MOTL, J., KELLUM, CORY A., WESTENDORF, JENNIFER J. & KAUFMAN, DAN S. Use of RUNX2 Expression to Identify Osteogenic Progenitor Cells Derived from Human Embryonic Stem Cells. *Stem Cell Reports,* 4**,** 190-198.